Functional characterization of a novel ENU-induced mutation in *Unc93b1* and its role in single-stranded RNA virus infection

Erin Isabel Lafferty

Division of Experimental Medicine

McGill University, Montréal

April 2014

A thesis submitted to McGill University in partial fulfillment of the requirements of the degree of Doctor of Philosophy

Acknowledgements

I would like to thank my supervisor Dr. Salman Qureshi for providing me with the opportunity, tools, and guidance to tackle this stimulating project and for always challenging me to achieve excellence. In addition, I would like to thank the members of my supervisory committee, Dr. Silvia Vidal, Dr. Ciriaco Piccirillo, and Dr. Danuta Radzioch, for helpful advice both during and between my yearly committee meetings. I would also like to thank all manuscript co-authors, in particular Adam Flaczyk and Sean Wiltshire, for their technical, intellectual, and editorial contributions.

A big thank you to past and present members of the Qureshi Lab for experimental and general support and to members of the MGH L11 for smiles in the hall and lunchtime conversations. In particular, thank you to Dr. Scott Carroll for teaching me how to be a PhD student and Isabelle Angers for her technical expertise, friendship, and French translation skills.

Thank you to the people I have met and worked with through SKILLSETS, Let's Talk Science, and the PGSS Equity Committee for your friendship and advice on life, careers, and graduate school; with special thanks to my thesis writing buddy Heather. To my incredible friends who live near and far; Carolyn, Monique, Sophia, Marie-Claire, Iona, and many more; you have been beside me through so much, both in person and on the phone/over Skype. Your support, words of encouragement, amazing personal successes, and outlook on life inspire me everyday.

A special thank you to Colin for your genuine interest in what I have spent the last six years of my life studying (even if you did not always understand it!), and for reminding me that a Doctor of Philosophy is, in its most basic definition, an advanced degree in the 'love of wisdom'. Your belief in my abilities, calm and rational outlook, and constant support and love through the successes and challenges of thesis and manuscript writing has been truly incredible. I look forward to a bright future together!

Finally, thank you to my wonderful family – Mom, Dad, and Megan. You have always been so proud of my accomplishments and picked me up and dusted me off every time I stumbled in life. Thank you for your unwavering belief that I could do this. You are my role models of hard work and determination and your love and support keep me strong.

Table of Contents

List of Figures and Tables

CHAPTER 1:

CHAPTER 2:

CHAPTER 3:

Author Contributions

This thesis has been organized in accordance with the guidelines of the McGill University Office of Graduate and Postdoctoral Studies for the preparation of a manuscript-based thesis. Each manuscript contains an abstract, introduction, results, discussion, and materials and methods section as well as figures, tables, and appropriate legends. These manuscripts have been accepted or submitted to a peer-reviewed journal. To integrate manuscript findings into a cohesive thesis, a detailed introduction to the relevant literature, a statement on the overall project rationale, hypothesis and experimental objectives, a discussion of conclusions and future questions that arise, and between-chapter linking statements have been included.

Chapter 2: An ENU-induced splicing mutation reveals a role for *Unc93b1* in early immune cell activation following influenza A H1N1 infection. Erin I Lafferty, Adam Flaczyk, Isabelle Angers, Robert Homer, Eva d'Hennezel, Danielle Malo, Ciriaco A Piccirillo, Silvia M Vidal, and Salman T Qureshi. *Genes and Immunity.* 2014 May 22.

Erin I Lafferty was involved in experimental design, conducted all infections and harvests, and, unless otherwise stated, performed all of the experiments in this manuscript, as well as named the mutant allele, carried out all statistical analyses, prepared all figures, and wrote and edited the manuscript. **Adam Flaczyk** performed the ELISAs in figure 2.1 and 2.6, harvested the lymph nodes and provided critical review of the manuscript. **Isabelle Angers** conducted the initial screen for the ENU-derived mouse, and identified and determined the genetic location of the *Letr* mutation. **Dr. Robert Homer** provided an expert opinion regarding lung pathology and critical review of the manuscript. **Dr. Eva d'Hennezel** provided advice regarding flow cytometry. **Dr. Danielle Malo** provided critical review of the manuscript. **Dr. Ciriaco A Piccirillo** provided flow cytometry facilities and critical review of the manuscript. **Dr. Silvia M Vidal** provided critical research and manuscript review and is the Principal Investigator on the grant that supported this project. **Dr. Salman T Qureshi** envisaged and designed the initial study and experiments, provided the facilities and equipment to conduct the research, and extensively edited the manuscript.

Chapter 3: *Unc93b1*-dependent endosomal TLR signaling regulates inflammation and mortality during Coxsackievirus B3 infection. Erin I Lafferty[*], Sean A Wiltshire[*], Silvia M Vidal, and Salman T Qureshi. *Submitted to Journal of Innate Immunity – May 2014.* *Authors contributed equally to this publication.

Erin I Lafferty and **Sean A Wiltshire** contributed equally to this publication and were involved in experimental design, conducted infections and harvests, and quantified multi-organ viral load and myocarditis. In addition, **Erin I Lafferty** performed the microarray analysis, captured the histology images, conducted the real-time PCR, carried out all statistical analyses, prepared all figures and tables, and wrote and edited the manuscript. **Sean A Wiltshire** optimized the infection model, prepared samples for microarray analysis, and provided critical review of the manuscript. **Dr. Silvia M Vidal** and **Dr. Salman T Qureshi** were involved in experimental design, provided the facilities and equipment to conduct the research, and edited the manuscript.

Original scholarship and contributions

The original contributions of this thesis are:

1. Validation of a chemically induced loss-of-function mouse model of *Unc93b1* that can be used to study its role in diverse infections and to examine the structure-function relationship for different domains of the UNC93B1 protein.
2. These are the first studies to delineate a role for *Unc93b1* in the immune response to influenza A/PR/8/34 (H1N1) and acute CVB3-induced myocarditis.
3. *Unc93b1* and endosomal TLRs activate innate immunity but have a non-essential role in dictating host outcome during influenza A/PR/8/34 (H1N1) infection.
    a. *Unc93b1*-mediated immune signaling contributes to early cellular and inflammatory mediator activation at the site of infection.
    b. *Unc93b1*-mediated endosomal TLR activation contributes to the control of lung viral load and tissue pathology but is not essential for survival.

4. In acute CVB3-induced myocarditis, *Unc93b1*-mediated immune signaling is a crucial mediator of host defense and survival.
    a. *Unc93b1* activation of endosomal TLR-mediated immune signaling provides protection against increased multi-organ viral load and cardiac tissue damage.
    b. The loss of *Unc93b1* and endosomal TLR signaling leads to increased early activation of inflammatory response genes.
    c. The loss of *Unc93b1* function decreases the early expression of genes associated with antigen processing and presentation of exogenous peptide antigen via MHC class II.
    d. Early expression of *Lcn2* and *Serpina3n*, genes associated with tissue injury and fibrosis, is elevated in the heart of *Unc93b1*$^{Letr/Letr}$ mice, linking their early expression to increased susceptibility in acute CVB3-induced myocarditis.

Other contributions

Though not a component of this thesis, I was the principal author of an invited review article:

1. **Lafferty E.I.,** Qureshi S.T., and Schnare M. (**2010**) The role of toll-like receptors in acute and chronic lung inflammation. *J Inflamm*.7:57.

I was also involved in additional studies during my PhD work for which my contribution was recognized:

1. Kornete, M., Mason, E., Girouard, J., **Lafferty, E.I.,** Qureshi, S.T., Piccirillo, C.A. ICOS regulates the homing of Th1-like CXCR3^{+} Foxp3^{+} T_{reg} cells to β-islets during pre-diabetes in non-obese diabetic mice. *Eur J Immunol.* (**Submitted: January 2014**)

2. Flaczyk, A., Duerr, C.U., Shourian, M., **Lafferty, E.I.,** Fritz, J.H., Qureshi, S.T. (**2013**) IL-33 signaling regulates innate and adaptive immunity to *Cryptococcus neoformans*. *J Immunol.* 191: 2503-13.

3. Goulet, M.L., Olagnier D., Xu Z., Paz S., Belgnaoui S.M., **Lafferty E.I.,** Janelle V., Arguello M., Paquet M., Ghneim K., Richards S., Smith A., Wilkinson P., Cameron M., Kalinke U., Qureshi S.T., Lamarre A., Haddad E.K., Sekaly R.P., Peri S., Balachandran S., Lin R. and Hiscott J. (**2013**) Systems Analysis of a RIG-I Agonist Inducing Broad Spectrum Inhibition of Virus Infectivity*. PLoS Pathog*. 9(4): e1003298.

4. Carroll S.F., **Lafferty E.I.,** Flaczyk A., Fujiwara T.M., Homer R., Morgan K., Loredo-Osti J.C., and Qureshi S.T. (**2012**) Susceptibility to progressive *Cryptococcus neoformans* pulmonary infection is regulated by loci on chromosomes 1 and 9. *Infect Immun*. 80(12): 4167.

List of Abbreviations

3d	Triple defect
5'-ppp	5'-triphosphate
AM	Alveolar macrophage
APC	Antigen-presenting cell
ARDS	Acute respiratory distress syndrome
ASC	Apoptosis-associated speck-like protein containing a CARD
BAL	Bronchoalveolar lavage
bp	Base pair
C	Carboxy-terminus
C. elegans	*Caenorhabditis elegans*
CAR	Coxsackievirus-adenovirus receptor
CARD	Caspase activation and recruitment domain
CCL	Chemokine (C-C motif) ligand
CCR	C-C chemokine receptor type
CD	Cluster of differentiation
cDC	Conventional dendritic cell
cDNA	Complementary DNA
CNS	Central nervous system
CpG DNA	Unmethylated CpG dinucleotides
CpG ODN	CpG oligodeoxynucleotide
CTD	C-terminal domain
CVB3	Coxsackievirus group B type 3
CXCL	Chemokine (C-X-C motif) ligand
D. melanogaster	*Drosophila melanogaster*
DAF	Decay-accelerating factor
DAMP	Damage-associated molecular pattern
DAVID	Database for Annotation, Visualization and Integrated Discovery
DC	Dendritic cell
DCM	Dilated cardiomyopathy
DGalN	D(+)-Galactosamine hydrochloride
dsRNA	Double-stranded RNA
ECM	Extracellular matrix
ENU	*N*-ethyl-*N*-nitrosourea
ER	Endoplasmic reticulum
ExM	Exudate macrophage
FBS	Fetal bovine serum
gDNA	Genomic DNA
GO	Gene ontology
H&E	Hematoxylin and eosin
HA	Hemagglutinin
HSE	Herpes simplex encephalitis

HSV	Herpes simplex virus
IFN	Interferon
IKK	IκB kinase
IKMC	International Knockout Mouse Consortium
IL	Interleukin
IL-1R	IL-1 receptor
IL-1Ra	IL-1R antagonist
IMPC	International Mouse Phenotyping Consortium
ILC	Innate lymphoid cell
IRAK1	IL-1 receptor-associated kinase 1
IRF	Interferon regulatory factor
ISG	Interferon-stimulated gene
ISGF3	IFN-stimulated gene factor 3
IκBα	Inhibitor of NFκB
L. major	*Leishmania major*
LALN	Lung-associated lymph node
Lcn2	Lipocalin 2
Letr	Loss of endosomal TLR response
LGP2	Laboratory of genetics and physiology 2
LN	Lymph node
LPS	Lipopolysaccharide
LRR	Leucine-rich repeat
M2	Matrix protein 2
MAPK	Mitogen-activated protein kinase
MAVS	Mitochondrial antiviral signaling protein
MCMV	Mouse cytomegalovirus
MDA5	Melanoma differentiation-associated protein 5
MDCK cells	Madin-Darby canine kidney cells
MFI	Mean fluorescence intensity
MGI	Mouse Genome Informatics
MHC	Major histocompatibility complex
MyD88	Myeloid differentiation primary response gene 88
N	Amino-terminus
NA	Neuraminidase
NFκB	Nuclear factor kappa-light-chain-enhancer of activated B cells
NK cell	Natural killer cell
NLR	Nucleotide-binding domain and leucine-rich-repeat containing receptor
NLRP3	NLR pyrin domain containing 3
NOD	Nucleotide-binding oligomerization domain-containing protein
NOS2	Nitric oxide synthase 2
NS1	Non-structural protein 1
NSV	Neuroadapted Sindbis virus
$\mathbf{P_{adj}}$	Adjusted p-value

PAMP	Pathogen-associated molecular pattern
PBMC	Peripheral blood mononuclear cell
PBS	Phosphate-buffered saline
PCA	Principal component analysis
pDC	Plasmacytoid dendritic cell
Phyre	Protein Homology/analogY Recognition Engine
polyI:C	Polyinosinic:polycytidylic acid
polyU	polyuridylic acid
poly-Ub	Poly-ubiquitination
PRR	Pattern recognition receptor
PYD	Pyrin domain
qRT-PCR	Quantitative RT-PCR
RIG-I	Retinoic acid-inducible gene 1
RLR	RIG-I-like receptors
rSerpin	Recombinant serpin A 3N
RT-PCR	Reverse transcription polymerase chain reaction
Se	Selenium
SerpinA3N	Serine (or cysteine) peptidase inhibitor, clade A, member 3N
SLE	Systemic lupus erythematosus
SNP	Single nucleotide polymorphism
ssRNA	Single-stranded RNA
STAT	Signal transducer and activator of transcription
T. cruzi	*Trypanosoma cruzi*
T. gondii	*Toxoplasma gondii*
TAB	TAK1 binding protein
TAK1	TGF-β activated kinase 1
TANK	TRAF family member-associated NFκB activator
TBK1	TANK-binding kinase 1
TF	Transcription factor
TGF-β	Transforming growth factor-β
Th	T helper
TIR	Toll/IL-1 receptor
TLR	Toll-like receptor
TNF-α	Tumour necrosis factor-α
TRAF6	TNF receptor associated factor 6
TRAIL	TNF-related apoptosis-inducing ligand
TRIF	TIR-domain-containing adapter-inducing IFN-β
TRIM25	Tripartite motif-containing 25
type I IFN	IFN-α/β
type I IFNAR	Type I IFN receptor
type II IFN	IFN-γ
Unc93b1	*Unc-93 homolog b1* (*C. elegans*)
WHO	World Health Organization

Abstract

Pattern recognition receptors (PRRs) of the innate immune system are on the front line of host defense against an invading pathogen. These proteins recognize highly conserved pathogen-associated molecular patterns (PAMPs) and initiate signaling cascades that lead to immune activation. The first PRRs discovered were toll-like receptors (TLRs) that can recognize a broad range of microbial structures. While some TLRs localize to the cell membrane, recognition of foreign nucleic acid frequently occurs at the endosome through TLR3, TLR7, and TLR9. Though endosomal TLRs recognize conserved PAMPs, their contribution to host defense and infection outcome varies according to the pathogen under consideration.

To investigate the contribution of TLR-associated proteins to immune activation we conducted random chemical mutagenesis using *N*-ethyl-*N*-nitrosourea (ENU) and found a deviant mouse that was hyporesponsive to TLR3-, TLR7-, and TLR9-specific PAMP stimulation *in vitro* and *in vivo.* This was caused by a mutation in *Unc93b1,* a chaperone that trafficks nucleic acid-sensing TLRs from the endoplasmic reticulum to the endosome for immune activation. The ENU-induced mutation in *Unc93b1*, which we termed *Letr* for 'loss of endosomal TLR response', causes a splicing defect that removes two transmembrane domains of the UNC93B1 protein.

A protective role for UNC93B1 has been previously defined following infection with parasites or DNA viruses but its role in ssRNA viral infection has been less well characterized. Therefore, we studied the contribution of UNC93B1-mediated immune activation following infection with two ssRNA viruses; influenza A/PR/8/34 (H1N1) – an important global respiratory pathogen, and coxsackievirus group B type 3 (CVB3) – the most common etiological agent of viral myocarditis. As both pathogens are capable of activating TLR3 and TLR7, we used *Unc93b1*$^{Letr/Letr}$ mice to define a specific role for endosomal TLR-mediated immune activation in each infection.

Following influenza infection, *Unc93b1*$^{Letr/Letr}$ mice had diminished innate immune activation at the site of infection that was characterized by decreased activated exudate macrophage recruitment, T cell activation, and inflammatory mediator production. The *Letr* defect led to delayed lung viral clearance and increased tissue inflammation but did not significantly alter infection survival. This suggests that *Unc93b1*-mediated signaling in influenza

infection plays a role in early immune activation but is not required to define a positive infection outcome, a scenario that is most likely explained by the activation of additional host immune mechanisms.

In contrast to influenza, *Unc93b1*$^{Letr/Letr}$ mice were significantly more susceptible to acute CVB3-induced viral myocarditis, accompanied by increased multi-organ viral load and cardiac injury with substantial fibrosis. Cardiac transcriptome analysis revealed dysregulated expression of inflammatory response genes as well as genes for antigen processing and presentation of exogenous peptide antigen via MHC class II in *Unc93b1*$^{Letr/Letr}$ mice. In particular, *Unc93b1*$^{Letr/Letr}$ hearts had increased expression of *Ifn-b, Lcn2*, and *Serpina3n* at day 2 post-infection. The latter two genes have been previously linked to tissue injury and fibrosis and may be contributing to the severe cardiac pathology observed during CVB3 infection.

In conclusion, these studies have characterized a unique loss-of-function mutation in *Unc93b1,* and illustrated the varying contributions of the endosomal TLR pathway to immunity following infection with two different ssRNA viruses. Further detailed analysis of this mutant mouse could provide additional insights on the role of endosomal TLRs in immune activation and better define the process of host-pathogen interaction during virus infection.

Résumé

Les récepteurs de reconnaissance de motifs (PRRs) constituent la première ligne de défense du système immunitaire inné contre les agents pathogènes envahissants. Ces protéines reconnaissent des motifs moléculaires associés aux pathogènes (PAMPs) parfaitement conservés et déclenchent la signalisation en cascade à l'origine de l'activation de la réponse immunitaire. Les premiers PRR mis en évidence étaient des récepteurs de type Toll (TLRs) qui peuvent identifier un large éventail de motifs microbiens. Alors que certains d'entre eux se trouvent à la surface des membranes cellulaires, la reconnaissance des acides nucléiques d'origine étrangère à l'hôte s'effectue fréquemment à la surface des endosomes (TLR3, TLR7, et TLR9). Bien que ces TLRs endosomaux reconnaissent des PAMPs hautement conservés, leur contribution dans la défense immunitaire de l'hôte et le résultat en termes d'infection varient selon l'agent pathogène étudié.

Pour étudier la contribution des protéines associées aux TLR dans l'activation du système immunitaire, nous avons mené une étude en mutagénèse chimique aléatoire en utilisant l'agent mutagène N-nitroso-N-éthylurée (ENU). Cette étude a permis d'identifier une souris hyporéactive aux PAMPs associés aux récepteurs TLR3, TLR7, et TLR9 lors de stimulations *in vitro* et *in vivo*. La cause de cette absence de réponse est une mutation dans le gène *Unc93b1*, le chaperon moléculaire qui accompagne les TLRs endosomaux du réticulum endoplasmique vers l'endosome. Cette mutation induite par ENU, appelée *Letr* (loss of endosomal TLR response, perte de réponse du TLR endosomal), cause une défaillance dans l'épissage du gène *Unc93b1* qui se traduit par la perte de deux domaines transmembranaires de la protéine UNC93B1.

Auparavant, le rôle protecteur d'UNC93B1 lors d'infections par des parasites ou des virus à ADN a été bien défini. En revanche, son rôle lors d'infections par des virus à ARN simple brin (ARNsb) est beaucoup moins caractérisé. Par conséquent, nous avons étudié la contribution de l'activation immunitaire contrôlée par UNC93B1 lors de deux modèles infectieux par deux virus à ARNsb différents, à savoir le virus de l'influenza A/PR/8/34 (H1N1), un important agent pathogène respiratoire à l'échelle mondiale, et le virus Coxsackie B3 (CVB3), l'agent étiologique le plus courant des myocardites virales. Comme ces deux virus peuvent

activer les récepteurs TLR3 et TLR7, nous avons utilisé pour chaque infection notre lignée de souris *Unc93b1*$^{Letr/Letr}$ pour définir un rôle spécifique à l'activation immunitaire contrôlée par les TLR endosomaux.

Suivant une infection par le virus de l'influenza, les souris *Unc93b1*$^{Letr/Letr}$ présentaient une activation immunitaire innée réduite au site de l'infection, caractérisée par une diminution du recrutement des macrophages exsudats activés, de l'activation des cellules T et de la production des médiateurs inflammatoires. La défaillance *Letr* a entraîné un retard de la clairance virale pulmonaire et une augmentation de l'inflammation des voies respiratoires, mais n'a pas modifié la survie après infection de manière représentative. Ces résultats suggèrent que la signalisation contrôlée par UNC93B1 dans l'infection par le virus de l'influenza joue un rôle dans l'activation immunitaire précoce, mais qu'elle n'est pas requise pour déterminer un dénouement positif en cas d'infection, ce dernier étant plus susceptible d'être expliqué par l'activation de mécanismes immunitaires complémentaires de l'hôte.

Par opposition à l'influenza, les souris *Unc93b1*$^{Letr/Letr}$ étaient plus sensibles aux myocardites virales aiguës induites par le CVB3, accompagnées d'une augmentation de la charge virale multi-organe et de lésions cardiaques avec présence d'une fibrose importante. L'analyse du transcriptome cardiaque suivant une infection au CVB3 a mis en évidence un dérèglement de l'expression des gènes de la réponse inflammatoire, ainsi que des gènes d'apprêtement et de présentation des antigènes exogènes au niveau du CMH de classe II chez les souris *Unc93b1*$^{Letr/Letr}$. En particulier, l'expression des gènes *Ifn-b, Lcn2,* et *Serpina3n* avaient augmenté dans les tissus cardiaques des souris *Unc93b1*$^{Letr/Letr}$ au jour 2 suivant l'infection. Par le passé, ces deux derniers gènes, *Lcn2* et *Serpina3n*, ont tous les deux été impliqués dans les lésions tissulaires et la fibrose. Ils sont donc deux contributeurs possibles à la pathologie sévère que nous observons durant une infection virale au CVB3.

En conclusion, ces études ont caractérisées une mutation unique dans le gène *Unc93b1* qui cause une perte de fonction. Nous avons aussi illustré une contribution variable des voies de signalisation activées par les TLR endosomaux à l'immunité de l'hôte après l'infection par deux virus à ARNsb différents. Dans le futur, des analyses plus détaillées de cette souris mutante pourraient nous donner une connaissance plus approfondie sur le rôle des TLR

endosomaux dans l'activation immunitaire et pourraient nous aider à mieux définir les interactions hôte-pathogène durant une infection virale.

CHAPTER 1. Introduction

According to a World Health Organization (WHO) survey of global mortality in 2011, two of the five most common causes of death were attributed to infectious diseases, a statistic that is unchanged from over a decade ago.[1] The significant impact of infectious diseases is particularly obvious in low-income countries where half of the top ten causes of mortality are infection-related.[1] Global infectious causes of morbidity and mortality derive from established pathogens, newly emerging pathogens, and pathogens that have re-emerged due to the development of drug-resistance or as a result of increased susceptibility in an expanding global pool of immunocompromised individuals.

How the host responds to an infection is dependent upon both host factors (age, sex, genetics, nutritional status) as well as microbial factors (dose, strain, virulence factors, resistance to treatment, route of infection). The dynamic interaction between the host and the pathogen is a key determinant of whether the host will succumb to the disease or recover from infection with or without clinical sequelae. The in-depth study of this interaction and identification of the specific host factors that mediate infection outcome can reveal novel mechanisms to be exploited or targeted for infection prevention or treatment with the potential to decrease the significant global morbidity and mortality caused by infectious diseases.

I. Studying host-pathogen interactions

The ideal study of host-pathogen interactions would be conducted in humans.[2] However, the inherent genetic variation within and among different populations and the lack of control over external environmental factors make these studies challenging to design and interpret.[2] In addition, the numerous ethical and practical limitations that go with experimentation in humans create a further restriction.[2] To circumvent these challenges, *in vivo* research of host-pathogen interactions is conducted using animal models.

Mice are the most commonly used model of human disease as a homologous gene between mice and humans has been discovered in 99% of cases, mice are easy to work with and maintain, they breed well to produce large groups in a short period of time, and are amenable to experimental manipulation and analysis using a wide variety of tools.[3-5] As

laboratory mice can be bred to have genetically identical backgrounds and are used in a controlled setting, researchers can more easily manage potential confounding host and environmental factors.[4, 6] Nevertheless, there are several caveats to the use of mouse models when studying host-pathogen interactions. Individual mouse strains can respond to the same infection with a dramatically different phenotype,[6] leading to divergent conclusions as to the importance of host genes in protective immunity. Also, mouse models of infection frequently differ from natural human infection in terms of the route of entry, dose required to cause disease, relevance of the experimental strain to human infection, and clinical symptoms.[2] These limitations can create problems when trying to extrapolate findings from experimental mouse studies to natural human infection. Despite these limitations, studies of host-pathogen interactions using mouse models of infection have revealed important insights into the human immune response. To conduct these studies researchers will often adopt either a reverse or a forward genetic approach.

Reverse genetics

This is a hypothesis-based approach that begins with manipulation of a targeted region of the host genome and examines the ensuing effect on one or more selected phenotypes.[3, 4] A reverse genetic strategy is generally guided by previous information on the relationship between the genetic region being manipulated and the phenotype under study.[4] While reliance on previous conclusions can provide supportive evidence for the experimental hypothesis, it biases potential experimental findings towards already established knowledge.[4, 7] In addition, if the previous conclusions used for hypothesis generation are not robust, the extensive investment required to create a new genetic model may not yield relevant biological discoveries.[7]

In reverse genetics, a variety of techniques can be used to increase, ablate, or conditionally alter gene expression.[8] An interesting contemporary technique is the creation of humanized mice, whereby human immune cells are grafted into an immunodeficient mouse to more closely recapitulate the human immune response in an experimentally versatile mouse model.[9, 10]

Forward genetics

Forward genetic approaches begin with a phenotype of interest and subsequently search for the responsible genes. This strategy analyzes the relationship between genotype and phenotype in the opposite way to reverse genetic approaches.[3, 4] Forward genetics is an unbiased and hypothesis-free approach that can reveal novel genes or novel roles for known genes causing a phenotype of interest.[3, 11] An advantage of forward genetics is that a phenotypic difference is established prior to a substantial investment into genetic mapping and further characterization.[4]

A key tool used in forward genetics is the genetic diversity of the over 450 available inbred mouse strains.[6] As these strains can have widely divergent phenotypes following infection, they can be crossed to create interval-specific congenic mice where a novel phenotype is transferred to mice with a known genetic background and the causative mutation is subsequently mapped to a specific interval.[12] A challenge in congenic studies is that mapping the responsible gene requires extensive backcrossing and gene sequencing, which can be laborious.[12] In addition, there is a limited pool of genetic and phenotypic diversity available among inbred strains.[13] While crossing inbred strains with wild-derived strains can increase genetic diversity, the genomes of wild-derived strains are not as well characterized which can further complicate genetic mapping.[12] To circumvent this issue, many forward genetic studies have adopted the use of mutagens such as radiation or noxious chemicals to randomly alter the mouse genome and create unique mutant strains.[14, 15]

II. ENU mutagenesis

The most potent chemical mutagen that is used to alter the genome of both plant and animal species is *N*-ethyl-*N*-nitrosourea (ENU).[15, 16] This chemical is an alkylating agent that randomly inserts its ethyl group at the nitrogen or oxygen site of DNA nucleotides to significantly alter the nucleotide such that, during replication, the strand is misread and a new base pair (bp) is substituted at this site, producing a point mutation in the genomic DNA (gDNA) (Figure 1.1).[17, 18] ENU is injected into male mice and specifically targets spermatogonial cells to cause heritable mutations.[3, 15, 17]

Mutations caused by ENU occur at approximately 1 bp per million and are therefore more frequent in larger genes.[3, 19] Though ENU mutagenesis is considered random, insertion of its ethyl group is biased towards A:T bps and occurs more frequently in GC-rich genes.[18, 20] Analysis of published ENU-induced mutations revealed that 44% caused a transversion from an A:T to a T:A while 38% caused an A:T to G:C transition with G:C bps rarely affected.[18] At the protein level, 64% of ENU-induced mutations resulted in a missense mutation, 26% induced a splicing error during DNA processing, and 10% caused nonsense mutations.[18] The reason for these mutation biases is currently unknown.

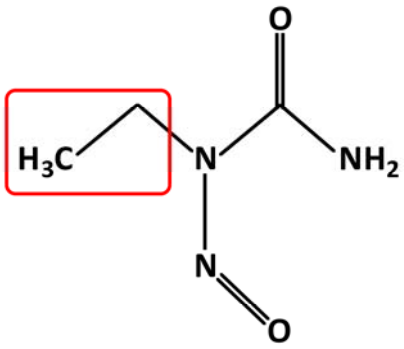

Figure 1.1. Chemical structure of N-ethyl-N-nitrosourea ($C_3H_7N_3O_2$)
A potent mutagen for inducing random heritable point mutations in host DNA nucleotides through ethyl group (indicated in red) insertion.[15, 17, 18]

Mutagenesis and screening

The basic protocol for ENU mutagenesis and screening is as follows:

1. Male mice are injected intraperitoneally with ENU at the G0 generation.[13] An optimal dose of ENU induces sterility within two weeks of injection and is tested by pairing a mutagenized male with a wild type female mouse during this time. The male usually regains fertility within 10-12 weeks.[3, 21]
2. Following fertility recovery, mutagenized mice are paired with wild type female mice from a known inbred strain in order to create G1 mice.[13] As all G1 mice are heterozygous for the ENU-induced mutations, screening for dominant mutations is conducted at this generation.[13] The advantage of dominant screens is that they require less breeding, which can minimize housing costs and decrease experimental complexity

(Figure 1.2A).[22] Nevertheless, dominant mutations causing a phenotype of interest are rare; occurring about 2% of the time,[23] meaning that mutants demonstrating the phenotype of interest will be more challenging to discover.

3. An alternative strategy is to screen for recessive mutations. This approach increases the likelihood of uncovering a phenotype-causing mutation and breeding from healthy heterozygous parents can allow for the study of recessive mutations that may affect reproduction.[13] Methods for uncovering recessive ENU-induced mutations include:
    a. Mating G1 progeny to a mouse carrying a known chromosomal deletion followed by screening at the G2 generation. Recessive mutations that induce a phenotype when following this breeding strategy will be on a gene that localizes to the deleted chromosome only (Figure 1.2B).[13, 22] While this cuts down on breeding time, cost and complexity, it limits the genetic diversity available for study.[13]
    b. Mating two G1 mice, the progeny from separate ENU injections at G0, to produce G2 progeny that are subsequently intercrossed to create G3 mice for screening (Figure 1.2C).[13, 16] This technique allows an unbiased investigation for mutations on any chromosome.[13, 16] Mating two mutagenized mice at the G1 generation, as opposed to a mutagenized and wild type inbred mouse, increases the pool of mutations at the G3 screening generation.[13, 16]

c.

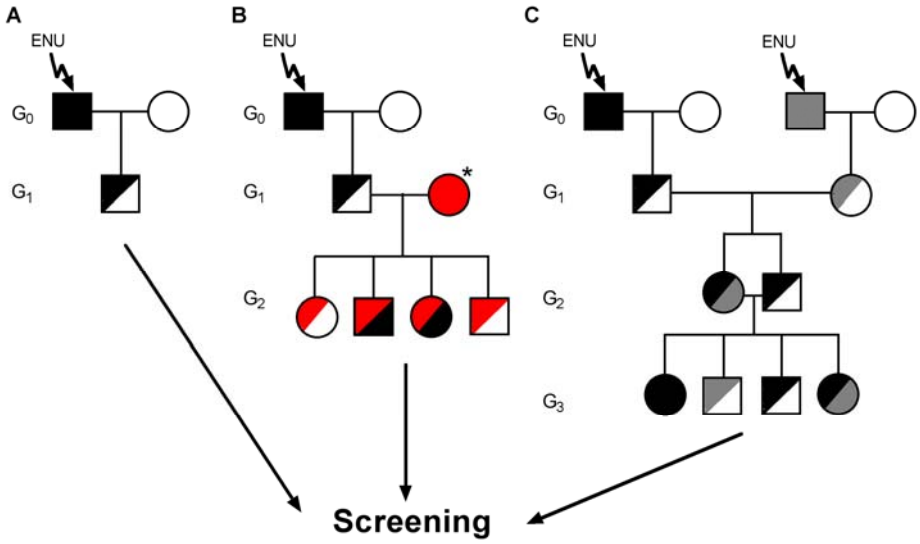

Figure 1.2. Breeding and phenotyping strategies to uncover ENU-induced mutations
Distinct breeding strategies allow for phenotypic analysis of (A) dominant and (B, C) recessive ENU-induced mutations at different generations. (*) denotes a female mouse with a known chromosomal deletion. (A, B) were adapted from:[13, 16, 22] and (C) was adapted from Figure 2.1A of chapter 2.

4. Once a phenotypically relevant mutagenized mouse is discovered, a panel of genetic markers that are spaced throughout the genome are used to determine the initial chromosomal location of the mutation followed by intra-chromosomal fine mapping techniques.[13] Within a defined region, the specific gene and causative mutation can then be uncovered through detailed gene sequencing. These studies can use a targeted approach to mutation discovery, sequencing only specific genes in the defined region based on previous functional knowledge, or may sequence all genes in the defined interval.[13]
5. Finally, studies must confirm that the ENU-induced mutation truly localizes to the predicted gene. This can be done in one of two ways. The first is through insertion of a wild type transgene into mutant mice or cells.[21] If this reverses the phenotype of interest then the ENU-induced mutation is indeed in the predicted gene. The second method is allelic complementation, conducted by breeding the ENU-mutagenized

mouse with an existing independent mouse that carries a known loss-of-function mutation in the predicted gene.[21] If the phenotype of interest persists in the compound heterozygote then the predicted mutation and gene are responsible for inducing the phenotype of interest.

Designing phenotypic screens for ENU mutagenesis

To increase the likelihood of uncovering novel findings, the phenotype that is selected for screening following ENU mutagenesis should address a phenomenon or disease for which there are unanswered questions.[11] The screen should also be robust, allowing for the same results to be obtained in multiple independent experiments with minimal interexperimental variability, and specific, yielding results that exclusively pertain to the phenotype of interest.[11, 13] This is essential to ensure that the screen is not overly sensitive, which may generate false positive results, while at the same time remaining sensitive enough so that subtle mutations are not missed.[11, 16] In studying host-pathogen interactions, the screen selected can focus on a specific pathogen or more generally examine the immune response to an experimental stimulus such as a chemical or nucleic acid structure.[3, 11]

Phenotypic screens can occur *in vitro*, examining a response in a singe or multiple cell types, or directly *in vivo*. *In vivo* screens allow the researcher to examine a phenotype at the whole organism level or focus on a specific organ or cellular response following infection. There are also several options for how a screen can be conducted, depending on the pathogen or phenotype under study. Non-lethal screens allow the researcher to continue breeding directly following phenotyping and permit phenotype confirmation in subsequent tests, though they limit the characteristics that can be studied following mutagenesis.[13, 16] Lethal screens can expand the phenomena available for study but require the maintenance of parental generations to rederive the mutation in further breeding.[16] Though not always possible, a sub-lethal screen is a third option in which mice that are positive for a lethal phenotype are rescued through curative treatment so that further breeding can occur without the need to maintain the parental generation.[16]

Advantages and challenges of ENU mutagenesis

The key advantage of ENU is that it can produce point mutations at different sites of the same gene leading to a variety of effects on protein function.[13] This more closely imitates human mutation and has the potential to reveal specific functions of a particular protein site or domain in a given biological process.[13, 22] Compared to other methods of mutagenesis, ENU is the most powerful mutagen available and has a greater propensity to cause discrete point mutations instead of large deletions or chromosomal breaks.[15]

The largest barrier to ENU studies is the cost and organization required to set-up and maintain a successful mutagenesis, breeding, screening, and mapping program.[21] Another disadvantage of ENU mutagenesis studies is that, as it relies on a testable phenotype, discovery can be biased away from subtle mutations in favour of genes linked to more easily detectable phenotypes.[13] Finally, despite the theoretically valid concept that ENU mutagenesis can randomly mutate any gene, its inherent bias towards larger genes and specific nucleotides means that this is unlikely to be true in practice.[18, 20] Therefore, the frequency of mutagenesis is not equivalent across the genome and may limit the genes that can be studied using this method. Despite these challenges, the field of host-pathogen interactions has been significantly advanced as a direct consequence of findings derived from ENU mutagenesis studies, demonstrating the value of this approach.

III. The immune response to viral infection

Pattern recognition receptors (PRRs) initiate the primary host response to a pathogen. Following infection they recognize conserved, essential structures produced by microbes known as pathogen-associated molecular patterns (PAMPs).[24] This initiates a complex immune signaling network that leads to the production of proinflammatory cytokines and type I interferon (IFN) (IFN-α/β), which further orchestrates immune activation.[24] PRRs can be classified as membrane-bound, localized to the surface of a cell or intracellular organelle, or located freely in the cytosol.[24, 25] The following sections will outline the general pattern of immune activation following viral infection with pathogen-specific details discussed in later sections.

Toll-like receptors

Toll-like receptors (TLRs) are the oldest known PRRs and were first discovered in *Drosophila melanogaster* (*D. melanogaster*) where they were named 'Toll' and observed to have a role in dorsal-ventral patterning during embryonic development as well as an important role in mediating protection against fungal infection.[26, 27] Since their initial discovery, 10 human and 12 mouse TLRs have been elucidated and implicated in immune activation but not embryonic development, representing a functional specialization of these TLRs that is distinct from *D. melanogaster* Toll.[28, 29] All TLRs are classified as type I transmembrane proteins containing a variable number of leucine-rich repeats (LRRs) for PAMP recognition, a transmembrane domain, and a cytosolic toll/interleukin(IL)-1 receptor (TIR) domain to mediate adaptor binding.[29] Despite their conserved structure, TLRs are present in distinct locations in the cell. TLR1, TLR2, TLR4, TLR5, and TLR6 are localized to the cell surface and recognize highly conserved proteins including lipopolysaccharide (LPS), flagellin and lipoproteins.[24] On the other hand, TLR3, TLR7, and TLR9 localize to the endosome and recognize nucleic acids, including those derived from viruses during infection and replication.[24]

Endosomal TLRs

Each endosomal TLR recognizes unique structural features of nucleic acids. TLR3 recognizes double-stranded (ds)RNA as well as the chemical agonist polyinosinic:polycytidylic acid (polyI:C).[30] TLR7 recognizes single-stranded (ss)RNA and can also be activated by specific synthetic agonists that include polyuridylic acid (polyU) and imidazoline compounds such as Imiquimod.[31, 32] TLR9 recognizes DNA containing unmethylated CpG dinucleotides and can be activated by synthetic CpG oligodeoxynucleotides (CpG ODN).[33] As one or more of these structures may be present during infection and viral replication, more than one endosomal TLR can simultaneously trigger immune signaling. Expression of TLR3, TLR7, and TLR9 in the host occurs primarily in immune cells such as dendritic cells (DCs) and macrophages, with a particular role for TLR7-specific immune activation in plasmacytoid (p)DCs.[25, 31] These TLRs activate further immune signaling at the endosome but they localize to the endoplasmic reticulum (ER) in the unstimulated cell. Owing to this compartmentalization, endosomal TLR-

mediated immune activation only occurs once these TLRs have been trafficked from the ER to the endosome by UNC93B1.[34-36]

TLR3 activation by dsRNA at the endosome causes PRR dimerization and subsequent recruitment of the TIR-domain-containing adapter-inducing IFN-β (TRIF) adaptor that binds the cytosolic TIR domain of TLR3 (Figure 1.3).[25, 28] This is followed by recruitment of TANK-binding kinase 1 (TBK1) and IKKi which complex and phosphorylate the IFN regulatory factor (IRF)3 transcription factor (TF).[28] Phosphorylation of IRF3 allows it to dimerize and translocate into the nucleus to upregulate type I IFN transcription.[28, 37] Newly derived IFN-α and IFN-β can then exit the host cell and bind to the cell-surface localized IFN-α/β receptor (type I IFNAR) to activate IFN-stimulated gene factor 3 (ISGF3), a TF complex composed of IRF9, and the phosphorylated form of signal transducer and activator of transcription (STAT)1 and STAT2.[38] Following activation, ISGF3 enters the nucleus and upregulates the expression of multiple IFN-stimulated genes (ISGs) that modulate diverse immune functions in the host including destruction of virally infected cells, PRR upregulation, cytokine and chemokine expression, and antigen presentation.[39]

Type I IFN expression can also be elicited following TLR7 activation.[28, 31] The interaction between ssRNA and TLR7 recruits the myeloid differentiation primary response gene 88 (MyD88) adaptor to the endosome (Figure 1.3), which initiates the formation of a complex consisting of the IL-1 receptor-associated kinase 1 (IRAK1) and tumour necrosis factor receptor associated factor 6 (TRAF6) ubiquitin ligase.[28] This leads to IRAK1-dependent phosphorylation of the IRF7 TF which, similar to IRF3, dimerizes and enters the nucleus to upregulate type I IFN expression.[28] Activation of type I IFN by TLR7-MyD88 signaling occurs exclusively in pDCs,[28] a restriction that may prevent immune hyperactivation.

In addition to type I IFN expression, TLR3-TRIF and TLR7-MyD88 can also activate the transcription of proinflammatory cytokines through the nuclear factor kappa-light-chain-enhancer of activated B cells (NFκB) TF (Figure 1.3).[28] Following TLR-adaptor binding, TRAF6 recruitment and activation induces the formation of a complex consisting of transforming growth factor- (TGF)-β activated kinase 1 (TAK1) and TAK1 binding proteins (TAB)1-3 that subsequently activates the IκB kinase (IKK) complex.[28, 37] Activated IKK phosphorylates the

inhibitor of NFκB (IκBα), which targets it for degradation.[37] As the physical binding of IκBα to NFκB normally restricts its localization to the cytosol, IκBα dissociation activates NFκB, allowing it to translocate into the nucleus to initiate proinflammatory cytokine gene transcription.[37]

Cytosolic receptors

Immune recognition of viruses that directly enter the cell and localize in the cytosol is facilitated by PRRs in the RIG-I-like receptor (RLR) and nucleotide-binding domain and leucine-rich-repeat containing receptor (NLR) families.[38-40]

RLRs

RLRs, similar to TLRs, activate type I IFN and proinflammatory cytokine transcription via the IRF3/IRF7 and NFκB TFs, respectively (Figure 1.3).[39] RLRs are ubiquitously expressed and play a role in both immune and non-immune cells in the host but are not required for pDC-specific production of type I IFN.[39, 41] The RLR family consists of three known members, retinoic acid-inducible gene 1 (RIG-I), melanoma differentiation-associated protein 5 (MDA5) and laboratory of genetics and physiology 2 (LGP2).[39] While a specific ligand for LGP2 has not been elucidated, several studies have implicated it in either positive or negative regulation of RIG-I and MDA5 activation, depending on the specific stimulus.[42-44] The basic structure of the RLRs consists of two N-terminal caspase activation and recruitment domains (CARDs) for adaptor binding, a DExD/H RNA helicase domain and a C-terminal domain (CTD).[44, 45] LGP2 is distinguished from other RLRs by the absence of the N-terminal CARD domains.[44]

RIG-I signaling is activated in response to 5'-triphosphate (5'-ppp) structures on viral ssRNA in addition to a secondary structural pattern such as a 5' panhandle conformation.[45-48] In resting cells, RIG-I is auto-repressed by its CTD that sequesters the CARD binding sites.[39, 42] Ligand binding to the helicase domain of RIG-I de-represses the CARDs and exposes them to tripartite motif-containing 25 (TRIM25)-mediated polyubiquitination. Upon full activation, polyubiquitinated RIG-I dimerizes and binds the mitochondrial antiviral signaling protein (MAVS) adaptor at the mitochondrial membrane through CARD-CARD interactions.[42, 49-53] MAVS

localization at the mitochondrial membrane is sustained through a C-terminal transmembrane region and is required to facilitate downstream TF activation.[52]

MDA5 is activated in response to polyI:C or dsRNA stimulation and has an established role in the immune response to picornavirus infection.[54, 55] MDA5 also utilizes the MAVS adaptor to activate proinflammatory cytokine and type I IFN gene transcription.[50, 51] Unlike RIG-I, MDA5 activation is not repressed in the resting state[42] however, similar to RIG-I, polyubiquitination is required for MDA5 activation, although the causative protein is not yet known.[56]

NLRs

To date, 23 human and 34 mouse NLRs have been identified.[24] The common structure of NLRs consists of a sequence of C-terminal LRRs, a nucleotide-binding domain and an N-terminus with either a pyrin domain (PYD) or a CARD.[57] NLRs contribute to immune activation through two distinct mechanisms (Figure 1.3). The first is via nucleotide-binding, oligomerization domain-containing protein (NOD)1 and NOD2.[40] These PRRs typically elicit proinflammatory cytokine and type I IFN expression in response to peptidoglycan;[40] however, NOD2 has also been implicated in type I IFN activation during ssRNA viral infection via the MAVS-IRF3 pathway.[58] NLRs can also be involved in initiating the formation of a multi-protein complex known as the inflammasome. The inflammasome typically consists of three proteins; a PRR, an adaptor and pro-caspase-1.[40] This cytosolic complex cleaves pro-IL-1β and pro-IL-18, produced following NFκB activation mediated by other PRRs, into fully functional cytokines.[40, 59] Unlike other PRRs, the inflammasome has no role in activating the transcription of proinflammatory cytokine or type I IFN genes.[40] During RNA viral replication the NLR family, pyrin domain containing 3 (NLRP3) PRR, expressed predominantly in hematopoietic cells, is activated and initiates inflammasome formation.[40] NLRP3 activation can occur through a variety of PAMPs, such as nucleic acid from DNA or RNA viruses, as well as damage-associated molecular patterns (DAMPs) derived from virus-mediated tissue damage.[40] Activated NLRP3 binds to the apoptosis-associated speck-like protein containing a CARD (ASC) adaptor via PYD-PYD interactions.[59] The ASC CARD subsequently binds to the CARD of pro-caspase-1, allowing protein cleavage and

activation of caspase-1.[60] Active caspase-1 can then mediate cleavage of pro-IL-1β and pro-IL-18.[59, 61]

Activation of TLRs, RLRs, and NLRs in the immune response to viral infection provides partially overlapping yet highly specialized pathways to effectively respond to diverse stimuli. Following PRR activation, the immune response progresses in two distinct waves. Innate immunity is a non antigen-specific response that occurs rapidly following infection and controls initial viral replication and spread while instructing adaptive immunity.[62, 63] The adaptive immune response is not genetically pre-programmed like the innate immune response but instead provides a specific and tailored response to the infecting strain.[62, 63] This allows the host to more effectively combat the viral infection and provides a long term antibody-mediated memory response that can be rapidly mobilized in future homologous infections.[62, 63]

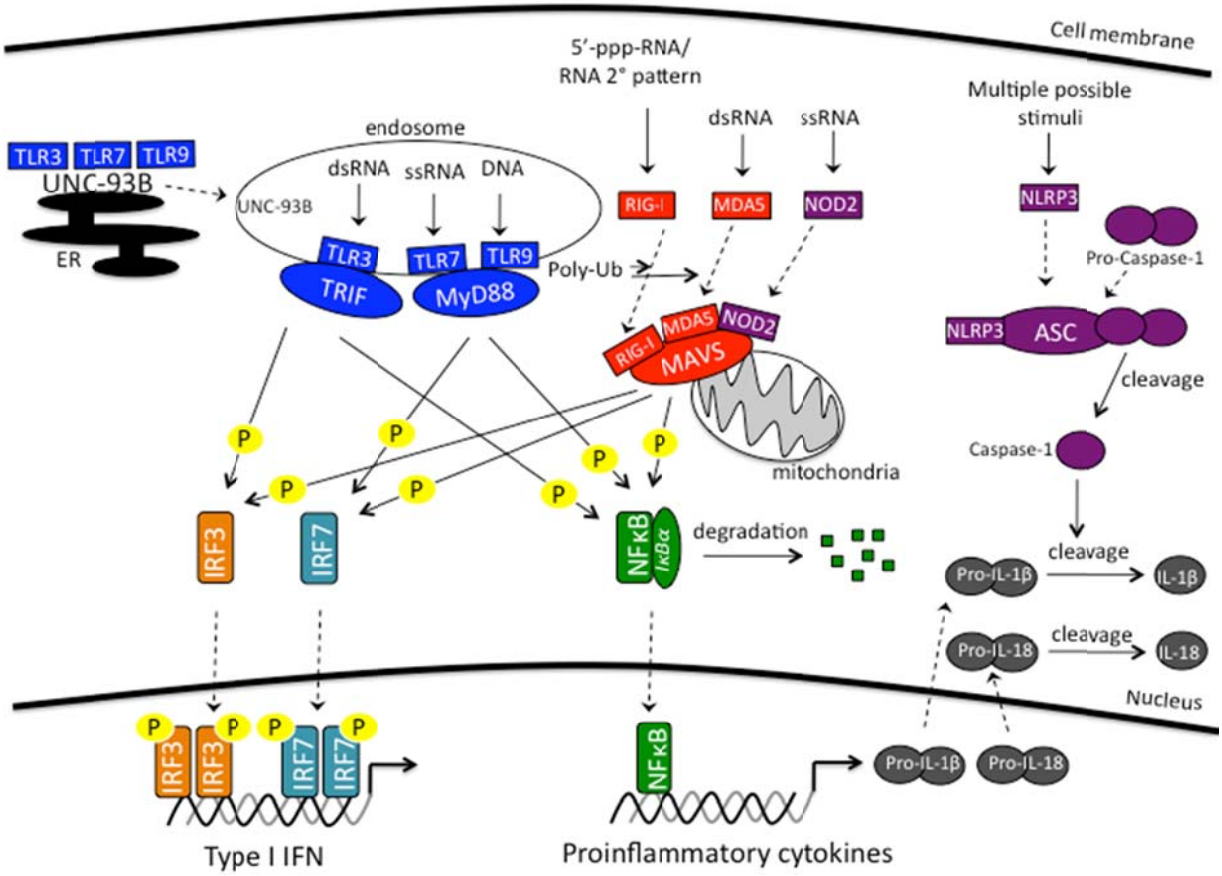

Figure 1.3. Pattern recognition and immune activation in viral infection
Viruses can activate both endosomal and cytosolic immune signaling cascades leading to TF activation and the transcription or activation of type I IFN and proinflammatory cytokines. At the endosome TLR3, TLR7, and TLR9 recognize dsRNA, ssRNA, and DNA, respectively and use the TRIF (TLR3) or MyD88 (TLR7, TLR9) adapter to activate TFs. TLR3 mediates type I IFN activation via phosphorylation of IRF3 while TLR7 and TLR9 do so by phosphorylating IRF7. All endosomal TLRs activate NFκB-mediated proinflammatory cytokine transcription through phosphorylation and degradation of the NFκB-bound IκBα anchor, allowing NFκB to translocate into the nucleus. The RLRs, RIG-I and MDA5, recognize 5'-ppp/secondary RNA structures or dsRNA, respectively and are further activated by poly-ubiquitination. Subsequent binding to the mitochondrial outer membrane-localized MAVS adaptor protein mediates TF activation. In viral infection, the NOD2 NLR is activated in response to ssRNA leading to MAVS-mediated IRF3 activation. NLRP3 activation with various PAMP or DAMP stimuli initiates the formation and activation of the inflammasome that is completed following binding with the ASC adaptor and pro-caspase-1. The formation of this multi-protein complex induces caspase-1 activation by cleavage. Caspase-1 then mediates pro-IL-1β and pro-IL-18 activation through cleavage, allowing functional cytokines to be released from the cell. Solid lines, unless otherwise indicated, delineate activation. Dashed lines symbolize trafficking. (P) phosphorylation, (poly-Ub) poly-ubiquitination. Blue: TLRs; Red: RLRs; Purple: NLRs. Figure adapted from:[28, 39, 40]

Innate immunity

Infection of epithelial cells, such as those in the lung or intestine, is often the first indication of a viral infection.[64, 65] This stimulates the production of proinflammatory cytokines including IL-1β, IL-6, tumour necrosis factor alpha (TNF-α), and type I IFN and an array of chemokines at the local infection site.[65] Localized inflammatory mediator production leads to the recruitment of innate immune cells including macrophages, DCs, pDCs, neutrophils, and innate lymphoid cells (ILCs) – a relatively new family of innate effector cells that includes natural killer (NK) cells.[62, 64, 66] Neutrophils, NK cells, and macrophages control the infection through the release of proinflammatory cytokines and cytotoxic molecules as well as phagocytosis and destruction of virally infected cells.[63, 67, 68] Non-NK cell ILCs contribute to innate immune activation through cytokine release following infection and can additionally activate mechanisms of host repair subsequent to tissue damage.[66] pDCs are specially designed cells that produce large quantities of type I IFN at the site of infection.[69, 70] While conventional (c)DCs can also contribute to the local production of proinflammatory mediators, their primary role is antigen presentation to naïve T cells.[70]

Adaptive immunity

The adaptive immune response begins when cDCs take up antigen at the site of infection.[70] Activated cDCs migrate via C-C chemokine receptor type (CCR)7-mediated signals to the local lymphoid tissue where naïve T cells are located.[63, 69] There are two types of T cells activated in the local lymphoid tissue; cluster of differentiation (CD)8^+ and $CD4^+$ T cells. The primary role of activated $CD8^+$ T cells is to migrate back to the site of infection and elicit an antigen-specific cytotoxic effect that destroys virally infected cells.[62, 63, 65] $CD4^+$ T cells are classically defined as helper cells in the adaptive immune response, controlling the activation of cytotoxic $CD8^+$ T cells and initiating B cell activation.[63, 69]

DC-mediated T cell activation in the lymphoid tissue requires three signals. The first is antigen presentation on the DC surface by a major histocompatibility complex (MHC) molecule. MHC class I presents antigen that entered the DC through direct cytosolic uptake, such as during viral infection, and activates $CD8^+$ T cells.[63] MHC class II presents antigen that entered

the DC via phagocytosis and stimulates $CD4^+$ T cell activation.[63] An exception to this division of labour is antigen cross-presentation in which antigen taken up through phagocytosis is presented via MHC class I to allow for $CD8^+$ T cell activation.[62, 69] The second signal required for T cell activation is costimulatory molecule expression, including CD80 or CD86 produced by DCs.[64, 69] The third signal, specific to $CD4^+$ T cells, involves the local expression of cytokines that dictates T cell differentiation into T helper (Th)1, Th2, Th17, or Treg lineages, each of which express a specific pattern of cytokines (Table 1.1):[63, 65]

Table 1.1. $CD4^+$ T cell differentiation

T cell subset	DC-derived differentiation signal	Cytokines expressed upon activation
Th1	IFN-γ, IL-12	TNF-α, IFN-γ, IL-10
Th2	IL-4, IL-5	IL-4, IL-5, IL-13
Th17	IL-6, TGF-β	IL-17, IL-22, TNF-α
Treg	TGF-β	TGF-β, IL-10, IL-35

In addition to the production of cytokines, activated $CD4^+$ T cells can amplify $CD8^+$ T cell activation by increasing the costimulatory capacity of antigen-presenting cells (APCs), a process mediated by increased IL-2 production from $CD4^+$ T cells.[63, 65, 69] Unlike Th1, Th2, and Th17 cells which activate the immune response, Tregs act to dampen immune activation by blocking proinflammatory cytokine expression and controlling T cell activation.[63, 65]

A humoral response, which complements the T cell-mediated cellular adaptive immune response, is activated through B cells and leads to the production of antigen-specific antibodies. B cell activation is mediated by $CD4^+$ T cells and, similar to naïve T cell activation, requires antigen presentation, costimulatory molecule expression, and the production of specific cytokines, which direct the subsequent antibody response.[64, 69] These antigen-specific antibodies assist the host in clearing the current infection and form an important component of the long term memory response.[64]

The general mechanisms of immune activation and patterning that are described above are seen in response to many viruses; however, the relative contribution of these components to host protection against a particular virus, discussed in greater detail in the subsequent sections, may vary. Owing to the specificity of host-virus interactions, infection-specific studies of innate and adaptive immunity are important.

IV. Influenza

Influenza infection is a prevalent cause of respiratory disease that is responsible for significant worldwide morbidity and mortality.[71] Different strains circulate globally and can cause mild or severe disease depending on the age of the infected individual, the immune competence of the host, and the infecting viral strain. According to the WHO, seasonal strains of influenza cause 250 000-500 000 deaths globally each year.[72] Seasonal influenza, though it causes a mild respiratory infection in healthy adults, can be severe in infants, the elderly and patients with a chronic disease or immunodeficiency.[71] Besides seasonal influenza, there remains the threat of a novel influenza strain rapidly evolving to infect humans and causing a pandemic. Pandemic influenza strains commonly originate in an animal reservoir and can cause severe disease in an immunologically naïve human population that has had no prior exposure to this novel strain.[73, 74] Since the beginning of the 20th century, there have been four major influenza pandemics occurring in 1918, 1957, 1968, and 2009.[74] The 1918 pandemic killed 20-50 million people globally, making it the most deadly.[75] During this pandemic, mortality occurred predominantly in individuals younger than 65 years of age, with nearly 50% of deaths reported in individuals 20-40 years of age.[71, 76] Mice infected with a 1918-like influenza strain, compared to less pathogenic strains, revealed dramatically increased inflammatory cell infiltration and a higher lung viral load suggesting a role for dysregulated immune activation and viral clearance in causing significant host pathology.[77] Increased mortality during the 1918 pandemic was also attributed to reduced host immune capacity to respond to a secondary bacterial infection caused by impaired lung bacterial clearance, TLR desensitization to additional pathogen exposure, and dysregulated immune activation following the preceding viral infection.[78-82] The H5N1 influenza strain is currently considered a likely cause of a future influenza pandemic, pending viral mutation to allow for efficient human-to-human transmission.[74, 83] Originating in birds, H5N1 was first reported in humans in 1997 with cases occurring in families that lived in close quarters or through direct transmission from birds.[74, 83] Its spread has resulted in 386 deaths globally since 2003 with a mortality rate of ~60%, caused predominantly by acute respiratory distress syndrome (ARDS).[74, 84]

The virus

Influenza is a negative-sense ssRNA virus and is a member of the *Orthomyxoviridae* family.[71, 73, 74] It is divided into three types; influenza A, B, and C. Influenza type A has a broad host range including birds, humans, pigs, and horses and has been implicated in both seasonal and pandemic infections.[71] Influenza type B and C viruses mostly infect humans, and, due to this limited host range, are unlikely to cause a pandemic.[71]

The influenza virus has a segmented genome that, in influenza type A and B viruses consists of eight RNA segments while type C consists of seven.[71, 73, 74] Each RNA segment is surrounded by a nucleoprotein and a protein coat envelops the entire virus.[73] The nomenclature to differentiate influenza strains describes the virus type (A, B, or C), the geographic location of viral isolation, the viral strain number and the year of isolation, each separated by a slash and followed by the strain-specific hemagglutinin and neuraminidase protein subtype in brackets.[71] An example of this is the commonly used mouse-adapted influenza strain A/PR/8/34 (H1N1), originally isolated in Puerto Rico in 1934.

The evolution of new influenza viral strains can occur in two ways:

1. Antigenic drift: The lack of a proofreading mechanism during influenza viral replication causes a high mutation rate. Over time, pressure from the host immune response allows these mutations to accumulate, changing the viral genome and protein structure.[73, 85] This leads to the gradual evolution of a new influenza strain that can no longer be recognized by the host immune response, even if the individual was previously infected with the parent strain.[73, 85, 86] This is seen in seasonal influenza strains and is why the influenza vaccine must be reformulated on a yearly basis.[85, 86]
2. Antigenic shift: Rapid viral evolution caused by the exchange of entire RNA segments that code for functional proteins between unrelated viral strains to form a completely novel strain.[85] The segmented genome of the influenza virus allows for this rapid evolution.[73, 74] The genetic material from two influenza strains can mix when both strains infect the same host, a process that occurred in pigs during the 2009 H1N1 outbreak.[74]

Viral mechanisms of entry and immune evasion

Influenza viral proteins control replication and viral packaging, allow for entry and exit from the host cell, and mediate viral evasion of the immune response. Key influenza viral proteins include:

1. Hemagglutinin (HA): A protein that protrudes from the viral protein coat and binds to host sialic acid-containing receptors on airway epithelial cells to allow for viral entry by endocytosis.[73, 87] There are 16 different HA subtypes currently identified.[71, 74, 86]
2. Neuraminidase (NA): An additional protein at the virus surface with 9 subtypes currently known.[71, 74, 86] Subsequent to viral replication and virion assembly, it mediates the release of nascent viral particles from the host cell through sialic acid residue cleavage.[74]
3. Matrix protein 2 (M2): Similar to the HA protein, the M2 protein is involved in host cell entry through the formation of an ion channel in the viral protein coat thereby facilitating uncoating of the virus.[73, 74]
4. Non-structural protein 1 (NS1): This protein uniquely mediates evasion and antagonization of the host immune response by inhibiting host type I IFN production[88, 89] or by binding TRIM25 to prevent poly-ubiquitination and activation of RIG-I.[90, 91]

Clinical features and diagnosis

The influenza virus is transmitted through close contact with an infected person or object.[92] Most infected patients present with fever, head and muscle ache, and respiratory problems while severe infection can lead to ARDS and death.[71, 87, 92]

As most symptoms of influenza infection are non-specific, a definitive diagnosis is dependent on the confirmation of viral presence. Currently available diagnostic procedures include viral culture, immunofluorescence, reverse transcription polymerase chain reaction (RT-PCR), and rapid diagnostic tests.[93] RT-PCR is presently the most optimal in terms of rapidity and sensitivity, although the facilities to conduct this test are not universally available.[92]

Treatment

The two classes of antiviral therapeutics that are currently available and used to treat influenza infection are NA inhibitors and M2 ion channel inhibitors.[87] While antiviral treatment should be started soon after infection to minimize virus-mediated damage, this timing is challenging to achieve from a clinical perspective as a result of the non-specific nature of initial infection symptoms.[87] Another challenge is that antiviral resistance is increasingly seen in circulating seasonal H3N2 and H1N1 influenza strains and was also observed in the 2009 pandemic H1N1 strain.[87, 94] While new antiviral drugs continue to be developed, their introduction and widespread use is likely to cause continued viral evolution and drug resistance.

An alternative therapeutic option for infected patients is immunomodulatory therapy, targeting the host instead of the virus.[87] These drugs can specifically up or downregulate key immune pathways or can cause general immunosuppression.[87] As immunomodulatory drugs act independently of the infecting virus, their use does not lead to drug resistance and the same drug may be effective at treating a broader range of influenza subtypes.[87]

Vaccines

An ideal influenza vaccine would protect the host against multiple virus strains and subtypes.[86] The high mutation rate and interstrain variation of the virus however makes this a challenge.[86] The two types of vaccine currently used are inactivated and live attenuated vaccines; with relatively high efficacy in adults and children respectively.[95, 96] These vaccines are trivalent, meaning that they are formulated with a cocktail of influenza A H3N2, influenza A H1N1, and influenza B strains.[92] Inactivated vaccines are grown in eggs, delivered through intramuscular injection, and cause an antibody-driven response to strain-specific viral proteins.[86, 95] Live attenuated vaccines are delivered intranasally and can induce an additional mucosal immune response, providing enhanced protection at the site of infection.[86, 95] Current research to produce novel vaccines is focused on targeting more highly conserved influenza genetic signatures or proteins and developing new methods for more rapid vaccine strain production in cell lines or with plasmids instead of in eggs.[86, 95]

Animal models

As influenza type A can infect many species, several animal models exist. Large animal models that develop similar clinical and histopathological features to humans include non-human primates and pigs.[71, 74, 97] These models are not frequently used however due to issues with cost, housing, and a lack of widely available research tools.[97] Ferrets are another model of influenza infection that also present with clinical and histopathological changes similar to humans and, along with pigs, are capable of transmitting the virus to other animals in close proximity.[71, 74, 97] As both pigs and ferrets can be naturally infected with the influenza virus, an issue with the use of these models is ensuring that uninfected animals are obtained prior to experimentation.[97]

Due to these constraints, the mouse is the most frequently used model of influenza infection. Though the influenza virus does not naturally infect mice, human strains can be adapted by serial passage to be virulent in mice.[71, 98] Though mice lack outward clinical features of human influenza infection such as fever or the production of respiratory secretions, they display many features of lung tissue damage and immune activation that are similar to humans[71, 74, 97] making them a valuable tool with which to study the immune response to influenza infection.

Immune recognition of the influenza virus

Endosomal TLR signaling

The expression of TLR3, TLR7, TLR8, and TLR9 is upregulated following influenza infection.[31, 99-101] TLR3 and TLR7, owing to their established role in RNA viral recognition,[30, 31, 101] are the most widely studied.

TLR3 expression in human bronchial and alveolar epithelial cells is significantly upregulated following *in vitro* stimulation with influenza virus leading to increased proinflammatory cytokine expression.[102] Activation of TLR3 at the primary site of influenza infection suggests that it plays a role in the early control of viral replication. Indeed, the loss of TLR3 *in vivo* delayed lung viral clearance and led to dampened early expression of airway inflammatory mediators and a lower frequency of airway macrophages and $CD8^+$ T cells

following infection with an influenza A H3N2 strain.[99] Somewhat surprisingly, these TLR3-deficient mice had a dose-dependent decrease in mortality compared to C57BL/6 mice that was accompanied by reduced lung pathology.[99] This suggests that TLR3 activation leads to excessive inflammation and immune-mediated pathology.[99] In contrast to this, a protective role for TLR3 has been proposed in a small study of patients with influenza-associated encephalopathy.[103] One patient had a missense mutation in *TLR3* leading to dampened NFκB activation and IFN-β expression, thereby implicating TLR3-mediated immune signaling in host protection against infection-related sequelae.[103] The TRIF adaptor is not essential for influenza infection survival, a surprising result considering the above findings on TLR3.[104] Further studies specifically examining the role of either TLR3 or TRIF in the adaptive immune response to influenza infection have demonstrated a non-essential role for this immune pathway in both $CD4^+$ and $CD8^+$ T cell activation as well as formation of a humoral response.[105] Therefore, the above studies suggest that TLR3 is primarily involved in activating the innate immune response at the site of infection. While this can contribute to viral clearance it may also cause immune-mediated pathology. Despite a widely accepted role for TLR3 in immune upregulation, the influenza-specific PAMP it recognizes is unclear. Though the acknowledged stimulus of TLR3 is dsRNA,[30] *in vitro* studies have been unable to detect dsRNA during influenza infection.[47, 106] This may be because very small quantities of dsRNA can upregulate an antiviral response or the formation of dsRNA as a replicative intermediate is transient during viral replication, making it challenging to detect.[106]

It is well established that TLR7 recognizes ssRNA following influenza infection and can activate a potent type I IFN response in pDCs.[31, 101] Further studies of TLR7 and its adaptor MyD88 in the immune response following influenza infection however have yielded conflicting findings. Several groups, following infection with both influenza A H1N1 and influenza A H3N2 strains, demonstrated that the loss of MyD88 does not increase mortality compared to wild type mice, suggesting that this immune pathway is non-essential for infection recovery.[99, 107] In a separate study, increased susceptibility, lung tissue damage, and airway wall thickening was observed in MyD88-deficient mice infected with influenza A H1N1.[104] Increased mortality and

pathology in these mice was attributed to dampened immune activation, as decreased immune cell infiltration and IL-6, TNF-α, and IFN-γ expression was observed in the airway.[104]

In the adaptive immune response to influenza infection, several studies have revealed that the production of IFN-γ^+CD8^+ T cells can occur independently of TLR7-MyD88-mediated immune activation.[104, 105, 108, 109] While a study of MyD88-deficiency implicated this adaptor in $CD4^+$ T cell proliferation and IFN-γ production,[108] it is unclear if this is directly attributable to immune activation through TLR7 or if immune signaling through the IL-1 receptor (IL-1R), the receptor for IL-1α/β that also signals through the MyD88 adaptor, is playing a role.[110] Further analysis of TLR7-deficient mice revealed that activation of this PRR was not required for the production of IFN-γ^+CD4^+ T cells, however this same study was also unable to implicate MyD88 in this response.[105] Studies of the humoral response have revealed that the loss of MyD88 affects antibody isotype switching by decreasing serum expression of IgG2a and IgG2c following infection.[105, 108] Further, analysis of TLR7- and MyD88-deficient mice following infection with an inactivated influenza virus and subsequent lethal infection led to decreased total IgG and IgG2a in the serum and increased mortality in both mouse models.[108] This suggests that vaccination was ineffective in mice missing either TLR7 or MyD88[108] and supports a role for TLR7-MyD88-mediated immune activation in patterning the memory response to influenza. This is in direct opposition to a study of MyD88/TRIF-double deficient mice that observed no defect in the ability of the double deficient host to mount an immune response to a secondary lethal dose of virus following a primary low dose infection.[104] Conflicting reports in the literature may be due to differences in the viral strain or dose used for infection and vaccination as well as the distinct knockout models studied.[104, 105]

Cytosolic PRR signaling – RIG-I

RIG-I signaling can activate both a proinflammatory and type I IFN response following influenza infection.[111] As RIG-I-deficiency causes severe liver damage and is often embryonic lethal, *in vivo* infection studies with these mice are a challenge.[41] Most research is therefore conducted in MAVS-deficient mice as this adaptor is activated by RIG-I but not MDA5 following influenza infection.[55] Studies in MAVS-deficient mice have revealed that immune activation

through this pathway is neither required for infection survival nor for the development of the cellular or humoral arms of the adaptive immune response following influenza infection.[104, 108] The ability of the RIG-I-MAVS-mediated immune pathway to activate type I IFN in diverse cell types such as respiratory epithelial cells, compared to the specialization of TLR7-MyD88-mediated activation of type I IFN in pDCs, suggests that the former is important in the innate immune response to influenza infection.[111] Other PRRs and immune mechanisms that activate type I IFN production however, can compensate for the loss of RIG-I-MAVS-mediated signaling in the whole lung.[108] Indeed, only the combined loss of MAVS and MyD88 significantly decreased lung type I IFN expression and elevated lung viral titer 24 hours post-infection.[108] Though there is a lack of evidence indicating an essential role for the RIG-I-MAVS pathway in influenza infection survival, augmented RIG-I activation with a 5`-triphosphate agonist prior to infection significantly decreased lung viral load and provided protection against influenza-induced mortality,[112] suggesting that this pathway does indeed contribute to host protection and can improve infection outcome when activated, making it a potentially favourable target for immunomodulatory therapy.

Cytosolic PRR signaling – NLRP3

NLRP3 activation and inflammasome formation in influenza infection is elicited by the M2 viral protein[113] and has been specifically shown to occur in macrophages, dendritic cells and respiratory epithelial cells.[107, 114, 115] *In vivo*, the loss of NLRP3, the ASC adaptor, or caspase-1 decreased airway expression of IL-1β and IL-18, and delayed viral clearance beginning at day 7 post-infection.[107, 114, 116] In addition, both NLRP3- and caspase-1-deficient mice had significantly increased collagen deposition, a marker of tissue fibrosis, compared to wild type mice and increased mortality was observed following influenza infection in NLRP3-, ASC-, and caspase-1-deficient mice.[107, 116] These findings suggest that the inflammasome plays a non-redundant role in host protection following influenza infection that may be mediated through the activation of IL-1β and IL-18.

A further demonstration of a protective role for IL-1β and IL-18 can be seen in IL-1R-deficient mice following influenza infection.[117] IL-1R deficiency increased mortality and lung

viral load despite causing a decrease in lung cell recruitment and tissue damage.[117] This suggests that, while activation of this pathway may cause immune-mediated damage, its ability to activate viral clearance mechanisms is essential for host survival. In the adaptive immune response, IL-1R has specifically been demonstrated to be essential for activation of antigen-specific $CD8^+$ T cells following influenza infection with no requirement for TLR7 and MAVS in this process.[118]

Conflict on PRR significance

Many of the studies described above present dissimilar conclusions as to the relative role of the PRRs and adaptors activated in the immune response to influenza infection. Experimental variables including virus strain and dose, mouse genetic background and time points of analysis have all been implicated in interstudy variability.[99, 104, 105, 107, 114, 116] Indeed, even studies using different infectious doses in the same host model can yield disparate conclusions. For example, high dose infection of TLR7/MAVS-double deficient mice significantly increased pulmonary viral load compared to wild type mice while low dose infection demonstrated significantly higher viral load in the wild type mice suggesting that, at low dose infection, TLR7- and MAVS-mediated mechanisms of immune activation can augment viral replication in the host.[119] While there was ultimately no difference in infection survival between TLR7/MAVS-double deficient and wild type mice at either infectious dose,[119] these findings demonstrate the model-dependent variability that can exist between studies.

Immune mechanisms of protection and pathogenesis

The influenza virus primarily infects epithelial cells that line the respiratory tract, leading to rapid activation and recruitment of local and blood-derived macrophages and DCs.[64] Further activation and recruitment of innate neutrophils and NK cells as well as adaptive T and B cells leads to infection resolution.[120] The expression of proinflammatory cytokines and chemokines over the course of an influenza infection in both the lung and airway orchestrates this immune cell migration and contributes to antiviral processes.[64] These mediators include the proinflammatory cytokines: IL-1β, IL-6, IFN-γ, type I IFN, TNF-α, and chemokines: chemokine (C-

X-C motif) ligand (CXCL)1, CXCL2, CXCL10, chemokine (C-C motif) ligand (CCL)2, CCL3, CCL4, and CCL5.[85, 121, 122]

Macrophages

Two types of macrophages have been described in influenza infection. Alveolar macrophages (AMs) reside in the respiratory tract and are one of the first cells exposed to the influenza virus.[123] In resting conditions AMs are involved in maintaining airway homeostasis while respiratory infection upregulates AM-mediated mechanisms of phagocytosis.[69, 123]

Exudate macrophages (ExMs) derive from $CCR2^+$ monocytes that are recruited from the bloodstream to the airway by epithelial cell-mediated expression of CCL2 following infection.[124] ExMs are distinct from AMs because they can express costimulatory molecules CD80 and CD86 similar to DCs but, unlike DCs, can only activate memory antigen-specific T cells and not naïve T cells.[124] Key proteins produced by ExMs following influenza infection include nitric oxide synthase 2 (NOS2) and TNF-α.[124] Depletion of either of these mediators significantly decreased mortality following influenza infection, suggesting that ExM activation may contribute to pathology.[125, 126] Studies in CCR2-deficient mice demonstrated increased survival following influenza infection with minimal to no impact on viral clearance, suggesting a non-essential, and even pathogenic, role for $CCR2^+$ cells in mediating infection outcome.[124, 127, 128] One study correlated improved host protection in CCR2-deficient mice with decreased expression of NOS2[124] while another attributed protection to reduced expression of TNF-related apoptosis-inducing ligand (TRAIL) from ExMs.[128] A specific pathogenic role for TRAIL, a mediator of epithelial cell apoptosis, was further demonstrated in studies with a TRAIL-blocking antibody.[128] This led to diminished alveolar epithelial cell apoptosis and improved survival following intravenous influenza infection.[128] These studies suggest that $CCR2^+$ cells, and perhaps excessive ExM recruitment and cytokine production, may contribute to host pathology following influenza infection. Conversely, an additional study demonstrated that blocking airway infiltration of $CCR2^+$ cells using a CCL2-specific antibody instead increased epithelial apoptosis following influenza infection though, similar to other studies,[124] this did not affect lung viral clearance.[129] This suggests a protective role for CCL2 signaling in influenza infection,

which the authors attributed to macrophage recruitment to the site of infection.[129] As the $CCR2^+$ cells that are recruited from the bloodstream by CCL2 expression during infection include both ExMs and monocyte-derived DCs, further studies that specifically deplete ExMs in the host will better clarify their specific role in host protection and pathogenesis following influenza infection.

Dendritic cells

DCs are involved in mediating antiviral mechanisms,[69] producing chemokines to recruit immune cells,[130] and activating naïve T cells in the lymph node (LN).[131] Both pDCs and distinct subsets of resident and recruited cDCs are activated in the lung following influenza infection. cDCs can be classified as either $CD103^+CD11b^{lo}$ DCs ($CD103^+$ DCs) that reside in the mucosal space adjacent to airway epithelial cells or $CD103^-CD11b^{hi}$ DCs ($CD11b^{hi}$ DCs) that are present in the lung parenchyma or recruited to the airway from the bloodstream as $CCR2^+$ monocytes following infection.[124, 132, 133]

There is some evidence in the literature that $CD11b^{hi}$ DCs are the dominant APC population involved in antigen presentation in the LN.[131, 134] A direct interaction between $CD11b^{hi}$ DCs and $CD8^+$ T cells in the LN was observed in one study following infection, however this group did not study $CD103^+$ DCs in comparison.[131] A further study, which did contrast $CD103^+$ and $CD11b^{hi}$ DCs, found an early role for both cDC subsets in $CD8^+$ T cell activation but a predominant role for the $CD11b^+$ population as the infection progressed, a finding which they attributed to continual recruitment of these DCs from the lungs.[134] Indeed, studies have shown that $CD11b^+$ but not $CD103^+$ DC recruitment to the lungs is increased early after influenza infection,[135, 136] which may allow for prolonged recruitment of these cells to the LN. Conversely another study found that, while the peak of $CD103^+$ recruitment to the LN occurred earlier than the peak of $CD11b^{hi}$ DC recruitment, $CD103^+$ and not $CD11b^+$ DCs are the dominant $CD8^+$ T cell activating APCs; though both subsets were capable of activating $CD4^+$ T cells.[137] This is in agreement with several other studies that demonstrated that $CD103^+$ DCs are the primary APC for $CD8^+$ T cell activation.[135, 138] One study showed that $CD11b^+$ DCs, despite a poor antigen presenting capacity, could carry influenza antigen to the LN and suggested that the role of

recruited $CD11b^+$ DCs may be to provide antigen to the $CD11b^-CD8\alpha^+$ LN-resident DCs which can subsequently activate naïve $CD8^+$ T cells, implicating $CD11b^+$ cells in indirect antigen presentation and activation of $CD8^+$ T cells.[135, 139] This is still to be validated however as others have reported that $CD11b^+$ cells do not migrate to the LN following infection, implicating them instead in TNF-α production and continued activation of the proinflammatory state at the site of infection.[138] Controversy regarding which DC subset is responsible for antigen presentation following influenza infection may be based on differences in the viral and host model used or may be attributable to differences in flow cytometry gating strategies when differentiating cDCs as these subsets can be challenging to define.[138]

Compared to cDCs, the role of pDCs following influenza infection is more clearly defined. As major type I IFN producers, pDCs have a strong antiviral capacity but cannot effectively present antigen to $CD4^+$ or $CD8^+$ T cells.[69, 137, 140] pDCs are not essential for host recovery from an influenza infection as pDC-depleted mice had normal survival, lung viral clearance, and antigen-specific $CD8^+$ T cell activation following infection.[135, 140] These mice however had an early delay in airway T cell recruitment suggesting a non-essential contribution of pDCs in the adaptive immune response to influenza infection.[140] Further work supporting their role in adaptive immunity demonstrated a contribution for pDCs in antibody formation as part of the humoral response.[135]

T cells

The timing of T cell activation in the LN and subsequent lung recruitment during infection is partially dependent on the infecting influenza strain, which can dictate the rate of DC recruitment to the LN and therefore the subsequent timing of T cell activation.[141] Typically, an activated $CD4^+$ or $CD8^+$ T cell that is recruited to the influenza-infected lung is classified as $CD62L^{lo}$, $CCR7^{lo}$, $CD44^{hi}$, $CD69^{hi}$, and $CD49d^{hi}$ with each marker providing a distinct contribution to the state of cell activation.[142, 143] CD69 expression is correlated with exposure to antigen.[142] Its expression is immediately upregulated during naïve T cell activation in the LN followed by a subsequent decrease in expression as T cells proliferate in the LN and are no longer in contact with antigen.[142] Once activated, T cells interact with antigen-carrying infected cells in the lungs

and CD69 expression is upregulated once more.[142] CD44 is also a marker of activated T cells, allowing T cell adhesion to the tissue at the site of infection as well as promoting T cell survival though, unlike CD69, its expression following activation is not dictated by antigen interaction.[144, 145] CD62L, CCR7, and CD49d are determinants of T cell location. CD62L and CCR7 expression localizes T cells to the LN and therefore expression must be downregulated for activated T cells to migrate to the site of infection.[143, 146] CD49d upregulation is only seen on activated T cells at the site of infection and its expression is required for homing to the lungs.[143]

Interestingly, while T cell activation following influenza infection is typically thought to occur exclusively in the LN,[131] recent studies suggest that DCs continue to activate antigen-specific $CD8^+$ T cells at the site of infection.[147, 148] This was elegantly shown with the depletion of DCs at the site of infection following initial DC recruitment to the LN during influenza infection.[147, 148] Naïve T cell priming in the LN was normal in these mice however DC depletion at the site of infection increased mortality and lung viral titer and led to significantly fewer influenza-specific lung $CD8^+$ T cells compared to wild type mice.[147, 148] These studies suggest that $CD8^+$ T cells are not fully differentiated when they exit the LN and only elicit an optimal antiviral response through continued DC-mediated activation at the site of infection.[147-149]

Classically $CD4^+$ T cells act as helpers for B cell activation in the LN and contribute to cytokine production at the site of infection while $CD8^+$ effector T cells destroy virally-infected cells at the site of infection through the release of cytotoxic molecules or apoptosis.[69, 150] In influenza infection however, these cell types have been shown to play additional roles. $CD4^+$ T cells have been demonstrated to have a cytolytic role, with adoptive transfer of Th1 $CD4^+$ T cells increasing host protection following lethal influenza infection.[151, 152] $CD8^+$ T cells, in addition to their cytolytic actions, can play an immunoregulatory role through production of the anti-inflammatory cytokine IL-10.[153] Unlike proinflammatory IFN-γ expression from $CD8^+$ T cells, which is detectable in both the LN and lung,[142] IL-10 is predominantly produced by $CD8^+$ T cells in the lung,[153] suggesting that continued $CD8^+$ T cell activation in the lung during the infection is required to upregulate this response.[154] Antibody-dependent depletion of IL-10 increased immune-mediated damage and mortality following influenza infection, demonstrating an important role for this cytokine in inflammation control and host protection.[153]

V. Coxsackievirus-induced myocarditis

Myocarditis, or inflammation-induced cardiac necrosis and remodeling, is an important global health problem with limited diagnostic and treatment options.[155, 156] It has been estimated to cause 4-20% of acute cardiac deaths in young and otherwise healthy individuals.[156-158] The majority of myocarditis cases are diagnosed in individuals less than 40 years of age with declining incidence in older cohorts.[156] Other host factors such as nutritional status, pregnancy, and sex can also impact host susceptibility to infection and myocarditis severity.[156]

A variety of pathogens can cause myocarditis in humans. *Trypanosoma cruzi* (*T. cruzi*) is the primary causative agent in Central and South America while viruses are implicated in the majority of cases in North America and much of Europe.[156, 159, 160] Viruses that can cause myocarditis include influenza, human immunodeficiency virus, cytomegalovirus, adenoviruses, coxsackieviruses, and hepatitis C virus.[159, 161] Coxsackieviruses are the most common etiological agent with the coxsackievirus group B type 3 (CVB3) strain implicated most frequently.[155, 162] The majority of CVB3 infections are asymptomatic and can be easily cleared with no obvious sequelae while other infections cause a mild self-resolving febrile or gastrointestinal illness.[156] More severe CVB3 infections can cause myocarditis, pancreatitis, or aseptic meningitis.[156] CVB3-induced myocarditis can result in three possible outcomes:[156, 163, 164]

1. Limited cardiac inflammation and tissue damage with host recovery around two weeks after infection.
2. Severe and rapid tissue damage resulting in death during an acute infection.
3. Dilated cardiomyopathy (DCM) characterized by chronic inflammation and structural changes to the extracellular matrix (ECM).

Cardiac damage during viral myocarditis can occur through both viral- and immune-mediated mechanisms. The outcome of CVB3 infection in the host is dictated by the degree and timing of tissue damage, the extent of virus persistence, and the subsequent cardiac tissue repair processes.[156] Compared to most other tissues, cardiac inflammation is particularly harmful as cardiomyocytes cannot regenerate and host-mediated attempts to repair cardiac tissue

damage, such as increased collagen expression, lead to extensive fibrosis, cardiac architecture disruption, and reduced cardiac function.[164]

The virus

CVB3 is one of six serotypes of coxsackievirus group B and is a positive-sense ssRNA enterovirus of the *Picornaviridae* family.[155, 156, 164] It is a ubiquitous, non-enveloped virus that is transmitted to humans via the fecal-oral route and primarily infects the spleen, liver, pancreas, and heart following transport through the bloodstream.[155, 156]

Viral mechanisms of entry and immune evasion

To infect host cells, the CVB3 virus utilizes two host receptors. The decay-accelerating factor (DAF) receptor mediates viral binding to the host cell membrane and localization to endothelial tight junctions where the virus can then bind the coxsackievirus-adenovirus receptor (CAR) to permit viral entry through receptor-mediated endocytosis.[156, 165] CAR expression is important for viral infection as cardiac depletion of CAR expression blocks CVB3 infection in the heart and results in an absence of cardiac inflammation and tissue necrosis.[166] Once inside the host cell, the CVB3 virus replicates its ~7400 nucleotide viral transcript that is then packaged, along with newly formed structural proteins, viral proteases, and polymerases, into a viral capsid and cytolytically released from the cell.[155, 156, 164] Cell lysis during viral replication is a mechanism through which virus-mediated tissue damage occurs in CVB3 infection.[167] Another mechanism of virus-mediated pathology is orchestrated by the protease 2A protein that can damage cardiomyocytes by cleaving dystrophin, a protein involved in cardiac muscle stability.[168] To evade immune-mediated degradation, viral proteases 2B, 2BC, and 3A can cause MHC class I endocytosis, allowing the virus to evade the $CD8^+$ T cell response and normal destruction of infected cells.[169, 170] In addition, the CVB3 $3C_{pro}$ cysteine protease provides viral protection by inducing cleavage of the MAVS and TRIF adaptors to dampen immune activation and allow for virus persistence.[171]

Diagnosis

The current gold standard for diagnosing myocarditis involves classifying patient endomyocardial biopsies using the Dallas criteria; a system which grades the degree of inflammation and the presence or absence of tissue damage and repair. [156, 172] Though widely used, there are several limitations associated with this technique. Acquiring an endomyocardial sample for analysis requires the patient to undergo an unpleasant and invasive procedure while subsequent scoring of the tissue sample is not an easy or sensitive procedure.[156, 158, 173] In addition, it can be a challenge to determine if the cause of myocarditis was infectious because, while molecular identification of the CVB3 virus in heart tissue is possible, the infection may have been cleared by the time the disease is diagnosed.[174, 175] The ideal tool for diagnosing myocarditis would be a non-invasive marker that not only determined if there was an infectious cause of disease but also predicted disease progression and severity. To date, a marker that is this sensitive and specific does not exist.

Treatment

As both the virus and the immune response can cause cardiac tissue destruction following CVB3 infection, it is unclear what the most effective treatment should target. Current treatment options for patients with CVB3-induced myocarditis are limited. Treatment of an acute infection is supportive and symptom-driven while the progression to DCM often requires a heart transplant;[176] neither of which address the underlying viral- and immune-mediated pathological mechanisms of disease.

Several clinical studies have examined the effectiveness of general immunosuppressants in reducing immune-mediated pathology following CVB3 infection. These studies however revealed disappointing results in patients with myocarditis as heart function and patient survival were not increased over a 24-week treatment period compared to patients given normal therapy.[177, 178] Though general immunosuppression was not effective, a refined approach to immune modulation has shown promise. Studies in both mouse models and patient populations have demonstrated that IFN-β treatment can improve CVB3 infection outcome, abrogating both excessive viral load and inflammation. In susceptible Balb/c mice,

IFN-β treatment decreased viral load, inflammatory cell recruitment, and cardiomyocyte injury leading to improved survival during acute myocarditis.[179] The exogenous addition of IFN-α also provided some protection but nearly double the dose was required to produce the same outcome, suggesting that IFN-β may be more relevant clinically.[179] In a small nonrandomized clinical trial of CVB3-infected patients with unresolving DCM, IFN-β therapy improved heart function and reduced both inflammation and persistent cardiac viral load over 24 weeks.[176] Despite some side effects associated with IFN-β treatment that can range from flu-like symptoms to depression,[180] it is currently the most favourable therapeutic option for the treatment of viral myocarditis though further clinical trials are required.

Animal models

CVB3 infection of murine cardiomyocytes demonstrated that, similar to human infection, the virus enters mouse cells through CAR-mediated endocytosis and infected mice follow a similar disease course to human infection.[156, 162, 181, 182] Resistant strains, including C57BL/6, 129/S1, and DBA/1J mice, have a self-limiting infection with minimal mortality while susceptible strains, including A.BY/SnJ, SWR/J, and Balb/c mice, first develop an acute infection that is followed by chronic disease by day 28 post-infection.[156, 158, 183]

To effectively study both acute and chronic myocarditis as well as delineate virus- and immune-mediated pathological mechanisms, three models are used in mice:

1. Acute viral infection: Mice are infected with the CVB3 virus and studies are conducted during an acute 7-28 day period at the end of which mice either recover from or succumb to infection.[184, 185]
2. Experimental autoimmune myocarditis: This model studies immune-mediated pathology in the absence of viral infection by injecting adjuvant and cardiac myosin protein into the host to activate immune signaling in response to host-derived antigen.[186]
3. Infection-induced autoimmune myocarditis: This is a hybrid model of the above two strategies and is used to model virus-induced chronic DCM. Mice are infected with a heart-passaged strain of CVB3 that is extracted from a previously infected mouse and

contains a cocktail of heart proteins and infectious virus. This induces both viral- and immune-mediated pathology following infection.[187]

Immune recognition of the CVB3 virus

Endosomal TLR signaling

While uninfected human cardiac tissue and cells have basal expression of all TLRs,[188] CVB3 infection predominantly activates endosomal TLRs.[188-190] In human cardiac cells, virus infection increased the expression of TLR7 and TLR8, along with MyD88, at the endosome.[188] Blocking TLR7 or TLR8 expression reduced IL-6, TNF-α, and IFN-β production, further implicating these PRRs in immune activation following CVB3 infection.[188] *In vivo* studies on the role of TLR7 in CVB3 infection however have not been conducted to date.

TLR9, though classically a PRR for DNA recognition, is also upregulated in the heart during acute CVB3-induced myocarditis.[190] Following infection, TLR9-deficient mice had reduced tissue inflammation and repair compared to wild type mice.[190] This was accompanied by decreased cardiac recruitment of $CD4^+$, $CD8^+$, and $CD11b^+$-positive cells and an altered pattern of cytokine expression that included decreased TNF-α but increased IFN-β.[190] As there was no difference in cardiac viral load between wild type and TLR9-deficient mice, this study proposed that TLR9 signaling is non-essential for viral clearance but may contribute to immune-mediated pathology in acute CVB3-induced myocarditis.[190]

Similar to the studies conducted in TLR9-deficient mice, MyD88 deficiency decreased cardiac as well as pancreatic tissue pathology, accompanied by decreased cardiac expression of IL-1β, TNF-α, and IFN-γ but increased IFN-β at day 4 and 7 post-infection.[191] This led to improved survival and multi-organ viral clearance in MyD88-deficient mice.[191] As both TLR9 and MyD88 deficiency led to decreased cardiac tissue pathology without negatively impacting viral clearance, the loss of immune upregulation through this pathway may provide host protection through a selective increase in IFN-β but dampened expression of other proinflammatory mediators and cells.

Immune activation through TLR3 and its adaptor TRIF is also upregulated following CVB3 infection.[189, 192, 193] Unlike MyD88 deficiency however, TRIF deficiency in CVB3 infection

increased mortality, cardiac viral load, and tissue necrosis and repair at day 7 post-infection.[193] Though this study analyzed survival over a chronic 80-day infection, >60% of the mortality occurred before day 28 in the acute phase of infection,[193] indicating an early role for TRIF in immune-mediated protection following infection. TRIF-deficient mice had increased recruitment of activated T cells, B cells, and macrophages and elevated IL-1β, IL-18, and TNF-α compared to wild type mice at day 7 post-infection,[193] suggesting that excessive immune activation may be contributing to worsened disease in this model and that TRIF activation may mediate immune control during CVB3 infection.

TLR3-deficient mice are also significantly more susceptible to acute CVB3 infection accompanied by increased serum viral load, cardiac inflammation, and fibrosis.[189] Unlike TRIF-deficient mice however, TLR3-deficient mice had decreased cardiac expression of proinflammatory cytokines, including IL-12p40, IFN-γ and IL-1β at day 3 and 6 post-infection with no change in cardiac IFN-β expression compared to wild type mice.[189] In TRIF-deficient mice a more dynamic change in IFN-β expression was observed with significantly less expression at day 3 post-infection but increased expression compared to wild type mice at day 7 post-infection, though the addition of IFN-β ultimately improved protection and viral clearance in TRIF-deficient mice.[193] In further support of a protective role for TLR3-mediated immune activation following CVB3 infection, a clinical study of more than 50 patients correlated viral myocarditis with an increase in *TLR3* polymorphisms.[192] Transgenic expression of these *TLR3* variants *in vitro* led to increased viral replication and decreased type I IFN expression,[192] illustrating the immune protection induced through this pathway.

Cytosolic PRR signaling

Both the MDA5 PRR and MAVS adaptor are required for survival of an acute CVB3 infection with the loss of either signaling mediator leading to increased hepatic and pancreatic damage,[194, 195] a finding that is distinct from the predominant cardiac damage seen in studies of TLR3- and TRIF-deficient mice. While the loss of MDA5 or MAVS did not affect IFN-β expression in the pancreas,[194, 195] MAVS-deficient mice had decreased serum IFN-β at day 2 post-infection.[195] *In vitro* studies support a role for MAVS in type I IFN expression following CVB3

infection as HeLa cells transfected with MAVS had less cell death along with reduced CVB3 RNA presence and increased expression of type I IFN compared to untransfected cells.[196]

To date no publications have determined a role for the NLRP3-dependent inflammasome in CVB3 infection. It is unclear if this is because these studies have yet to be conducted or if the CVB3 virus does not elicit inflammasome-dependant immune signaling during infection.

Immune mechanisms of protection and pathogenesis

Following CVB3 infection, NK cells and macrophages are the predominant innate immune cells that infiltrate the heart 4-5 days post-infection followed shortly thereafter by a significant T cell infiltration.[155] Though these cells can provide host-protective immune functions, dysregulated activation can also elicit immune-mediated pathology.

NK cells

NK cells are recruited to the heart through cardiomyocyte-derived CXCL10 expression and can both phagocytose virally infected cells and produce proinflammatory mediators.[155, 197] NK cell activation is correlated with a significant reduction in cardiac viral titer following CVB3 infection, suggesting that their recruitment and activation following CVB3 infection is important for infection resolution.[198, 199] Indeed, depletion of NK cells *in vivo* increased cardiac viral load as well as cardiomyocyte death and fibrosis in mice.[198, 199]

NK cell-mediated host protection following infection may be related to IFN-γ expression as co-culture of peripheral blood mononuclear cells (PBMCs) with CVB3-infected HeLa cells *in vitro* led to a significant increase in NK-cell derived IFN-γ production.[200] Further *in vivo* studies revealed that the specific depletion of IFN-γ significantly increased mortality, serum viral load, and liver damage following CVB3 infection.[189] In addition, vaccinating mice with a recombinant IFN-γ-expressing CVB3 strain provided significant host protection and control of multi-organ viral load during a subsequent lethal infection with wild type CVB3 virus.[201] Studies in IFN-γ receptor-deficient mice however could not define an important role for this receptor in mediating acute CVB3 infection outcome, suggesting that further studies are required.[202]

T cells

Similar to NK cells, T cells can lyse infected cells and upregulate cytokine production.[155] Unlike NK cells however, the T cell response is non-essential or even pathogenic following CVB3 infection.[185, 203] The specific depletion of $CD4^+$ T cells prolonged host survival despite increasing cardiac tissue damage and repair.[204] While this implicates $CD4^+$ T cell activation in a detrimental host response that contributes to increased mortality, it suggests that the remaining $CD8^+$ T cells also contributed to increased tissue pathology in this model. Indeed, $CD8^+$ T cell depletion in the $CD4^+$ T cell-deficient mice further improved host survival following infection, though it increased cardiac viral load.[204] Another study of $CD4^+CD8^+$ T cell-deficient mice also demonstrated improved host outcome compared to wild type mice.[205] This was accompanied by increased cardiac NK cell infiltration and IFN-γ expression, which may be a mechanism of host protection activated in the $CD4^+CD8^+$ T cell-deficient mice.[205] These studies demonstrate that T cell-mediated mechanisms of viral clearance may provide some benefit to the host however they can easily trigger mortality and immune-mediated tissue pathology, which may ultimately impact infection outcome in the host to a greater extent.

Proinflammatory mediators

TNF-α and IL-1β are proinflammatory cytokines that are activated throughout the acute phase of CVB3 infection[206, 207] and can contribute to pathogenesis. In B10.A mice, normally protected against myocarditis following CVB3 infection, injection with virus and IL-1β or TNF-α significantly increased cardiac inflammation compared to CVB3 infection alone, implicating these cytokines in immune-mediated tissue pathology.[208] In addition, blocking cardiac IL-1 signaling through an IL-1R antagonist significantly improved survival and decreased cardiac fibrosis, demonstrating a pathogenic and non-essential role of IL-1 in the immune response to CVB3 infection.[209] Evidence for cytokine-mediated pathology also exists in humans as elevated TNF-α has been observed in patients with acute heart failure or DCM, implicating TNF-α expression in host damage during both acute and chronic myocarditis.[210, 211]

The expression of type I IFN, similar to IFN-γ, is required for a positive outcome in acute CVB3-induced myocarditis. Type I IFNAR deficiency significantly increased the expression of serum alanine transaminase, a marker of liver injury, at day 3 post-infection and resulted in a dose-dependent increase in mortality compared to wild type mice.[202] The specific loss of IFN-β expression also increased mortality in acute CVB3 infection, which led to greater cardiac tissue damage and cell infiltration compared to wild type mice.[212] Interestingly, deficiency of either IFN-β or the type I IFNAR led to a non-statistically significant delay in cardiac viral load clearance by day 10 post-infection but significantly elevated hepatic viral load during the early phase of infection.[202, 212] These findings suggest that type I IFN signaling primarily mediates hepatic protection early in the infection while a protective role in cardiac viral clearance becomes evident as the infection progresses.

VI. Unc93b1

Unc93b1 is an 11-exon gene that codes for a 598 amino acid 12-transmembrane domain chaperone protein.[36, 213] Unc-93 was first described in *Caenorhabditis elegans (C. elegans)*, as a mediator of potassium ion transport with a role in muscle contraction and coordination.[214] The name 'Unc' derives from 'uncoordinated', an accurate description for *C. elegans* patterns of movement following Unc-93 mutation.[213, 214] In humans, *UNC93B1* is localized to chromosome 11q13 while in mice it is on chromosome 19.[36, 213] The expression of *UNC93B1* is fairly ubiquitous in humans but the highest expression is seen in the brain, heart, and kidney.[213] In addition to *Mus musculus* and *Homo sapiens, Unc93b1* homologs exist in other diverse organisms including *Arabidopsis thaliana*, *D. melanogaster*, and *Gallus gallus,* indicating that it is an evolutionarily conserved gene.[213] While *C. elegans* Unc-93 shares only 21% amino acid sequence homology with human *UNC93B1,*[213] mouse *Unc93b1* and human *UNC93B1* share greater than 90% amino acid sequence homology,[34] indicating that functional studies in mice may be applicable to humans.

Unc93b1 and endosomal TLR transport

The role of mammalian *Unc93b1* was discovered following an ENU-mutagenesis screen for a recessive defect in TLR signaling.[36] Primary macrophages were stimulated with specific agonists for TLR2, TLR3, TLR4, TLR7, and TLR9 and analyzed for TNF-α expression.[36] A mutant was discovered that lacked immune upregulation via TLR3, TLR7, and TLR9 but maintained normal TNF-α expression following TLR2- and TLR4-specific activation.[36] This mutant was termed *3d* for 'triple defect'.[36] Genetic mapping localized the ENU-induced mutation to the *Unc93b1* gene and confirmed its location by rescuing TNF-α expression in *Unc93b1*$^{3d/3d}$ bone marrow DCs by transfection of wild type *Unc93b1* complementary DNA (cDNA).[36] The *3d* mutation caused a bp transversion that led to a single amino acid substitution (H412R) in the 9th transmembrane-spanning domain of UNC93B1 (Figure 1.4).[36] Further analysis of this loss-of-function mutant revealed that it trafficks endosomal TLR3, TLR7, and TLR9, normally residing at the ER, to the endosome to allow for immune activation through these pathways. Interestingly, no role for *Unc93b1* in muscle coordination or movement has been observed in mice or humans, demonstrating an evolutionary divergence in function from *C. elegans.*[36] The chaperone function of UNC93B1 occurs following direct binding to the transmembrane domain of TLR3, TLR7, and TLR9.[34] The role of UNC93B1 in immune activation however is indirect as it is not required to recognize antigen, stimulate the recruitment of the MyD88 or TRIF adaptors molecules, or activate TFs following TLR activation.[35]

Unc93b1 and infection

Unc93b1-mediated immune signaling was first associated with protection following infection with mouse cytomegalovirus (MCMV), a DNA virus of the *Herpesviridae* family.[36] Following infection, *Unc93b1*$^{3d/3d}$ mice had significantly increased mortality that was accompanied by elevated spleen viral load and significantly diminished plasma IFN-γ, IL-12, TNF-α, and type I IFN expression.[36] A subsequent paper demonstrated that the loss of *Unc93b1* in MCMV infection caused a transient increase in liver damage and inflammatory cell infiltration, a finding that correlated with sustained hepatic viral load.[215]

Another DNA viral infection in which *Unc93b1* has been studied is herpes simplex virus (HSV) infection. Rare cases of human HSV infection can lead to herpes simplex encephalitis (HSE), a severe infection-induced sequela. In a mouse model of HSE, though the loss of *Unc93b1* caused a moderate but significant increase in mortality, this could not be linked to a specific viral- or immune-mediated mechanism suggesting that *Unc93b1* is not a major contributor to susceptibility or protection following HSE infection in mice.[216] Interestingly, this manuscript demonstrated that TLR2 expression played a major role in increasing mortality following HSV infection as TLR2-deficient mice had improved survival and significantly reduced cytokine production.[216] Despite this finding, *UNC93B1*-mediated protection against HSE has been observed in humans.[217] A study of pediatric patients with HSE revealed two children from consanguineous families with unique recessive mutations in *UNC93B1.*[217] *In vitro* stimulation of patient PBMCs or fibroblasts with HSV led to increased cell lysis and a selective loss of IFN-α, IFN-β, and IFN-λ but not TNF-α, IL-1β, or IL-6 expression compared to control cells.[217] Treatment of patient cells with recombinant IFN-α decreased cell lysis following HSV stimulation *in vitro*; demonstrating that IFN expression mediated by *UNC93B1* activation can provide host cell protection.[217] Additional *in vitro* studies of stem cell-derived neurons and oligodendrocytes from these patients confirmed an IFN signaling defect due to the loss of *UNC93B1* function that correlated with increased viral replication; extending the protective role of *UNC93B1* in mediating IFN induction to cells resident to the human central nervous system (CNS).[218] An association between *UNC93B1* and IFN-β was only seen in human cells *in vitro* but not in the mouse brain *in vivo*. This may suggest that *UNC93B1* expression is only required to elicit a type I IFN response in some cell types with the overall IFN response in total brain tissue compensated for through immune mechanisms activated in additional cells. Alternatively, these disparate experimental findings may be an artifact of differences in infection route and encephalitis induction in the mouse model compared to natural infection.

A role for *Unc93b1* has also been proposed during infection with neuroadapted Sindbis virus (NSV). NSV is a positive-sense ssRNA virus that is used in the mouse to model human alphavirus-induced encephalitis.[219] *Unc93b1*$^{3d/3d}$ mice had increased mortality following intracranial NSV infection that was not caused by an increase in viral load or a decrease in type I

IFN in the brain or spinal cord.[219] Though the *Unc93b1*$^{3d/3d}$ mice had less CD11b^{+} cells in both the brain and spinal cord, suggesting a myeloid cell recruitment defect due to the loss of *Unc93b1*, attempts to determine which myeloid cell type was specifically depleted were unsuccessful.[219] It is therefore clear that the specific contribution of *Unc93b1*-mediated immune activation to host protection in NSV infection as well as in other ssRNA viral infections requires further study.

Not only has a protective role for *Unc93b1* been demonstrated in models of both DNA and RNA viral infection, but it has also been implicated in protection against parasites. In *Leishmania major* (*L. major*) infection the loss of *Unc93b1* increased host susceptibility, as evidenced by an increase in footpad swelling, as well as augmented infection-site parasite burden.[220] A skew towards Th2 immune upregulation was also seen in the *Unc93b1*$^{3d/3d}$ mice with increased IL-10 and decreased IFN-γ expression measured in the LN following infection.[220] This Th1/Th2 imbalance, when reversed by the addition of an IL-10R-antibody or recombinant IL-12, abrogated the increase in susceptibility and parasite burden seen in the infected *Unc93b1*$^{3d/3d}$ mice.[220] Infection with *T. cruzi* also revealed a role for *Unc93b1*-mediated immune activation in host protection. The *3d* mutation caused increased mortality and parasitemia following *T. cruzi* infection.[221] This was accompanied by reduced expression of the proinflammatory mediators IL-12p40 and IFN-γ and a defect in CD4^{+} and CD8^{+} T cell-specific IFN-γ expression in *Unc93b1*$^{3d/3d}$ mice compared to wild type mice.[221]

Finally, several studies have implicated *Unc93b1* in protection following *Toxoplasma gondii* (*T. gondii*) infection. These studies revealed that *Unc93b1* is essential for *T. gondii* infection survival and control of multi-organ viral load.[222] Analysis of serum proinflammatory cytokine expression revealed a dysregulated response with a specific decrease in IL-12p40 and increased expression of IL-6 and CCL2 in *Unc93b1*$^{3d/3d}$ serum.[222] Treatment with recombinant IL-12 was able to rescue the *Unc93b1*$^{3d/3d}$ mice from *T. gondii*-induced mortality, suggesting an essential role for the *Unc93b1*-mediated upregulation of this proinflammatory mediator in *T. gondii* infection.[223] Further studies have revealed that TLR11 and TLR12, upregulated by the profilin protein of *T. gondii*, also require UNC93B1-mediated transport to the endosome to elicit an immune response.[224, 225] The absence of *Unc93b1* expression in splenic DCs stimulated with

profilin *in vitro* led to significantly decreased IL-12p40, TNF-α, and IL-6 expression compared to wild type cells.[224] This suggests that UNC93B1 is not only involved in transport of nucleic acid-recognizing TLRs but also aids in transport of TLRs that localize to the endosome and recognize protein-derived PAMPs. Despite this, TLR11 and TLR12 are non-functional or absent from the human genome respectively, indicating that the importance of these PRRs and their interaction with UNC93B1 in human *T. gondii* infection is minimal and suggesting a greater reliance on nucleic-acid recognizing TLRs for immune activation during human *T. gondii* infection.[223, 226]

The above mouse studies, conducted in diverse infection models, define a role for *Unc93b1* as a broadly protective and essential chaperone protein in the immune response to multiple pathogens. This therefore implies that further study of the role of *Unc93b1* in response to infection with additional pathogens may continue to reveal novel insights into immunity.

Unc93b1 and antigen presentation

The initial manuscript by Tabeta *et al.* that uncovered the role of UNC93B1 in endosomal TLR transport also demonstrated its role in antigen presentation via MHC class II and antigen cross-presentation.[36] In this study, defects in antigen presentation and cross-presentation were visualized as decreased *in vivo* proliferation of OVA-specific OT-II ($CD4^+$) T cells following OVA stimulation in *Unc93b1*$^{3d/3d}$ mice and significantly less IFN-γ^+CD8^+ T cells with significantly decreased cytolytic activity *in vitro* after *Unc93b1*$^{3d/3d}$ splenocyte restimulation with MHC class I-specific OVA, respectively.[36]

Despite these interesting findings, subsequent studies have not been able to replicate these conclusions. While knockdown of *UNC93B1* expression in human monocyte-derived DCs ablated TNF-α production, consistent with a role for *UNC93B1* in proinflammatory cytokine activation, it did not affect *in vitro* $CD4^+$ T cell proliferation following stimulation with house dust-mite antigen.[227] Differences between these studies may be due to residual *UNC93B1* expression following gene knockdown in cells or may reflect a broader role for *Unc93b1* in the mouse that is not recapitulated in the human host. A very recent study however suggests that *Unc93b1* does not play a role in antigen presentation in a mouse model either. Deguine *et al.,* using *Unc93b1*$^{3d/3d}$ mice, reproduced the stimulation conditions and experimental output of the

original manuscript by Tabeta *et al.* but failed to see a difference in OT-II cell proliferation or in the frequency of activated IFN-γ^+ or $CD44^+CD8^+$ T cells.[228] In response to these findings, Tabeta *et al.* suggested that differences in experimental conditions may have contributed to this distinction.[229] Alternatively, they proposed that additional ENU-induced mutations may have existed in the original mouse that induced the defect in antigen presentation but have subsequently been lost through breeding.[229] The former reason seems unlikely as the experimental set-up, according to a comparison of the methodology detailed by both papers, is similar. The latter however warrants further investigation as, following whole-genome sequencing, Tabeta *et al.* discovered additional coding mutations in the original *Unc93b1*$^{3d/3d}$ genome that have yet to be studied for their potential role in antigen presentation and may assist in resolving this issue.[229]

Infection studies in *Unc93b1*$^{3d/3d}$ mice have also, either directly or indirectly, investigated a role for *Unc93b1* in antigen presentation. Following *T. gondii* infection, *Unc93b1*$^{3d/3d}$ mice had significantly less activated spleen $CD11b^+$ or $CD11c^+$ cells (APCs), measured by the cell-specific expression of MHC class I, MHC class II, CD40, CD80, and CD86.[222] *T. gondii*-infected *Unc93b1*$^{3d/3d}$ mice also had significantly less activated (expressing CD25 and CD69) $CD4^+$ and $CD8^+$ T cells in the spleen at day 8 post-infection.[222] While this study did not directly link *Unc93b1* expression to antigen presentation or describe a mechanism through which this might occur, it suggests that the activation of *Unc93b1*-dependent signaling, either directly or indirectly, plays a role in APC and T cell activation in *T. gondii* infection. Further studies of TLR3/TLR7/TLR9/TLR11-quadruple deficient mice in *T. gondii* infection however were able to fully recapitulate the phenotype observed in the *Unc93b1*$^{3d/3d}$ mice, including increased mortality and dampened early expression of proinflammatory mediators IL-6, IL-12, CCL2, and IFN-γ,[223] though the activation of APCs and T cells was not specifically examined in the quadruple-deficient mice. In *T. cruzi* infection, TLR3/TLR7/TLR9-triple deficient mice also recapitulated the susceptible phenotype seen in *Unc93b1*$^{3d/3d}$ mice including identical mortality, systemic parasite burden, and defective $CD4^+$ and $CD8^+$ T cell-specific IFN-γ production.[221] These studies suggest that the role of *Unc93b1* in T cell activation during *T. gondii* and *T. cruzi* infection is not distinct from its role in the activation of endosomal TLRs.

Finally, in infection with both MCMV and NSV, *Unc93b1*$^{3d/3d}$ mice expressed similar or even elevated frequencies of activated (IFN-γ^{+} or TNF-α^{+}) CD8^{+} or (IFN-γ^{+} or IL-17^{+}) CD4^{+} T cells, further suggesting that *Unc93b1* does not play a direct role in antigen presentation in viral infection either.[215, 219] Despite these findings, additional studies are required to specifically determine if *Unc93b1* has a direct and distinct role in antigen presentation during infection or whether its activation of the immune response via endosomal TLRs allows it to indirectly affect antigen presentation during certain infections.

***Unc93b1* and autoimmunity**

Though the previous analyses of *Unc93b1*$^{3d/3d}$ mice clearly delineate a protective role for *Unc93b1*-mediated immune activation following infection, subsequent studies have determined that, under select conditions, the expression of *Unc93b1* may also contribute to an autoimmune response. Studies following targeted deletion of the UNC93B1 amino terminus determined that a single amino acid change (D34A) (Figure 1.4) selectively biased TLR transport, resulting in increased TLR7 and decreased TLR9 trafficking to the endosome.[230] In the literature it is well established that TLR7 overexpression can cause autoimmunity,[231, 232] suggesting that increased TLR7 trafficking and immune activation induced by the D34A mutation may increase the risk of developing an autoimmune disease. Indeed, *in vivo* studies demonstrated that the majority of *Unc93b1*$^{D34A/D34A}$ mice spontaneously developed severe liver damage and splenomegaly leading to death around 30 weeks of age.[233] Cellular analysis showed that the *Unc93b1*$^{D34A/D34A}$ mice had a significantly increased frequency of activated effector (CD62L^{lo}CD44^{hi}) CD4^{+} T cells compared to wild type mice and higher expression of CD69 on LN CD4^{+} T cells, suggesting increased T cell activation as a possible mediator of pathology.[233] B cells were also implicated in pathology in this model with the loss of B cells in *Unc93b1*$^{D34A/D34A}$ mice causing a significant improvement in survival.[233] This study further demonstrated that enhanced TLR7-mediated immune activation was the primary cause of increased immune activation and pathology in the *Unc93b1*$^{D34A/D34A}$ mice as the expression of the D34A mutation on a TLR7-deficient but not TLR9-deficient background abolished the autoimmune phenotype

and improved survival.[233] These studies therefore define a protective role for *Unc93b1* against autoimmunity if a bias towards TLR9-mediated signaling is maintained in the host.

Contrary to the above findings, studies of the *3d* mutation on a genetic background that is prone to lupus revealed that the complete loss of *Unc93b1* function decreased autoantibody production and prevented lupus development and subsequent mortality.[234] This suggests that the complete loss of normal *Unc93b1*-mediated immune activation protects against the development of autoimmunity. Differences between studies conducted in *Unc93b1*$^{D34A/D34A}$ and *Unc93b1*$^{3d/3d}$ mice may be attributable to a bias towards increased TLR7 activation resulting in autoimmunity in the former compared to the complete abolition of endosomal TLR signaling in the latter. Even though TLR9-mediated immune activation is missing in the *Unc93b1*$^{3d/3d}$ mice, the additional loss of TLR7-mediated immune activation in this model may be what is allowing for increased protection against autoimmunity in this host.

The above studies in *both Unc93b1*$^{D34A/D34A}$ and *Unc93b1*$^{3d/3d}$ mice reveal that different domains of UNC93B1 have distinct functions in the regulation of the immune response and suggest that the study of additional mutations of *Unc93b1* at other sites may reveal unique functions for this gene in immune regulation or activation in response to diverse infections.

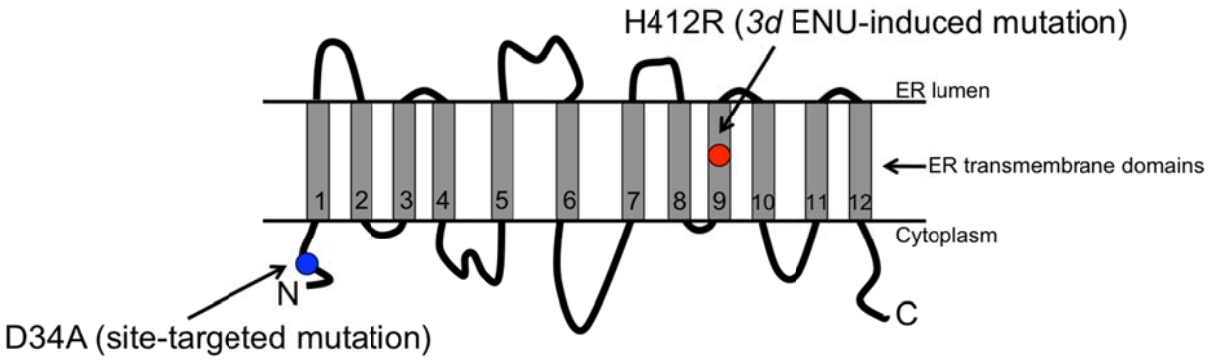

Figure 1.4. Schematic of the UNC93B1 12-transmembrane domain chaperone protein
Transmembrane domains, the amino- (N) and carboxy- (C) termini, and the relative positions of the previously characterized *3d* (red) and D34A (blue) mutations of UNC93B1 are indicated. Figure is adapted from.[34, 230]

VII. Rationale, hypothesis and experimental objectives

Rationale

The discovery of TLRs in the mammalian immune response by Charles Janeway Jr. and Ruslan Medzhitov in 1997[29] rapidly expanded the field of host-pathogen interactions. Since this time, studies have elucidated the cellular and intracellular location, activating PAMP(s), and mechanisms of downstream immune signaling for most of the 10 human and 12 mouse TLRs that are known.[28] These investigations have revealed a complicated network of interacting proteins whose importance in immune activation can vary depending on the cell type, organ, or pathogen being studied; with new discoveries continually restructuring how we understand immunity. Knowing this, our lab used ENU mutagenesis to look for novel mediators of TLR-mediated immune activation. This method of mutagenesis was selected as it permits an unbiased approach to discovering a novel gene or novel mutation responsible for a phenotype-of-interest. Our discovery of a mutant with an *in vitro* hyporesponsive phenotype to stimulation with PAMPs that activate endosomal TLR3, TLR7, and TLR9 led us, through sequencing, to the *Unc93b1* gene. Discovered in 2006, the role of *Unc93b1* in mammals is to chaperone TLRs from the ER to the endosome and therefore permit innate immune activation through this pathway.[34-36] Since then, multiple studies have defined the role of *Unc93b1* in parasite (*T. gondii, T. cruzi, L. major*) and DNA virus (MCMV and HSV) infection but only a single study, published in 2012, defined a role for *Unc93b1* in ssRNA viral infection using a model of alphavirus-induced encephalitis.[219] A specific role for *Unc93b1*-mediated immune activation in other ssRNA viral infections that are known to activate endosomal TLRs has yet to be elucidated.

Hypothesis

We hypothesize that the functional loss of *Unc93b1* and immune activation through endosomal TLRs during ssRNA virus infection will significantly impair the host's ability to activate a protective immune response and eliminate the infection. By characterizing our novel ENU-induced mutation of *Unc93b1* using two widespread and clinically relevant ssRNA viruses, influenza A/PR/8/34 (H1N1) and CVB3, we will confirm the utility of our novel loss-of-function

model for the investigation of host-pathogen interactions and gain novel insights into the contributions of *Unc93b1*-mediated immune activation to host outcome. These studies will yield new findings that may be beneficial at a clinical level.

Experimental objectives

Our main objective is to dissect the mechanisms of host resistance or susceptibility mediated by *Unc93b1* and endosomal TLRs using our novel ENU-induced loss-of-function mouse model. Our specific objectives include:

1. *Substantiate the hyporesponsive phenotype to PAMP stimulation in our novel mutant mice and describe the effect of the ENU-induced mutation on the gene and protein structure of UNC93B1 (Chapter 2).* Using ENU mutagenesis we screened for a recessive defect in innate immune signaling and discovered a mutant with impaired endosomal TLR-mediated activation that we mapped to *Unc93b1*. Continuing from this initial investigation, we will confirm the hyporesponsive phenotype observed *in vitro* using bigger groups of normal and deviant mice as well as determine if the ENU-induced mutation also elicits an *in vivo* defect in endosomal TLR activation. As a model of *Unc93b1* loss-of-function was previously generated using ENU-mutagenesis (*Unc93b1*$^{3d/3d}$) and has a similar phenotype to our ENU-mutagenized mice following PAMP stimulation,[36] we will contrast these unique mutations at the gene, amino acid, and predicted protein structure level. We will further confirm that our ENU-induced mutation is in the *Unc93b1* gene by analyzing the response to PAMP stimulation in compound heterozygous mice carrying our mutation and the *3d* mutation. If these mutations are in the same gene, the hyporesponsive phenotype of the original mutation will be recapitulated.

2. *Characterize the role of Unc93b1 in activation of a successful immune response following infection with influenza virus (Chapter 2).* Studies of a specific role for *Unc93b1* following infection with a negative-sense ssRNA virus or during a respiratory infection have not been conducted. Both TLR3- and TLR7-mediated mechanisms of immune activation have

been implicated in influenza infection, albeit with some discordant findings in the literature.[99, 103-105, 107, 108] Therefore, we want to determine how the host response to infection is affected following the complete loss of endosomal TLR signaling. These studies will be conducted using our ENU-derived mice with a mutation in *Unc93b1* that we have named '*Letr*' for 'loss of endosomal TLR response'. To study the immune response to influenza infection we will characterize the specific cellular and soluble mediator profile at the site of infection as well as determine how infection survival, lung viral load, and tissue damage are affected by the loss of *Unc93b1*. We expect that the loss of *Unc93b1*-mediated immune signaling in influenza infection will diminish immune activation and put the host at a significant disadvantage for recovery from infection.

3. *Identify the contribution of Unc93b1-mediated immune activation to the outcome of acute CVB3-induced myocarditis and delineate genes or pathways that may be mediating infection outcome in this model (Chapter 3).* As a protective role for *Unc93b1* in the immune response to positive-sense ssRNA viral infection with NSV has been shown,[219] we predict that infection studies with another positive-sense ssRNA virus will yield similar findings. Though the CVB3 virus can activate TLR3, TLR7, and TLR9,[188-190] the effect of the concurrent loss of multiple endosomal TLRs in acute CVB3-induced myocarditis has not been studied. We will therefore determine how the loss of *Unc93b1* function affects host survival, viral load in target organs, and cardiac tissue inflammation, necrosis, and repair using the *Unc93b1*$^{Letr/Letr}$ mice. As cardiac pathology is the primary mechanism of increased morbidity and mortality following CVB3 infection, we will examine early cardiac gene expression in the *Unc93b1*$^{Letr/Letr}$ hearts using a comprehensive microarray to gain insight into this process. Gene expression analysis has the potential to delineate novel mediators or pathways of host protection or pathogenesis in acute CVB3-induced myocarditis that are linked to *Unc93b1*-dependent endosomal TLR activation and may reveal interesting avenues for future research.

CHAPTER 2. An ENU-induced splicing mutation reveals a role for *Unc93b1* in early immune cell activation following Influenza A H1N1 infection

An ENU-induced splicing mutation reveals a role for *Unc93b1* in early immune cell activation following influenza A H1N1 infection

Erin I Lafferty[2], Adam Flaczyk[2], Isabelle Angers[3], Robert Homer[4], Eva d'Hennezel[5], Danielle Malo[3,6,7], Ciriaco A Piccirillo[3,5], Silvia M Vidal[3,6,7], and Salman T Qureshi[1,2,3#]

[1]Department of Critical Care, McGill University Health Centre, Montréal, Québec, Canada
[2]Division of Experimental Medicine, McGill University, Montréal, Québec, Canada
[3]Department of Medicine, McGill University, Montréal, Québec, Canada
[4]Yale University School of Medicine, New Haven, Connecticut, USA
[5]Department of Microbiology and Immunology, McGill University, Montréal, Québec, Canada
[6]Department of Human Genetics, McGill University, Montréal, Québec, Canada
[7]Complex Traits Group, McGill University, Montréal, Québec, Canada

[#]**Correspondence should be addressed to:**
Dr. Salman T Qureshi
Room L11-403, 1650 Cedar Avenue
Montréal, Québec, Canada
H3G 1A4
Telephone: 514-934-1934 x44626
Email: salman.qureshi@mcgill.ca

Published in: *Genes Immun*. **2014**. 15(5): 320-32.

Preface

As described in chapter one, ENU mutagenesis is a powerful tool that can be used to create novel mouse models to study host-pathogen interactions. An excellent example of the potential of this approach was demonstrated with the creation of a novel mutation, termed '*3d*', in UNC93B1; the chaperone protein that trafficks TLR3, TLR7, and TLR9 from the ER to the endosome. Studies using the *Unc93b1*$^{3d/3d}$ mutant model have revealed new and exciting insights into the role of *Unc93b1* and endosomal TLRs in the immune response to infection with the DNA viruses MCMV and HSV.

Our group also created a unique loss-of-function mutation in *Unc93b1* using ENU mutagenesis that is in a different location from the *3d* mutation. When we began these studies, a role for *Unc93b1* in ssRNA viral infection had not been defined. Therefore we decided to use our model to study how the loss of *Unc93b1* function affected infection outcome when the host was exposed to a ssRNA virus. The aim of these studies was to validate the use of our model for *in vivo* infection studies and generate novel insights into the role of *Unc93b1* and endosomal TLRs in ssRNA viral infection.

As detailed in chapter one, influenza is a negative-sense ssRNA virus that significantly contributes to global morbidity and mortality each year. The capacity of influenza virus to activate the immune response via TLR3 and TLR7, a well-established mouse model of influenza infection, and the paucity of current knowledge on the consequences of complete endosomal TLR deficiency made it an ideal pathogen for our investigation of the role of *Unc93b1* in ssRNA viral infection.

The research conducted in this chapter functionally dissected the specific contribution of *Unc93b1* and endosomal TLRs to immune activation following influenza infection *in vivo*. The use of our ENU-induced *Unc93b1* loss-of-function model allowed us to clearly define and differentiate the relative contributions of endosomal and cytosolic immune activation to host innate immune defense.

Abstract

Genetic and immunological analysis of host-pathogen interactions can reveal fundamental mechanisms of susceptibility and resistance to infection. Modeling human infectious diseases among inbred mouse strains is a proven approach but is limited by naturally occurring genetic diversity. Using ENU mutagenesis, we created a recessive loss-of-function point mutation in *Unc93b1* (*unc-93 homolog B1* (*C. elegans*)), a chaperone for endosomal TLR3, TLR7, and TLR9, that we termed *Letr* for 'loss of endosomal TLR response'. We used *Unc93b1*$^{Letr/Letr}$ mice to study the role of *Unc93b1* in the immune response to influenza A/PR/8/34 (H1N1), an important global respiratory pathogen. During the early phase of infection, *Unc93b1*$^{Letr/Letr}$ mice had fewer activated exudate macrophages and decreased expression of CXCL10, IFN-γ, and type I IFN. Mutation of *Unc93b1* also led to reduced expression of the CD69 activation marker and a concomitant increase in the CD62L naïve marker on $CD4^+$ and $CD8^+$ T cells in infected lungs. Finally, loss of endosomal TLR signaling resulted in delayed viral clearance that coincided with increased tissue pathology during infection. Taken together, these findings establish a role for *Unc93b1* and endosomal TLRs in the activation of both myeloid and lymphoid cells during the innate immune response to influenza.

Keywords: *Unc93b1*, ENU mutagenesis, influenza H1N1, exudate macrophages, $CD4^+$ and $CD8^+$ T cells

Introduction

Influenza virus infection causes an acute respiratory tract disease with a global annual mortality of 250 000 – 500 000.[72, 235] In addition to seasonal strains, humans face the persistent threat of novel strains that can emerge and spread quickly in a naïve population, potentially resulting in a pandemic.[236, 237] Seasonal influenza often affects individuals with weakened immune systems including very old, very young, and immunocompromised populations.[85, 238, 239] Conversely, certain highly pathogenic influenza viruses such as the 1918 H1N1 strain confer greater mortality in otherwise healthy individuals through a combination of enhanced inflammation leading to excessive tissue damage and secondary bacterial infection.[77, 79] To develop effective management strategies to combat both seasonal and pandemic influenza infection, a detailed understanding of the cellular and molecular mechanisms that regulate the quality and magnitude of the host immune response is essential.

Following influenza infection, a rapid yet nonspecific innate immune response is activated in an attempt to control initial viral replication and is followed by the mobilization of professional antigen-presenting cells (APCs), including dendritic cells (DCs) and macrophages. Activated APCs express class I or class II major-histocompatibility complex (MHC) molecules as well as co-stimulatory markers such as the cluster of differentiation (CD) molecules CD40, CD80, and CD86.[64] Expression of these markers, particularly by DCs, is required for the priming and activation of naïve T and B cells in the lung-associated lymph nodes (LALNs), leading to the formation of an adaptive immune response.[131, 137, 138, 240, 241] Activated T and B cells are recruited to the site of primary infection to mediate antigen-specific immunity through cell-mediated control of viral replication and the production of specific antibodies that provide lasting protection against the infecting strain, respectively.[64]

Initial recognition of the influenza virus and subsequent activation of innate immunity occurs through host pattern recognition receptors (PRRs). Two of the best-studied PRRs for influenza recognition are the endosomal toll-like receptors (TLR)3 and TLR7.[31, 101, 102, 108, 111] To initiate downstream signaling, TLR3 and TLR7 must be trafficked from the endoplasmic reticulum (ER) to the endosome by UNC93B1, an ER-resident transmembrane chaperone

protein that also transports TLR9 following activation.[34-36] At the endosome, TLR7 recognizes viral single-stranded RNA (ssRNA) and recruits the myeloid differentiation primary response 88 (MyD88) adaptor protein[31, 101] while TLR3 recognizes double-stranded RNA (dsRNA) and recruits the toll interleukin-1 receptor-domain-containing adapter inducing interferon-β (TRIF) adaptor protein.[242] One group has shown that MyD88-deficient mice are susceptible to influenza infection and have diminished recruitment of $CD11b^+$ neutrophils and monocytes as well as reduced expression of the proinflammatory mediators IL-6, TNF-α, and interferon (IFN)-γ in the airways.[104] A role for MyD88 in B cell activation and subsequent production of virus-specific IgG2a/c antibodies has also been demonstrated.[105, 108] Conversely, several other investigations have demonstrated that signaling via MyD88 is not essential for survival following influenza challenge.[99, 107]

Despite conflicting reports as to whether a true dsRNA replication intermediate forms during influenza virus replication, *TLR3* expression is upregulated in human alveolar and bronchial epithelial cells as well as mouse lungs following influenza infection, suggesting that it contributes to the host immune response.[99, 102, 106, 111] TLR3 has been specifically linked to the early production of proinflammatory mediators such as IL-6, IL-8, and CCL5 in human bronchial cells during influenza infection.[102, 111] Compared to wild type mice, TLR3-deficient mice have diminished production of IL-6 and IL-12 p40/p70, elevated expression of IL-9, IL-10, and IFN-γ, and fewer macrophages and $CD8^+$ T cells in the airways.[99] Somewhat unexpectedly, these mice had an improved rate of survival despite a higher lung viral load, suggesting that the TLR3-mediated host response during influenza infection is deleterious.[99] On the other hand, subsequent studies of TRIF-deficient mice that also lack TLR3 signaling did not reveal a significant role for this adaptor molecule following influenza infection.[104, 105] Finally, analysis of a single patient with influenza-associated encephalopathy revealed a loss-of-function missense mutation in *TLR3*, suggesting that this PRR may play a crucial role in protection rather than disease pathogenesis.[103] While the discordant experimental findings on the role of these TLRs and adaptor molecules in influenza infection may be attributable to differences in the strain, dose, and volume of virus administered to mice with distinct genetic backgrounds, complementary human studies have also failed to clearly identify the genes that are required

for protection of the host.[243] Thus, on the basis of current knowledge, it is not possible to draw firm conclusions about the contributions of the TLR7-MyD88 and TLR3-TRIF signaling pathways to innate immunity against influenza infection.

Studies of inbred mouse strains as well as gene-deficient mice have been essential for elucidating key features of the host response to viral infection that are relevant to human immunity.[3, 244] Owing to the limited number of available inbred and knockout strains, alternative approaches, such as the creation of random heritable mutations using the chemical N-ethyl-N-nitrosourea (ENU), have evolved in recent years.[3] Rather than abrogating gene expression, ENU mutagenesis can create unique point mutations that alter protein function.[18] Such mutations more closely mirror human genetic variation and can reveal specific roles for individual protein domains.[18] This forward genetic approach has been successfully used to study molecules and pathways that are crucial to host defense against various pathogens.[16] Here we report the creation of an ENU-induced point mutation in the mouse *Unc93b1* gene that results in the complete deletion of exon 4, which encodes the 3rd and 4th transmembrane domains of the full-length protein. We have named this mutation *Letr* for 'loss of endosomal TLR response' as it confers a lack of responsiveness to stimulation with nucleic acid structures that represent pathogen-associated molecular patterns (PAMPs) known to activate the TLR3, TLR7, and TLR9 signaling pathways.

Based on the previously demonstrated function of UNC93B1 as a chaperone for endosomal TLRs[34-36] as well as its contribution to the immune response against various parasites (*Toxoplasma gondii, Trypanosoma cruzi, Leishmania major*),[220-224] DNA viruses (Mouse cytomegalovirus (MCMV), Herpes simplex virus-1 (HSV-1))[215-217] and neuroadapted Sindbis virus (NSV, a positive-sense ssRNA virus),[219] we hypothesized that defective UNC93B1 function would impair the innate immune response to influenza A/PR/8/34 (H1N1), a negative-sense ssRNA virus that targets the respiratory mucosa. Using our ENU-induced mutant mice that lack endosomal TLR signaling, we found that *Unc93b1* contributes to the expression of type I and type II IFN (IFN-γ), recruitment of activated exudate macrophages (ExMs), and activation of T cells in the lung during the early phase of influenza infection. Importantly, despite a significant delay in viral clearance that coincided with increased tissue inflammation and epithelial

reaction, the failure of *Unc93b1*-mediated innate immune activation did not significantly alter mortality, suggesting that alternative pathways can compensate for the lack of endosomal TLR function in this model. Collectively, these results establish a distinct role for *Unc93b1* in the early activation of the innate immune response to influenza and demonstrate the importance of redundant mechanisms that protect the host against lethal infection.

Results

ENU mutagenesis induced a mutation that confers defective *in vitro* and *in vivo* responses to TLR3, TLR7, and TLR9 ligands

To identify novel genes or novel roles for known genes in TLR-specific immune signaling pathways, we injected male 129S1 G0 mice with ENU and screened cells from G3 mutagenized mice for defective responses to polyinosinic:polycytidylic acid (polyI:C), lipopolysaccharide (LPS), Imiquimod, and unmethylated CpG dinucleotides (CpG DNA). These structures were chosen as they are known to activate TLR3, TLR4, TLR7, and TLR9 signaling pathways respectively.[30, 32, 33, 245] The cytokines, cell types, and time points selected for analysis following *in vitro* and *in vivo* PAMP stimulation were based on data from the initial publications that identified these TLR ligands.[30, 32, 33, 245] Mutagenized G0 mice were bred to C57BL/6 female mice and the G1 progeny from independent G0 crosses were intercrossed to increase the number of recessive mutations available for screening at the G3 generation (Figure 2.1A). Thioglycollate-elicited peritoneal macrophages or splenocytes from G3 progeny of G2 brother-sister matings were tested for *in vitro* expression of IL-6 in response to PAMP stimulation. One pedigree (B28W6) showed a deviant phenotype in response to stimulation with polyI:C, Imiquimod, and CpG DNA but had normal expression following LPS stimulation (Figure 2.1B). Heterozygous G2 fathers from this pedigree were outcrossed to C57BL/6 female mice and the resulting F1 female progeny were backcrossed to create N2 progeny (Figure 2.1A). N2 mice were intercrossed and deviant lines carrying a homozygous mutation were identified by survival splenectomy and repeat *in vitro* phenotyping. Cells from heterozygous mice responded normally to CpG stimulation, confirming that the mutation has a recessive mode of inheritance (Figure 2.1B). To analyze the phenotype *in vivo*, progeny of deviant and normal N2 mice were injected intraperitoneally with LPS, polyI:C, Imiquimod, or CpG DNA and serum was collected three hours post-injection. Compared to the progeny of normal N2 mice, those from deviant N2 mice had significantly decreased expression of serum IL-12/IL-23 p40 in response to stimulation with polyI:C, Imiquimod, or CpG DNA but retained similar responses to LPS (Figure 2.1C).

An ENU-induced single nucleotide transversion in *Unc93b1* results in the loss of exon 4 due to alternative splicing

To map the gene responsible for the *Letr* phenotype, we performed a low-density genome scan using 375 single nucleotide polymorphisms (SNPs) among 54 mice derived from a (*Letr/Letr* x C3H/HeN) F1 x *Letr/Letr* backcross. The *Letr* mutation was localized to a 5.4 Mb region on chromosome 19 between markers rs31277487 and rs30935927. To test the heritability of the *Letr* mutation, an additional 281 mice from the same backcross were screened for IL-6 expression following *in vitro* stimulation of splenocytes with CpG DNA. Of these mice, 139 (49.5%) showed a normal IL-6 response while the other 142 (50.5%) animals lacked IL-6 expression with perfect concordance between the mutant phenotype and genotype for a recessive mutation.

Based on a previous ENU mutagenesis study that created a mouse, termed *3d,* with a similar hyporesponsive phenotype caused by a point mutation in *Unc93b1* on chromosome 19,[36] we took a targeted approach to identify the *Letr* mutation. Nucleotide sequencing of *Unc93b1* genomic DNA (gDNA) from normal and deviant (*Letr*) mice identified a single T to A transversion at the 5' splice donor site in the intron between exon 4 and 5 of *Unc93b1* that rendered the site ineffective (Figure 2.2A, non-coding strand shown). Sequencing of cDNA from both $Unc93b1^{+/+}$ and $Unc93b1^{Letr/Letr}$ mice determined that the mutation resulted in the loss of exon 4 in the 11-exon mRNA transcript (Figure 2.2C).

To confirm that the ENU-induced *Letr* mutation caused alternative splicing, spleen RNA from $Unc93b1^{Letr/Letr}$ and $Unc93b1^{+/Letr}$ mice as well as C57BL/6, C3H/HeN, and 129S1 inbred strains was reverse transcribed and a 918 base pair (bp) region of *Unc93b1* cDNA that included exon 4 was amplified and visualized by gel electrophoresis. All three inbred strains presented a single band at the predicted size while $Unc93b1^{Letr/Letr}$ cDNA presented a smaller band that is compatible with the 162bp deletion of exon 4 (Figure 2.2B). Analysis of heterozygous $Unc93b1^{+/Letr}$ cDNA showed both wild type and mutant *Unc93b1* transcripts.

To evaluate the relative importance of exon 4 to the integrity of the UNC93B1 protein, the degree of amino acid sequence conservation was compared among diverse species. Alignment of UNC93B1 amino acid sequences encompassing exon 4 demonstrated a 54 amino

acid deletion in *Unc93b1*$^{Letr/Letr}$ mice (Figure 2.2D). These missing amino acids were identical among all species examined, with the exception of *Xenopus tropicalis* that was distinguished by the substitution of nine amino acid residues. Protein modeling software was used to confirm that the wild type UNC93B1 amino acid sequence forms a 12-helix transport protein (Figure 2.2E).[36, 213] By mapping the amino acids encoded by exon 4 to the wild type model, the splicing defect caused by the *Letr* mutation is predicted to eliminate the 3rd and 4th transmembrane domains of the functional UNC93B1 protein and is distinct from the *3d* mutation which causes a single amino acid missense mutation (H412R) in the 9th transmembrane domain (Figure 2.2E).[36]

Allelic complementation does not rescue the hyporesponsive phenotype in *Unc93b1*$^{Letr/Letr}$ mice

To confirm that the *Letr* mutation was in the *Unc93b1* gene, we performed an allelic complementation study by generating *Unc93b1*$^{Letr/3d}$ F1 hybrids from *Unc93b1*$^{Letr/Letr}$ and *Unc93b1*$^{3d/3d}$ mice. If the *Letr* mutation were elsewhere in the genome, the lack of response to PAMP stimulation would be rescued in the compound heterozygotes. All genotypes were tested for IL-6 expression following *in vitro* stimulation with PAMPs, as done during the initial screen. Both thioglycollate-elicited peritoneal macrophages and splenocytes stimulated with media alone produced undetectable levels of IL-6 (data not shown). Thioglycollate-elicited peritoneal macrophages from *Unc93b1*$^{Letr/Letr}$, *Unc93b1*$^{3d/3d}$, and *Unc93b1*$^{Letr/3d}$ strains had a comparable IL-6 response to *Unc93b1*$^{+/+}$ mice following LPS stimulation (Figure 2.3A). Conversely, the *Unc93b1*$^{Letr/Letr}$, *Unc93b1*$^{3d/3d}$, and *Unc93b1*$^{Letr/3d}$ strains had significantly decreased or undetectable IL-6 expression compared to *Unc93b1*$^{+/+}$ mice following stimulation with polyI:C, Imiquimod, or CpG DNA (Figure 2.3B-D).

***Unc93b1*$^{Letr/Letr}$ mice have fewer activated ExMs in the lungs following influenza infection**

UNC93B1 functions as a chaperone for TLR3, TLR7, and TLR9 and plays a role in host defense against various pathogens including the DNA viruses MCMV and HSV-1 and the RNA virus NSV.[34-36, 215-217, 219] To determine if *Unc93b1* also mediates innate immunity against RNA viral infection of the respiratory mucosa, we characterized the response of *Unc93b1*$^{Letr/Letr}$ mice

to experimental challenge with influenza A/PR/8/34 (H1N1). TLR3, TLR7, and the MyD88 adaptor protein, have been implicated in the immune response to influenza infection, albeit with variable outcomes.[31, 99, 101, 102, 104, 105, 108] *Unc93b1*$^{Letr/Letr}$ mice provide a unique opportunity to determine the combined consequence of defective endosomal TLR3 and TLR7 activation in the presence of a functional MyD88 molecule that also participates in IL-1R- and IL-18R-mediated signaling.[110]

As a role for *Unc93b1* has been linked to antigen presentation during *T. gondii* infection,[222] we sought to determine whether the loss of *Unc93b1* function would affect the activation of lung macrophages and DCs during influenza infection.[246] Based on the literature, day 3 was selected as a representative time point for characterization of early immune differences following experimental influenza challenge.[99, 107, 116] Initially, CD11c and MHCII were used to distinguish macrophages (CD11c^{+}MHCII^{int}) from DCs (CD11c^{+}MHCII^{hi}) and CD11b expression was then used to separate the former population into resident alveolar macrophages (AMs) (CD11b^{-}) and monocyte-derived ExMs (CD11b^{+}) (Figure 2.4A). CD80 expression was used as a marker of cell activation (Figure 2.4A). Following influenza infection, the absolute number of DCs, macrophages, and ExMs was not significantly different between *Unc93b1*$^{+/+}$ and *Unc93b1*$^{Letr/Letr}$ mice in either the LALNs or lungs (Supplementary Figure 2.1A-C). Subsequent analysis of cellular activation status revealed that the loss of *Unc93b1* did not affect the number of CD80^{+} DCs at day 3 post-infection (Figure 2.4B); however, there were significantly fewer CD80^{+} ExMs in the lungs of *Unc93b1*$^{Letr/Letr}$ compared to *Unc93b1*$^{+/+}$ mice at this time point (Figure 2.4C). Simultaneous analysis of the LALNs showed that there was no significant difference in the number of CD80^{+} DCs while the number of CD80^{+} ExMs was too low for reliable detection (Supplementary Figure 2.1D), suggesting that the differential activation seen in the *Unc93b1*$^{Letr/Letr}$ mice was restricted to the site of infection.

Loss of *Unc93b1* function reduces CD4^{+} and CD8^{+} T cell activation in the lungs following influenza infection

As *Unc93b1* also has a role in the activation of CD4^{+} and CD8^{+} T cells during *T. gondii* infection,[222] we analyzed the number and activation status of these lymphoid cell subsets in our

model. Activated $CD4^+$ and $CD8^+$ T cells produce an antigen-specific response that contributes to control of lung viral load. Specifically, $CD8^+$ T cells function primarily through direct lysis of virally infected cells, while $CD4^+$ T cells are classically known as helper cells that enhance $CD8^+$ T cell and B cell activation and, more recently, have been shown to have a direct cytolytic function as well.[151, 247, 248]

Flow cytometry analysis at day 0, 3 and 7 post-infection did not reveal a difference in the total number of $CD4^+$ or $CD8^+$ T cells observed in the LALNs or lungs between *Unc93b1*$^{+/+}$ and *Unc93b1*$^{Letr/Letr}$ mice (Figure 2.5A, B, and Supplementary Figure 2.2G). To determine whether the loss of *Unc93b1* altered T cell activation during influenza infection, the surface expression of an early activation marker (CD69) as well as markers of a naïve (CD62L) and effector (CD44) T cell phenotype were evaluated at day 3 and 7 post-infection. Representative expression plots for T cell activation markers are displayed as histograms (Figure 2.5C-E, left panel). The basal level of all $CD4^+$ and $CD8^+$ T cell activation markers examined was similar between *Unc93b1*$^{+/+}$ and *Unc93b1*$^{Letr/Letr}$ mice (Figure 2.5C-E, right panel). At day 3 post-influenza challenge both $CD4^+$ and $CD8^+$ T cells in the lungs of *Unc93b1*$^{Letr/Letr}$ mice had significantly less expression of CD69 and significantly increased expression of CD62L compared to *Unc93b1*$^{+/+}$ mice (Figure 2.5C, D). No significant differences in the expression of CD44 on $CD4^+$ and $CD8^+$ T cells derived from *Unc93b1*$^{+/+}$ or *Unc93b1*$^{Letr/Letr}$ mice were observed at day 3 post-infection (Figure 2.5E). Finally, the difference in lung $CD4^+$ and $CD8^+$ T cell activation between *Unc93b1*$^{+/+}$ and *Unc93b1*$^{Letr/Letr}$ strains was not observed at day 7 in the lungs (Supplementary Figure 2.2A-C) nor was there a difference in the activation of $CD4^+$ and $CD8^+$ T cells in the LALNs at day 3 or 7 post-infection (Supplementary Figure 2.2D-F).

Unc93b1$^{Letr/Letr}$ mice have a selective decrease in type I/II IFN and CXCL10 expression during influenza infection

Following influenza infection, the lungs produce a variety of soluble mediators that are involved in the recruitment and activation of innate and adaptive immune cells as well as the destruction of virally infected host cells.[64] To determine whether the diminished cellular activation in *Unc93b1*$^{Letr/Letr}$ mice was associated with an altered pattern of inflammatory

mediator secretion in the airway or lungs, the expression of representative cytokines and chemokines that have been implicated in the host response to influenza was determined at serial time points. At day 3 post-infection the expression of type I IFN was significantly lower in the airways of *Unc93b1*$^{Letr/Letr}$ mice compared to the *Unc93b1*$^{+/+}$ strain; however, at day 7 post-infection a comparable increase was observed in both strains (Figure 2.6A). Significantly lower expression of CXCL10 (Figure 2.6B) and IFN-γ (Figure 2.6C) was also observed at day 3 post-infection in the airway and lungs of *Unc93b1*$^{Letr/Letr}$ mutants compared to the *Unc93b1*$^{+/+}$ strain. The expression of other proinflammatory mediators in the airway, including the cytokines IL-6 and TNF-α, and the chemokines CCL2, CCL3, CXCL1, and CXCL2 was not significantly different at day 3 or day 7 post-infection (Supplementary Figure 2.3). These findings demonstrate that soluble inflammatory mediator production at the site of infection was selectively altered by the loss of *Unc93b1* function.

Unc93b1$^{Letr/Letr}$ mice have delayed viral clearance and increased tissue inflammation following influenza infection

To determine if the significant differences in immune cell activation and inflammatory mediator expression caused by the loss of *Unc93b1* function had an impact on host outcome following influenza infection, a comparative analysis of lung viral load, inflammation, and mortality was conducted between *Unc93b1*$^{+/+}$ and *Unc93b1*$^{Letr/Letr}$ strains after intranasal challenge with 400 pfu of the virulent influenza A/PR/8/34 (H1N1) strain. In both genotypes, the peak lung viral load was observed at day 3 post-infection and decreased thereafter (Figure 2.7A).[99, 143] Notably, at day 7 post-infection, the lung viral load in *Unc93b1*$^{Letr/Letr}$ mice was significantly higher compared to *Unc93b1*$^{+/+}$ mice (Figure 2.7A).

In response to influenza challenge, both mouse strains showed a similar pattern of weight loss with a nadir at day 9 followed by recovery of initial weight in surviving animals by day 21 post-infection (Figure 2.7C).[116] Under these experimental conditions, *Unc93b1*$^{+/+}$ mice had a median survival time of 14 days and an overall mortality of 60% while *Unc93b1*$^{Letr/Letr}$ mice had a median survival time of 11.5 days and an overall mortality of 70% (Figure 2.7B). These data suggest that the loss of *Unc93b1* may be associated with an earlier onset of death

but does not significantly affect the overall survival rate following severe influenza infection. Finally, analysis of lung tissue sections stained with hematoxylin and eosin (H&E) at day 7 post-infection demonstrated that *Unc93b1*$^{Letr/Letr}$ mice had increased inflammation and signs of epithelial reactivity compared to *Unc93b1*$^{+/+}$ mice (Figure 2.7F, G). The differential tissue pathology was coincident with a significantly higher viral load in the *Unc93b1*$^{Letr/Letr}$ mice (Figure 2.7A), suggesting that inflammation in the *Unc93b1*$^{Letr/Letr}$ lungs may reflect a heightened response to increased viral replication. Analysis of lung tissue sections from uninfected mice did not show any difference between genotypes (Figure 2.7D, E). Taken together, these data indicate that impaired *Unc93b1* function predisposes the host to a more severe initial disease course following influenza challenge; however, this difference does not significantly alter the ability of the *Unc93b1*$^{Letr/Letr}$ mice to survive the infection.

Discussion

The intricate balance between host immunity and pathogen virulence determines the outcome of an infection. ENU mutagenesis is an advantageous strategy for interrogation of the immune response to infection because it efficiently creates random heritable point mutations throughout the genome that may not occur through natural variation in inbred strains.[3] ENU can also cause distinct single nucleotide alterations within a gene and create mutations that may closely resemble human conditions.[3] Using this technique we screened for a recessive defect in TLR signaling *in vitro* to target immune processes that play an important role in microbial infection.[16] We discovered an alternative splicing mutation in *Unc93b1*, a gene that has been implicated in host immunity to diverse pathogens, and have identified a specific role for this gene in the innate immune response to influenza. Our findings demonstrate that *Unc93b1* contributes to the early activation of ExMs and $CD4^+$ and $CD8^+$ T cells in the lungs as well as expression of type I IFN, type II IFN, and CXCL10 in the airways. Mutation of *Unc93b1* also delayed lung viral clearance and promoted tissue inflammation during infection, although it did not significantly alter survival. These findings establish the specific contribution of *Unc93b1*-dependent endosomal TLR activation during the initial host inflammatory response and highlight the role of complementary immune mechanisms that mediate survival and disease resolution following severe influenza infection.

Using a low-density genome scan, linkage analysis, and nucleotide sequencing, we determined that the *Letr* mutation causes a T to A transversion at the 5' splice donor site in the intron between exon 4 and 5 of the *Unc93b1* gene that results in the deletion of exon 4 in the spliced mRNA transcript. The *Letr* mRNA encodes a predicted protein that lacks the 3^{rd} and 4^{th} transmembrane domains of the full-length UNC93B1. The 54 amino acid residues eliminated by the *Letr* mutation are highly conserved between *Mus musculus*, *Homo sapiens,* and other diverse organisms, suggesting that the two missing transmembrane helices encode important protein domains. Functional analysis using *in vitro* and *in vivo* PAMP stimulation clearly demonstrate that the ENU-induced *Letr* mutation is recessive and confers a complete loss of endosomal TLR function with no detectable pattern of codominance. Residual IL-6 production

following polyI:C stimulation in mice or cells carrying the *Letr* mutation is most likely attributable to recognition by the cytosolic melanoma differentiation-associated protein 5 (MDA5) pathway.[55]

Due to the inherently random nature of ENU mutagenesis, one cannot control the genes, or sites within a gene, that are altered. A major advantage of this hypothesis-free approach is that screening for a particular phenotype can lead to the discovery of previously unknown genes as well as novel functions for known genes.[3] An earlier large-scale ENU mutagenesis study also identified a loss-of-function mutation, termed *3d,* in the *Unc93b1* gene and clearly established its role in immune responsiveness.[36] In contrast to the ENU-induced splicing mutation of *Unc93b1* that we describe here, the *3d* mutation causes a missense mutation in exon 9 that leads to a single amino acid substitution (H412R) in the 9th transmembrane domain of UNC93B1. Despite the different location and unique consequences of these two ENU-induced mutations, both produce a loss-of-function phenotype that confirms the essential contribution of the affected transmembrane-spanning domains to protein integrity. *In vitro* studies have shown that the *3d* mutation inhibits UNC93B1 binding and trafficking of endosomal TLRs from the ER to the endosome following PAMP stimulation.[34, 35] A similar defect in stimulus-dependent trafficking to the plasma membrane was also observed with naturally occurring deletions of multiple transmembrane domains of the SLC7A7 transport protein.[249] Although we have not formally demonstrated that TLR binding and translocation is inhibited by the *Letr* mutation, in light of the predicted deletion of two transmembrane domains of the UNC93B1 protein, it is tempting to speculate that a related mechanism occurs as a result of this ENU-induced allele. Alternatively, deletion of two transmembrane domains of UNC93B1 could also cause a severe structural defect that abrogates protein production, as observed following the loss of a single transmembrane span from the 10-transmembrane domain glucose-6-phosphate protein.[250]

Studies using *Unc93b1*$^{3d/3d}$ mice have demonstrated an enhanced pathogen load and increased susceptibility to *T. gondii*, *T. cruzi, L. major,* and MCMV infection in association with reduced expression of inflammatory mediators including IFN-γ (*T. cruzi*, MCMV, *L. major*), IFN-α (MCMV) and IL-12p40 (*T. gondii, T. cruzi*).[36, 215, 220-222] The current report using *Unc93b1*$^{Letr/Letr}$

mice extends the role of endosomal TLR-mediated inflammation to early host defense against influenza. Thus, the *Unc93b1*$^{Letr/Letr}$ and *Unc93b1*$^{3d/3d}$ mice represent alternative models for the study of diverse host-pathogen interactions. In contrast, Fukui *et al*. have shown that a point mutation in the cytoplasmic amino terminus of UNC93B1 (D34A) causes lethal inflammation. Specifically, *Unc93b1*$^{D34A/D34A}$ mice show preferential and constitutive transport of TLR7 over TLR9, resulting in a severe autoimmune phenotype in the absence of external stimulation.[230, 233] A comparison of the *3d, Letr,* and D34A mutations provides crucial insights into the structure-function relationship of UNC93B1 and demonstrates that unique point mutations of the *Unc93b1* gene can confer a deficient or overexuberant immune phenotype.

Following influenza challenge, macrophages and DCs are among the first cells recruited to the respiratory tract.[124, 251] Pulmonary macrophages may be classified into two types; AMs that reside in naïve lungs and elicit an early response along with respiratory epithelial cells, and monocyte-derived ExMs that are recruited from the bloodstream in a CCR2-dependent manner and differentiate into effector phagocytes that can lyse infected cells.[124, 128] Inflammatory DC subsets are also recruited from the bloodstream, take up antigen at the site of infection, and traffic in a CCR7-dependent manner to the LALNs to activate naïve T cells.[64] Both ExMs and inflammatory DCs express CD80; however, ExMs are relatively poor activators of naïve T cells.[124, 252] At an early time point after influenza infection we detected fewer activated CD80^{+} ExMs, but not CD80^{+} DCs, in the lungs of *Unc93b1*$^{Letr/Letr}$ mice. This data reaffirms a role for *Unc93b1* in APC activation following infection[222] and is consistent with a previous study in which a lack of endosomal TLR signaling did not affect co-stimulatory molecule expression on DCs.[109]

Residual APC activation in our model can be attributed to alternative pathogen recognition mechanisms such as the nucleotide-binding domain and leucine-rich repeat containing receptor family, pyrin domain containing 3 (NLRP3) inflammasome in macrophages and DCs[114] or the cytosolic retinoic acid-inducible gene 1 (RIG-I) pathway in DCs.[41, 47] Recognition of viral infection in conventional DCs (cDCs) preferentially utilizes RIG-I signaling[41, 109] while plasmacytoid DCs (pDCs) rely on TLR7.[31, 101] Since pDCs are the main producers of type I IFN, it is plausible that the delayed expression of type I IFN in the airways of *Unc93b1*$^{Letr/Letr}$

mice is due to defective TLR7-mediated activation of this specialized cell type. Conversely, the fact that cDCs produce type I IFN through a RIG-I-dependent mechanism[41, 45] may explain why the type I IFN response was diminished but not completely abolished in *Unc93b1*$^{Letr/Letr}$ mice. Only the combined loss of MyD88 and mitochondrial antiviral signaling protein (MAVS), the adaptor molecule for RIG-I and MDA5, has been shown to completely abolish type I IFN signaling following influenza infection *in vivo.*[108]

At day 2 or day 3 post-infection with influenza, T cells in the LALNs downregulate CD62L and CCR7, proliferate, and subsequently traffic to the site of infection where they express various activation markers and acquire the capacity to secrete IFN-γ.[142, 143] Consistent with an impaired activation state, $CD4^+$ and $CD8^+$ T cells in the lungs of *Unc93b1*$^{Letr/Letr}$ mice showed a decrease in CD69 and a concomitant increase in CD62L expression at day 3 post-infection. Importantly, TLRs have previously been shown to directly activate T cells.[253] *Tlr1, Tlr2, Tlr3, Tlr6* and *Tlr7* are expressed on both human peripheral blood and mouse C57BL/6 T cells[254-257] and direct stimulation with TLR3 or TLR7 ligands promotes T cell survival, CD38 and CD69 expression, and IFN-γ production.[253, 254, 258, 259] Studies in murine lymphocytic choriomeningitis virus and *T. gondii* infection have demonstrated that the selective loss of MyD88 in T cells leads to decreased survival and IFN-γ production[260, 261] and, in HIV-infected patients, direct TLR7 activation of $CD8^+$ T cells *in vitro* increased T cell proliferation and IFN-γ production.[262] As DC activation in *Unc93b1*$^{Letr/Letr}$ mice appeared to be normal, the delayed lymphocyte activation phenotype in our model may represent an intrinsic defect in $CD4^+$ and $CD8^+$ T cell activation caused by impaired *Unc93b1* function. Nevertheless, at day 7 post-infection, the $CD4^+$ and $CD8^+$ T cell activation profile in *Unc93b1*$^{Letr/Letr}$ lungs was comparable to the wild type strain and most likely reflects increased infiltration of primed $CD4^+$ and $CD8^+$ T cells from the LALNs.[142, 143] Indeed, the formation of antigen-specific $CD8^+$ T cells and IFN-γ^+CD4^+ T cells at later time points post-infection can occur in the absence of TLR7 activation.[105, 118] Studies in MyD88-deficient mice have also demonstrated that signaling through this adaptor protein is not required for antigen-specific $CD8^+$ T cell activation later in the infection, while evidence for the importance of MyD88 in $CD4^+$ T cell activation is variable.[105, 108]

Immune activation and cell migration following influenza infection is mediated by the expression of a large number of proinflammatory cytokines and chemokines.[64] In our model the loss of *Unc93b1* function led to a reduction in the expression of IFN-γ, CXCL10, and Type I IFN at day 3 post-infection. NK cells can produce IFN-γ in response to IFN-α production by macrophages.[263] Accordingly, the diminished IFN-γ response in the *Unc93b1*$^{Letr/Letr}$ mice at this early time point may be attributable to fewer activated ExMs in the lung. At day 7 post-infection the comparable level of IFN-γ between *Unc93b1*$^{+/+}$ and *Unc93b1*$^{Letr/Letr}$ mice is most likely attributable to production by antigen-specific T cells.[142, 143] CXCL10 primarily attracts lymphocytes to the lungs and can be produced in response to IFN-γ and by cells of both the innate and adaptive immune response, including ExMs.[264, 265] The reduced expression of CXCL10 in *Unc93b1*$^{Letr/Letr}$ mice at day 3 post-infection may also be linked to fewer activated ExMs with comparable induction at day 7 post-infection mediated by infiltrating $CD4^+$ and $CD8^+$ T cells.[142, 143] The selective defect in proinflammatory mediator expression by *Unc93b1*$^{Letr/Letr}$ mice following influenza infection is similar to observations in *Unc93b1*$^{3d/3d}$ mice following *T. gondii* infection as well as patients with HSV-1 encephalitis and natural *UNC93B1* mutations[217, 222].

In contrast to studies of *Unc93b1*$^{3d/3d}$ mice that have shown increased mortality following infection with MCMV, HSV, NSV, *T. cruzi,* and *T. gondii,*[36, 216, 219, 221, 222] the *Unc93b1*$^{Letr/Letr}$ mice and their wild type counterparts had a comparable rate of survival following influenza infection. Nonetheless, during the innate immune response to influenza, *Unc93b1*$^{Letr/Letr}$ mice exhibited several early immune defects including reduced myeloid cell recruitment, lymphoid cell activation, and soluble inflammatory mediator production that collectively led to impaired viral clearance as well as increased tissue inflammation and epithelial reactivity during the course of infection. The different disease outcome in previous studies of *Unc93b1* and the current report indicates that there is a limited requirement for *Unc93b1* in the generation of protective immunity against influenza. Indeed, previous studies have shown that influenza activates a series of inflammatory pathways that could provide compensatory immunity in *Unc93b1*$^{Letr/Letr}$ mice. For example, the cytosolic RIG-I signaling pathway, while not essential for survival, has been implicated in type I IFN expression from myeloid DCs, fibroblasts, and human lung epithelial cells following influenza infection.[41, 55, 108]

NLRP3-dependent activation of caspase-1 is also essential for survival of an influenza infection and the lack of either component leads to decreased recruitment of monocytes and neutrophils to the airways and lower expression of IL-1β, IL-18, CXCL1, and CXCL2 at day 3 post-infection.[107, 116] Remarkably, in the absence of pattern recognition through TLR7 and MAVS, IL-1R signaling in dendritic cells was shown to be necessary and sufficient for the generation of virus-specific $CD8^+$ T cell immunity against influenza.[118] Finally, our data highlight the differences in host response following systemic challenge with a purified PAMP that potently activates a single TLR and mucosal infection with a respiratory virus that activates multiple PRRs with complementary and overlapping immune functions.

In summary, we have demonstrated that *Unc93b1*$^{Letr/Letr}$ mice have defective endosomal TLR activation that diminishes innate immune responses at the site of infection during the early phase of influenza infection. Our study suggests two potential mechanisms by which *Unc93b1* may contribute to innate immunity against influenza. First, *Unc93b1*-dependent type I IFN expression may stimulate ExMs that, in turn, enhance initial IFN-γ production by NK cells and induces CXCL10. Second, *Unc93b1* may mediate endosomal TLR signaling on $CD4^+$ and $CD8^+$ T cells that triggers their activation at the site of infection. Further detailed investigations of *Unc93b1*$^{Letr/Letr}$ mice should reveal the exact mechanisms through which *Unc93b1* regulates the innate immune response to influenza and, potentially, other viral respiratory pathogens.

Materials and Methods

Ethics statement

All experiments using mice were performed according to the guidelines of the Canadian Council on Animal Care and approved by the Animal Use Care Committee of the McGill University Health Centre (Montréal, Canada).

Mice, virus, cell lines

C57BL/6 and 129S1 mice used for ENU mutagenesis and C3H/HeN mice used for breeding were purchased from Harlan Laboratories (Indianapolis, IN). *Unc93b1*$^{3d/3d}$ mice were obtained from the Mutant Mouse Regional Resource Center (UC Davis, Davis, CA). *Unc93b1*$^{+/+}$ and *Unc93b1*$^{Letr/Letr}$ F2 mice on the C57BL/6 background were bred in a specific pathogen-free facility (McGill University Health Centre). The influenza A/PR/8/34 (H1N1) virus was a generous gift from V. von Messling (INRS-Institut Armand-Frappier, Montréal, Canada). Madin-Darby canine kidney (MDCK) cells used for plaque assays were a generous gift from M. Divangahi (McGill University, Montréal, Canada). The B16-Blue IFN α/β cell line was purchased (InvivoGen, San Diego, CA).

ENU mutagenesis and breeding

Mutagenesis of 8-12-week-old G0 male 129S1 mice was conducted as previously described using 150mg/kg of ENU.[266] Following fertility recovery (8-12 weeks post-injection) mutagenized G0 males were crossed to C57BL/6 females in a three-generation breeding scheme for recessive ENU mutations.[267] G1 progeny from distinct G0 pairs were mated and G2 brother-sister matings were performed to produce 1200 G3 progeny for initial phenotypic screening. G2 fathers of G3 mice that displayed a deviant phenotype were outcrossed to C57BL/6 females and the resulting progeny were backcrossed to their G2 fathers. All backcross progeny were re-phenotyped using survival splenectomy and deviant male and female animals were selected for creation of homozygous lines. Deviant animals were outcrossed to C3H/HeN

mice and the F1 progeny were backcrossed to the deviant parent to generate 54 segregating mice used to map the genetic location of the mutation.

In vitro and *in vivo* phenotyping using PAMPs

Whole spleens were removed, placed in 4mL of RPMI (Gibco, Burlington, Canada) supplemented with 1% L-glutamine (Gibco), 1% penicillin/streptomycin (Gibco), 10% fetal bovine serum (FBS) (Gibco), and 0.1% β-mercaptoethanol (Gibco) and mechanically disrupted using the frosted end of a microscope slide (Fisher Scientific, Toronto, Canada). A single cell suspension was created by multiple passages through an 18G 1" and 21G 1" needle using a 5mL syringe (BD Biosciences, Mississauga, Canada). To obtain macrophages, mice were injected intraperitoneally with 1mL of thioglycollate, prepared according to the manufacturer's instructions (BD Biosciences). Seventy-two hours later, cells were recovered by intraperitoneal lavage with 10mL of incomplete RPMI. Following treatment with ACK lysis buffer (0.82% NH_4Cl, 0.1% $KHCO_3$, 0.0038% Na_2EDTA, pH 7.4), and collection by centrifugation, all cells were enumerated with a Coulter Z1 Particle Counter (Becton Coulter, Mississauga, Canada) and $2x10^5$ cells were plated on 96-well tissue culture plates (Sarstedt, Montréal, Canada). Peritoneal cells were incubated for 24 hours in RPMI supplemented with 1% L-glutamine, 1% penicillin/streptomycin, and 10% FBS to allow for macrophage adherence, washed with sterile phosphate-buffered saline (PBS) (Wisent, St-Bruno, Canada) and stimulated with 100ng/mL of LPS from *Escherichia coli* 055:B5[245] (Sigma-Aldrich, Oakville, Canada). Splenocytes were stimulated immediately after plating with 1μM unmethylated CpG oligodeoxynucleotide (CpG ODN)[33] (AlphaDNA, Montréal, Canada), 5μg/mL Imiquimod,[266] (InvivoGen) or 50-150μg/mL polyI:C (InvivoGen). Cell supernatants were harvested 24 or 48 hours after stimulation. For *in vivo* characterization, mice were injected intraperitoneally with 0.5mg/mL of LPS from *Escherichia coli* 055:B5[245], 150μg/mL Imiquimod, 2.5μg/g polyI:C in 20mg/mL D(+)-Galactosamine hydrochloride (DGalN)[30] (Sigma-Aldrich), or 50nmol/mL CpG ODN in 20mg/mL DGalN[33]; delivered in 1mL of sterile PBS. Mice were euthanized three hours post-injection, blood was collected by cardiac puncture and serum was separated using the Z-Gel microtubes

(Sarstedt). Cytokine and chemokine quantification was conducted using commercial ELISA kits (R&D systems, Minneapolis, MN).

Genotyping

gDNA from a panel of 54 (*Letr/Letr* x C3H/HeN) F1 x *Letr/Letr* mice was submitted for typing of 375 informative SNPs using a low-density Illumina genotyping platform and the *Unc93b1* gene was sequenced using gDNA and cDNA derived from normal and deviant mice (The Centre for Applied Genomics, Toronto, Canada). The primers used for gDNA sequencing were: EseqF 5'-GTAGTTGTAAAGAAGTGTGGCA-3', EseqR 5'-GCTAAAGTTGGCAAAGAAGT-3', FseqF 5'-CACCAGAGGCCATGTCCAA-3', FseqR 5'-GGCTGAGAAGACAATGGACTA-3', GseqF 5'-CAAACTGCCACCCCAAAG-3', GseqR 5'-GTTTGCTGGGTGACTGAGTG-3'. The primers used for cDNA sequencing were: UncP12 (reverse): 5'-CCATGAGCACGCTCTCTACA-3', UncP22 (reverse): 5'-GCCTGCCACCAGTGATAGAT-3', UncP23 (reverse): 5'-AAGGGCAGCTGGAAGATGT-3', UncP24 (forward): 5'-ACATCTTCCAGCTGCCCTTC-3', UncP31 (forward): 5'-CACACTCCTGGGCATCCTAT-3', UncP38 (reverse): 5'-CCATGTTGCCATACTTCACCT-3', UncP39 (forward): 5'-CCGGACATCGATAGCAAGAT-3', BGH (reverse): 5'-TAGAAGGCACAGTCGAGG-3', T7 (forward): 5'-TAATACGACTCACTATAGGG-3' (AlphaDNA).

***Unc93b1* PCR and gel electrophoresis**

RNA was extracted from spleens using the RNeasy Plus Mini kit (Qiagen, Toronto, Canada) with DNase digestion using the RNase-Free DNase Set (Qiagen) according to the manufacturer's instructions. Reverse transcription was carried out using the High Capacity cDNA Archive Kit (Applied Biosystems, Burlington, Canada). PCR was performed on 20ng of cDNA with 10µL 5x Herculase Buffer and 0.5µL Herculase Polymerase (Agilent, Mississauga, Canada), 5µL dNTP (Invitrogen, Burlington, Canada), and 100ng of each primer (forward: 5'-GGTGCCCAGAACTGCAAG-3' reverse: 5'-CCATGAGCACGCTCTCTACA-3') in a final volume of 50µL. The PCR cycling conditions were 94°C for 10 minutes, 35 cycles of 94°C for 30 seconds/52°C for 30 seconds/72°C for 1 minute, and 72°C for 7 minutes. The PCR product was visualized on a 1% agarose gel in TAE buffer containing 0.5µg/mL of ethidium bromide.

Analysis of *Unc93b1* sequence and protein structure

The relative size of the *Unc93b1* introns and exons was determined from the Ensembl database (ENSMUST00000162708). UNC93B1 amino acid sequences were derived from the NCBI nucleotide database for the following species *Mus musculus* (NM_019449.2), *Homo sapiens* (NM_030930.2), *Pan troglodytes* (XM_003313185.1), *Canis familiaris* (XM_540813.3), *Felis catus* (XM_003993751.1), *Bos taurus* (NM_001193147.1), *Equus caballus* (XM_001916968.2), *Ovis aries* (XM_004023404.1), and *Xenopus tropicalis* (NM_001100253.1). The amino acid sequences were aligned using Clustal Omega software, version 1.2 (European Molecular Biology Laboratory, Heidelberg, Germany).[268] To determine the predicted three-dimensional protein structure, the wild type UNC93B1 amino acid sequence was entered into the Protein Homology/analogY Recognition Engine (Phyre), version 2.0 (Structural Bioinformatics Group, Imperial College, London, UK).[269] The predicted model, including the location of the *3d* and *Letr* mutations, was visualized using the PyMol Molecular Graphics System, version 1.7 (Schrödinger, LLC).[270]

***In vivo* influenza infection**

6-week-old *Unc93b1*$^{+/+}$ and *Unc93b1*$^{Letr/Letr}$ F2 mice were anaesthetized by intraperitoneal injection of 150mg/kg of ketamine (Bioniche, Pointe-Claire, Canada) and 10mg/kg of xylazine (Bayer, Toronto, Canada) in sterile PBS and infected intranasally with 400 pfu of influenza A/PR/8/34 (H1N1). Infected mice were monitored daily for signs of sickness and sacrificed if they appeared moribund.

Flow cytometry

Lungs were extracted, placed in 5mL of incomplete DMEM, finely chopped with a no.23 scalpel and incubated with a further 5mL of RPMI supplemented with 300U/mL of Collagenase (Sigma-Aldrich) for 1 hour at 37°C in 5% CO_2. The tissue was then passed multiple times through a 16G 1" needle and a 100µM nylon strainer (BD Biosciences) and collected by centrifugation. LALN cells were prepared as described for splenocytes. Red blood cells were lysed with ACK

buffer and cells were counted using a hemocytometer. Cells were stained with Fixable Viability Dye-efluor780 (eBioscience, San Diego, CA) and, following a wash in sterile PBS, F_c receptors were blocked using the anti-mouse CD16/CD32 (clone 93) antibody (eBioscience). Cells were then fluorescently labeled using cocktails of fluorescence-conjugated antibodies: rat anti-mouse CD45-V500 (clone 30-F11), rat anti-mouse Ly6G-Alexa Fluor 700 (clone 1A8), rat anti-mouse CD45R/B220-PECF594 (clone RA3-6B2) (BD Biosciences); anti-mouse/human CD11b-Brilliant Violet 711 (clone M1/70), anti-mouse CD11c-Brilliant Violet 605 (clone N418), anti-mouse CD80-PE (clone 16-10A1), anti-mouse CD8a-Alexa Fluor 700 (clone 53-6.7), anti-mouse CD62L-Brilliant Violet 605 (clone MEL-14), anti-mouse CD69-PE/Cy7 (clone H1.2F3) (BioLegend, San Diego, CA); anti-mouse MHC class II (I-A/I-E)-PE/Cy7 (clone M5/114.15.2), anti-mouse CD3e-FITC (clone 145-2C11), anti-mouse CD4-eFluor450 (clone GK1.5), anti-mouse CD49b-allophycocyanin (clone DX5), anti-mouse CD44-PE (clone IM7) (eBioscience). Data was collected on the LSRFortessa using FACSDiva, version 6.2 (BD Biosciences) and analyzed using FlowJo, version 9.1 (Tree Star Inc., Ashland, OR) with fluorescence-minus-one gating controls.

Bronchoalveolar lavage and lung inflammatory mediator quantification

Following euthanasia, bronchoalveolar lavage (BAL) fluid was collected from the airways by inserting a 22G 1" catheter into the mouse trachea and slowly injecting and removing four-0.5mL aliquots of ice-cold sterile PBS. Cells were removed from BAL fluid by centrifugation. Lungs were perfused with 10mL of sterile PBS via the right ventricle, excised, and placed in 2mL of sterile PBS supplemented with 1x Halt protease inhibitor cocktail (Fisher Scientific). Lungs were processed using a rotor-stator homogenizer (Fisher Scientific) and samples were centrifuged to pellet insoluble material. BAL fluid and lung homogenate were stored at -80°C until further analysis. ELISAs were used for protein quantification according to the manufacturer's instructions (R&D Systems). Type I IFN was quantified using B16-Blue cells that were cultured using standard techniques in RPMI media supplemented with 1% L-glutamine, 0.5% penicillin/streptomycin, 10% FBS, and 0.2% Normocin (InvivoGen). After two passages, cells were washed with sterile PBS and cultured in the same media with the addition of 0.1% Zeocin (InvivoGen) for an additional two or three passages. 20µL/well of BAL sample,

recombinant IFN-β (positive control) (PBL Interferon Source, Piscataway, NJ), or sterile PBS (negative control) was added to a 96-well tissue culture plate and $7.56x10^4$ B16-Blue cells (in a volume of 180µL) were added to these wells and incubated at 37°C in 5% CO_2 for 24 hours. 20µL of this culture supernatant was added to a new 96-well plate containing 180µL of Quanti-Blue medium, prepared according to the manufacturer's instructions (InvivoGen), and incubated at 37°C for 3.5 hours. Absorbance was measured at 655nm and type I IFN quantified as the fold change in expression relative to uninfected airway.

Viral quantification by plaque assay

Lungs were extracted from mice at multiple time points post-infection and placed in incomplete DMEM (Wisent) at a 20% weight/volume ratio. Lungs were homogenized using a rotor-stator homogenizer and supernatants were collected by centrifugation. MDCK cells were cultured using standard techniques in DMEM supplemented with 1% L-glutamine, 1% penicillin/streptomycin, and 10% FBS. Three-six cell passages were conducted before one million cells were plated/well on a 6-well plate and incubated overnight at 37°C in 5% CO_2. Plaque assays were performed in a similar manner to a previous protocol.[98] Briefly, cells were washed twice with sterile PBS and 100µL of serially diluted lung homogenate in incomplete DMEM was added. Following a 30 minute incubation at 37°C in 5% CO_2, sample was removed and cells were covered with 3mL of a 1:1 mixture of 1.6% agarose and 2x MEM (Gibco) supplemented with 6% of a 7.5% $NaHCO_3$ solution (BioShop Canada Inc., Burlington, Canada), 1% L-glutamine, 2% penicillin/streptomycin, and 0.1% TPCK-trypsin (Sigma-Aldrich). After a 48 hour incubation at 37°C in 5% CO_2, 3mL of a 3:1 methanol (Sigma-Aldrich) and acetic acid (Fisher Scientific) solution was added. Four hours following, the solution and agarose plugs were removed and plates were allowed to dry for 24 hours. Plaques were visualized by staining with a 0.2% Crystal Violet solution in 20% ethanol (Sigma-Aldrich).

Lung histology

Lungs were flushed with 10mL of PBS via the right ventricle. A catheter was inserted into the trachea and lungs were allowed to expand to a pressure of 25cm using 10% buffered

formalin acetate (Fisher Scientific). Inflated lungs were then placed in 5mL of 10% buffered formalin acetate and subsequently embedded in paraffin, sectioned at 5µm, and stained with H&E at the Histology Facility of the Goodman Cancer Research Centre (McGill University, Montréal, Canada). Representative photographs of lung sections were taken using a BX51 microscope (Olympus, Richmond Hill, Canada), QICAM Fast 1394 digital CCD camera (QImaging, Surrey, Canada) and Image-Pro Plus software version 7.0.1.658 (Media Cybernetics, Rockville, MD).

Statistical analysis

Survival curve analysis was performed using the Logrank test. For comparison between multiple columns a 1-way ANOVA with Dunnett's or Tukey's post-hoc test was used. A two-tailed unpaired t-test was conducted for all other pairwise comparisons. Statistical analysis was performed using GraphPad Prism 4 (GraphPad Software, La Jolla, CA).

Acknowledgements

We thank Gregory Boivin and François Coulombe for advice with experimental procedures, Marie-Line Goulet for advice on experimental design as well as helpful comments on the manuscript, and Dr. David Logan Burk for help with three-dimensional protein modeling. We also acknowledge Dr. Veronika von Messling and Dr. Maziar Divangahi for providing materials and advice on working with the influenza virus.

This work was supported by a CIHR Team Grant in Mouse Mutagenesis and Infectious Diseases (CTP-87520), a Canada Research Chair in Host Resistance to Respiratory Infections (STQ), and the Fonds de Recherche du Québec – Santé. EIL is a recipient of awards from the CIHR Québec Respiratory Health Training Program, the McGill University Health Centre, and the McGill University Faculty of Medicine.

Conflict of Interest

The authors declare no potential conflicts of interest that are relevant to this manuscript.

Figures

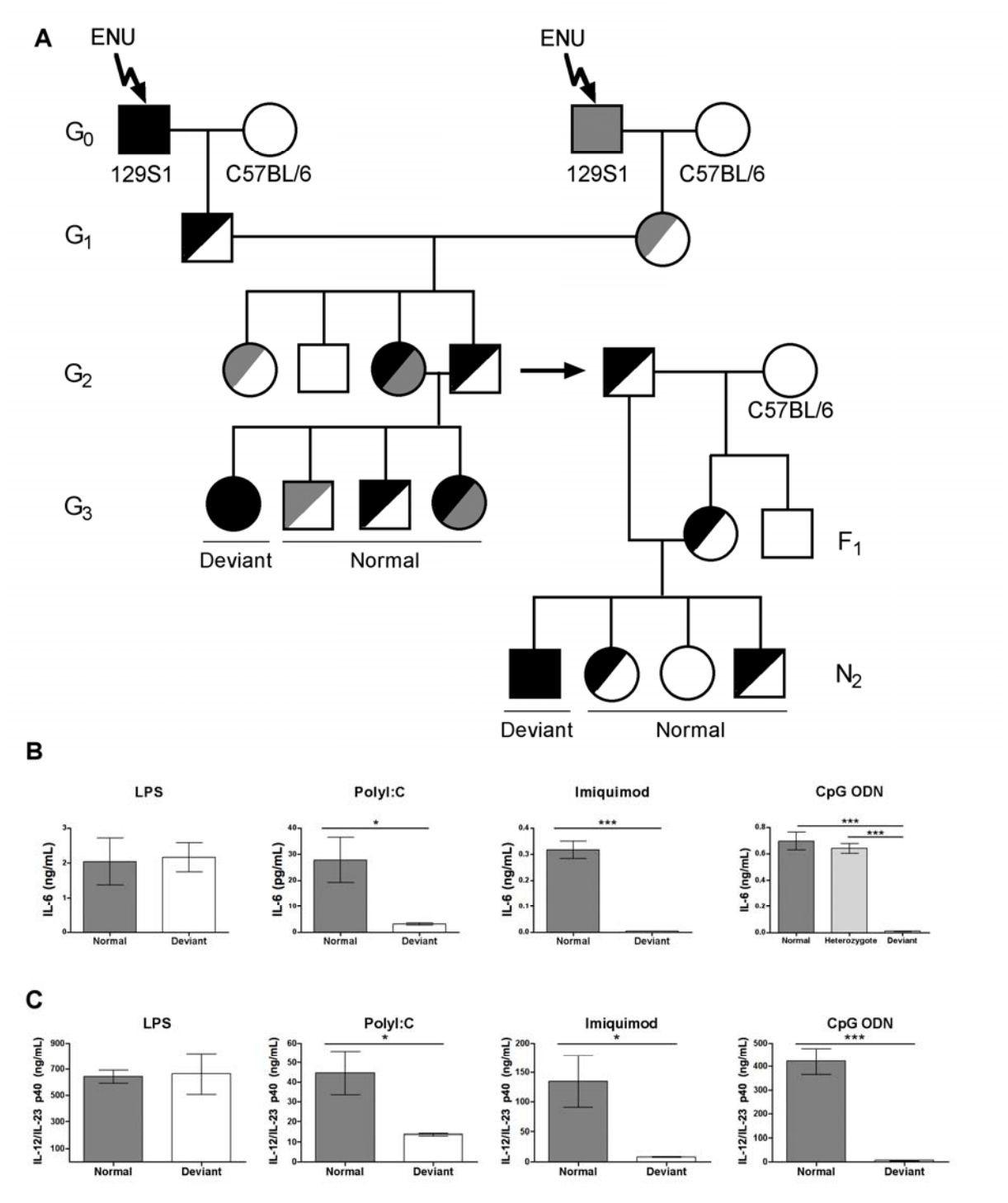

Figure 2.1

Figure 2.1. ENU mutagenesis establishes a mouse model with defective endosomal TLR signaling.

(A) Strategy used for the creation and characterization of mice with a recessive germline mutation caused by ENU. A detailed description of the breeding scheme can be found in the materials and methods section of this manuscript. Mice were screened at the G3 generation while N2 mice and their progeny were used for sequencing, phenotype confirmation, and creation of the F2 line for subsequent experiments. Black and grey shading denotes one (half-shaded) or two (fully-shaded) copies of an ENU mutation. (B) IL-6 expression in cell culture supernatants from normal (dark grey bars), heterozygous (light grey bars) and deviant (white bars) mice. Thioglycollate-elicited peritoneal macrophages were stimulated with LPS and splenocytes were stimulated with polyI:C, Imiquimod, or CpG ODN for 24 (LPS, Imiquimod, CpG ODN) or 48 (polyI:C) hours. (C) Serum IL-12/IL-23 p40 expression three hours post-intraperitoneal injection of LPS, polyI:C, Imiquimod, or CpG ODN. Data is representative of two independent experiments ($n \geq 3$/group or $n \geq 4$ technical replicates/group). *$p<0.05$; ***$p<0.001$ determined by two-tailed unpaired t-test or one-way ANOVA with Tukey's post-test. Main p value determined by one-way ANOVA for *in vitro* CpG stimulation: ***$p<0.0001$.

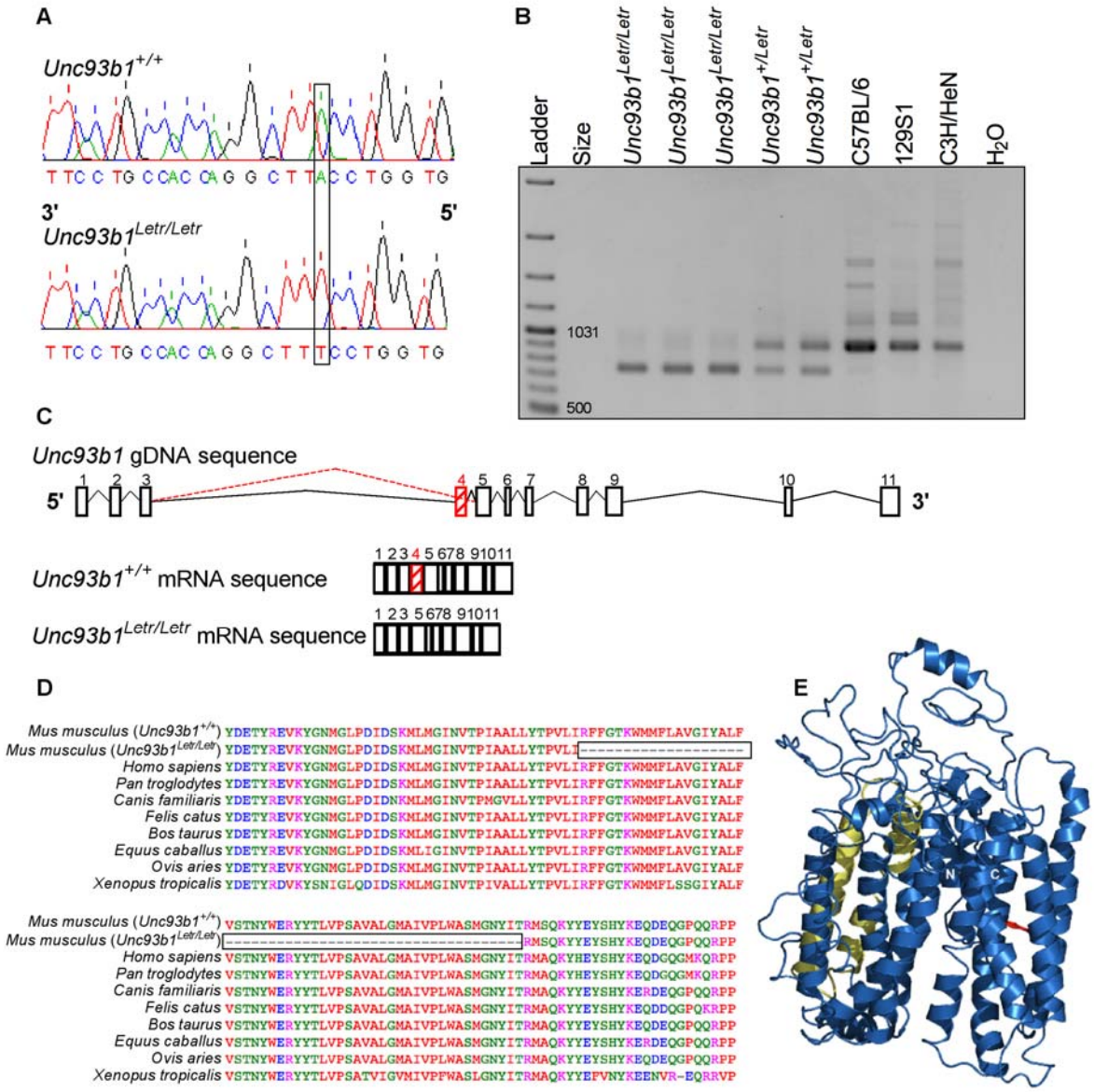
A
Unc93b1+/+
T T C C T G C C A C C A G G C T T A C C T G G T G
3'
5'
Unc93b1Letr/Letr
T T C C T G C C A C C A G G C T T T C C T G G T G
B
Ladder
Size
Unc93b1Letr/Letr
Unc93b1Letr/Letr
Unc93b1Letr/Letr
Unc93b1+/Letr
Unc93b1+/Letr
C57BL/6
129S1
C3H/HeN
H2O
1031
500
C
Unc93b1 gDNA sequence
5'
1
2
3
4
5
6
7
8
9
10
11
3'
Unc93b1+/+ mRNA sequence
1 2 3 4 5 6 7 8 9 10 11
Unc93b1Letr/Letr mRNA sequence
1 2 3 5 6 7 8 9 10 11
D
Mus musculus (Unc93b1+/+) YDETYREVKYGNMGLPDIDSKMLMGINVTPIAALLYTPVLIRFFGTKWMMFLAVGIYALF
Mus musculus (Unc93b1Letr/Letr) YDETYREVKYGNMGLPDIDSKMLMGINVTPIAALLYTPVLI----------
Homo sapiens YDETYREVKYGNMGLPDIDSKMLMGINVTPIAALLYTPVLIRFFGTKWMMFLAVGIYALF
Pan troglodytes YDETYREVKYGNMGLPDIDSKMLMGINVTPIAALLYTPVLIRFFGTKWMMFLAVGIYALF
Canis familiaris YDETYREVKYGNMGLPDIDNKMLMGINVTPMGVLLYTPVLIRFFGTKWMMFLAVGIYALF
Felis catus YDETYREVKYGNMGLPDIDSKMLMGINVTPIAALLYTPVLIRFFGTKWMMFLAVGIYALF
Bos taurus YDETYREVKYGNMGLPDIDSKMLMGINVTPIAALLYTPVLIRFFGTKWMMFLAVGIYALF
Equus caballus YDETYREVKYGNMGLPDIDSKMLIGINVTPIAALLYTPVLIRFFGTKWMMFLAVGIYALF
Ovis aries YDETYREVKYGNMGLPDIDSKMLMGINVTPIAALLYTPVLIRFFGTKWMMFLAVGIYALF
Xenopus tropicalis YDETYRDVKYSNIGLQDIDSKMLMGINVTPIVALLYTPVLIRFFGTKWMMFLSSGIYALF
Mus musculus (Unc93b1+/+) VSTNYWERYYTLVPSAVALGMAIVPLWASMGNYITRMSQKYYEYSHYKEQDEQGPQQRPP
Mus musculus (Unc93b1Letr/Letr) ----------RMSQKYYEYSHYKEQDEQGPQQRPP
Homo sapiens VSTNYWERYYTLVPSAVALGMAIVPLWASMGNYITRMAQKYHEYSHYKEQDGQGMKQRPP
Pan troglodytes VSTNYWERYYTLVPSAVALGMAIVPLWASMGNYITRMAQKYHEYSHYKEQDGQGMKQRPP
Canis familiaris VSTNYWERYYTLVPSAVALGMAIVPLWASMGNYITRMAQKYYEYSHYKERDEQGPQQRPP
Felis catus VSTNYWERYYTLVPSAVALGMAIVPLWASMGNYITRMAQKYYEYSHYKEQDDQGPQKRPP
Bos taurus VSTNYWERYYTLVPSAVALGMAIVPLWASMGNYITRMAQKYYEYSHYKEQDEQGPQQRPP
Equus caballus VSTNYWERYYTLVPSAVALGMAIVPLWASMGNYITRMAQKYYEYSHYKERDEQGPQQRPP
Ovis aries VSTNYWERYYTLVPSAVALGMAIVPLWASMGNYITRMAQKYYEYSHYKEQDEQGPQQRPP
Xenopus tropicalis VSTNYWERYYTLVPSATVIGVMIVPFWASLGNYITRMAQKYYEFVNYKEENVR-EQRRVP
E
N
C

Figure 2.2

Figure 2.2. The *Letr* allele causes a single nucleotide transversion and alternative splicing of *Unc93b1*.

(A) Chromatogram of the *Unc93b1*$^{+/+}$ (top) and *Unc93b1*$^{Letr/Letr}$ (bottom) gDNA sequence with the single T to A nucleotide change caused by the *Letr* mutation that is identified on the non-coding strand as A to T. (B) Gel electrophoresis of cDNA from *Unc93b1*$^{Letr/Letr}$, *Unc93b1*$^{+/Letr}$, and wild type inbred strains (C57BL/6, 129S1, C3H/HeN). The wild type transcript size is 918bp while the mutant transcript size is 756bp. (C) Schematic of *Unc93b1* introns (lines) and exons (blocks), including the mutant (dashed red line) splicing pattern and resulting mRNA transcripts for *Unc93b1*$^{+/+}$ and *Unc93b1*$^{Letr/Letr}$ mice. (D) Multiple species alignment of the UNC93B1 amino acid sequence surrounding and including exon 4. The boxed area delineates the missing sequence in *Unc93b1*$^{Letr/Letr}$ mice. (E) Predicted three-dimensional structure of wild type UNC93B1 with the *3d* (red) and *Letr* (yellow) mutations mapped to their respective protein domains. The amino- and carboxy-termini are indicated as N and C, respectively.

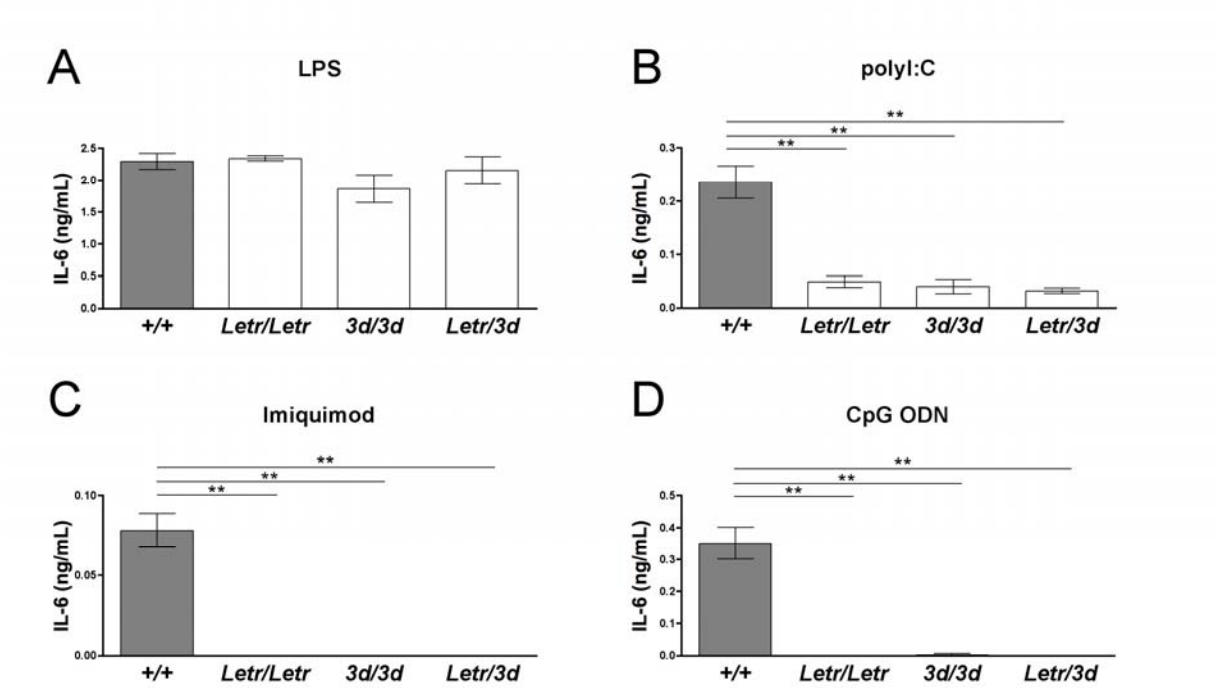
A
LPS
IL-6 (ng/mL)
2.5
2.0
1.5
1.0
0.5
0.0
+/+
Letr/Letr
3d/3d
Letr/3d
B
polyI:C
**
**
**
IL-6 (ng/mL)
0.3
0.2
0.1
0.0
+/+
Letr/Letr
3d/3d
Letr/3d
C
Imiquimod
**
**
**
IL-6 (ng/mL)
0.10
0.05
0.00
+/+
Letr/Letr
3d/3d
Letr/3d
D
CpG ODN
**
**
**
IL-6 (ng/mL)
0.5
0.4
0.3
0.2
0.1
0.0
+/+
Letr/Letr
3d/3d
Letr/3d

Figure 2.3

Figure 2.3. Lack of complementation confirms that the *Letr* mutation is in *Unc93b1*.

IL-6 expression of (A) thioglycollate-elicited peritoneal macrophages or (B-D) splenocytes from *Unc93b1*$^{+/+}$, *Unc93b1*$^{Letr/Letr}$, *Unc93b1*$^{3d/3d}$, and *Unc93b1*$^{Letr/3d}$ F1 mice following *in vitro* stimulation with (A) LPS, (B) polyI:C, (C) Imiquimod, or (D) CpG ODN for 24 (LPS, Imiquimod, CpG ODN) or 48 (polyI:C) hours. Data is representative of duplicate stimulations (n≥3/group). **p<0.01 determined by one-way ANOVA with Dunnett's post-test comparing all mutant strains to the *Unc93b1*$^{+/+}$ strain. Main p values determined by one-way ANOVA: (A) ns (B-D) ***p<0.001.

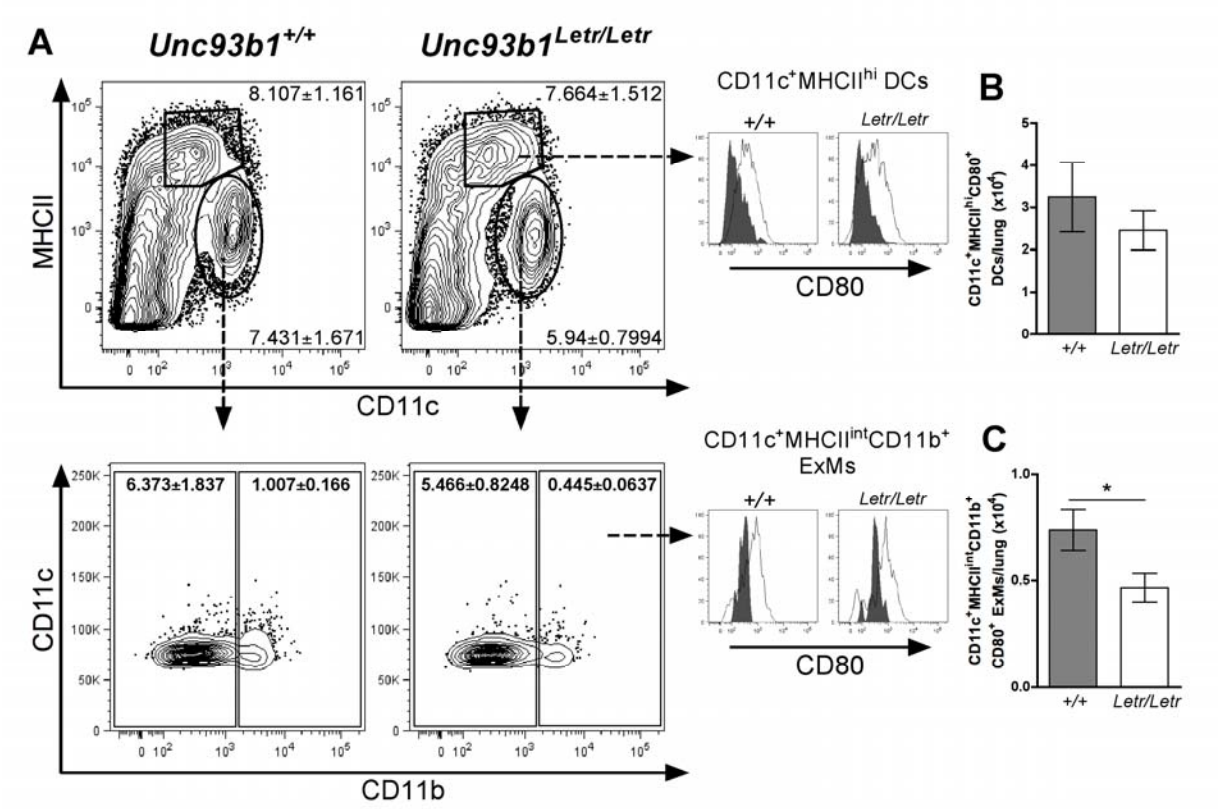
A
Unc93b1+/+
Unc93b1Letr/Letr
8.107±1.161
7.664±1.512
7.431±1.671
5.94±0.7994
MHCII
CD11c
CD11c+MHCIIhi DCs
+/+
Letr/Letr
CD80
B
CD11c+MHCIIhiCD80+ DCs/lung (x10⁴)
6.373±1.837
1.007±0.166
5.466±0.8248
0.445±0.0637
CD11c
CD11b
CD11c+MHCIIintCD11b+ ExMs
C
CD11c+MHCIIintCD11b+ CD80+ ExMs/lung (x10⁴)
*

Figure 2.4

Figure 2.4. *Unc93b1*$^{Letr/Letr}$ lungs have fewer activated ExMs but not DCs following infection.
(A) Representative dot plots of CD11c^{+}MHCII^{hi} DCs, CD11c^{+}MHCII^{int} macrophages, CD11b^{-} AMs, and CD11b^{+} ExMs. For precise analysis, all samples were gated on live, CD45^{+}, B220^{-}, Ly6G^{-} cells to eliminate potentially confounding B cell and neutrophil populations prior to identification of specific myeloid cell subsets. Numbers on each dot plot represent the percentage (mean ± SEM) of total live, CD45^{+} cells in each subset at day 3 post-infection. Histograms represent CD80 expression on DCs (top) and ExMs (bottom) in *Unc93b1*$^{+/+}$ and *Unc93b1*$^{Letr/Letr}$ lungs at day 0 (grey peaks) and day 3 (white peaks) post-infection. Absolute number of (B) CD80^{+} DCs and (C) CD80^{+} ExMs in the lungs of *Unc93b1*$^{+/+}$ (grey bars) and *Unc93b1*$^{Letr/Letr}$ (white bars) mice at day 3 post-infection. Data is representative of two independent experiments (n=6/group). *$p<0.05$ determined by two-tailed unpaired t-test.

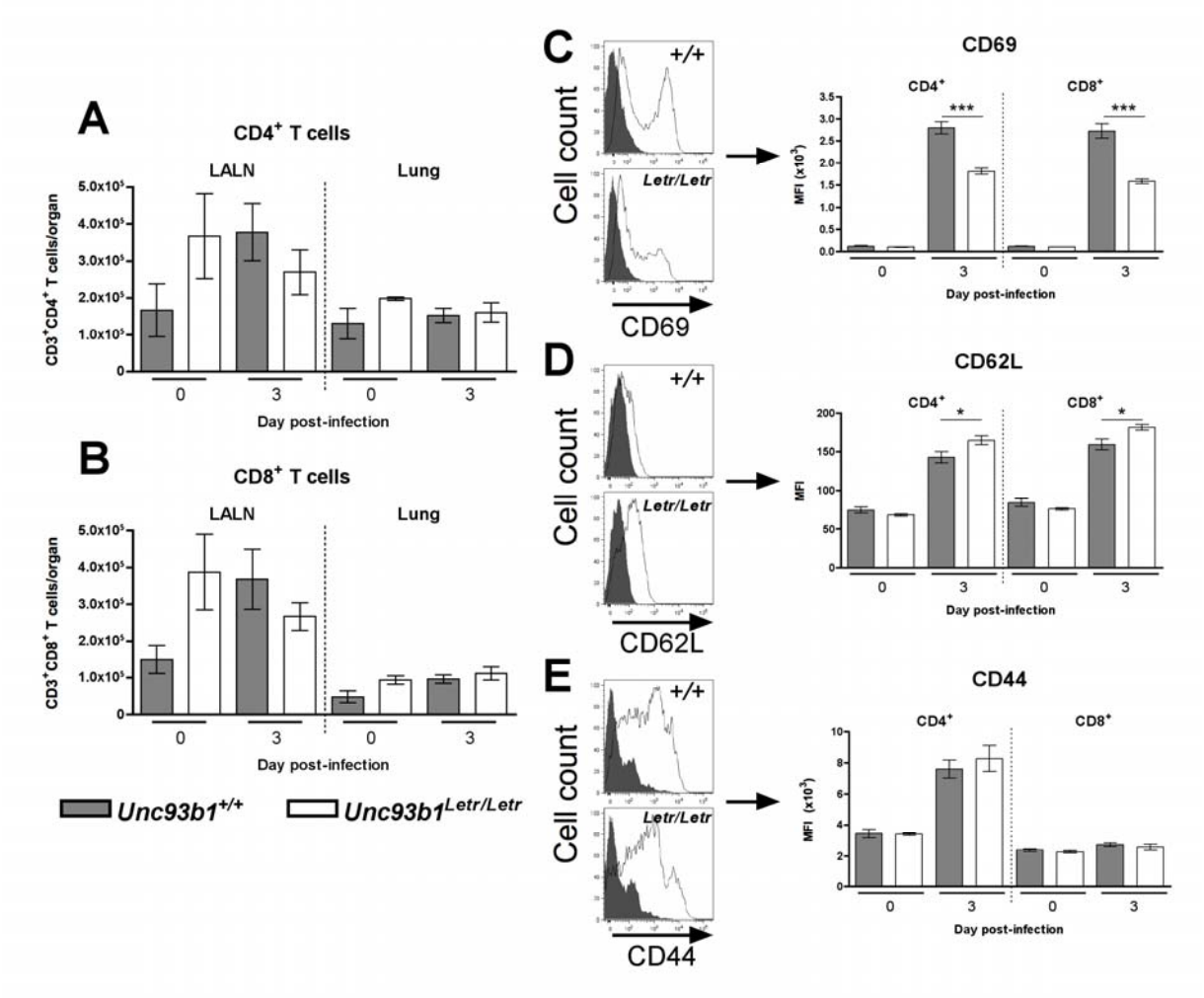
A
CD4+ T cells
LALN
Lung
CD3+CD4+ T cells/organ
5.0x10⁵
4.0x10⁵
3.0x10⁵
2.0x10⁵
1.0x10⁵
0
0
3
0
3
Day post-infection
B
CD8+ T cells
LALN
Lung
CD3+CD8+ T cells/organ
5.0x10⁵
4.0x10⁵
3.0x10⁵
2.0x10⁵
1.0x10⁵
0
0
3
0
3
Day post-infection
Unc93b1+/+
Unc93b1Letr/Letr
C
Cell count
+/+
Letr/Letr
CD69
CD69
CD4+
CD8+
***
***
MFI (x10³)
3.5
3.0
2.5
2.0
1.5
1.0
0.5
0.0
0
3
0
3
Day post-infection
D
Cell count
+/+
Letr/Letr
CD62L
CD62L
CD4+
CD8+
*
*
MFI
200
150
100
50
0
0
3
0
3
Day post-infection
E
Cell count
+/+
Letr/Letr
CD44
CD44
CD4+
CD8+
MFI (x10³)
10
8
6
4
2
0
0
3
0
3
Day post-infection

Figure 2.5

Figure 2.5. Early activation of $CD4^+$ and $CD8^+$ T cells is diminished in *Unc93b1*$^{Letr/Letr}$ lungs following infection.

Absolute number of live, $CD45^+$, $CD3^+$, $CD49b^-$ (A) $CD4^+$ and (B) $CD8^+$ T cells in the LALNs and lungs of *Unc93b1*$^{+/+}$ (grey bars) and *Unc93b1*$^{Letr/Letr}$ (white bars) mice. Mean fluorescence intensity (MFI) of (C) CD69, (D) CD62L, and (E) CD44 on *Unc93b1*$^{+/+}$ and *Unc93b1*$^{Letr/Letr}$ lung $CD4^+$ and $CD8^+$ T cells. Representative histograms for each activation marker show expression at day 0 (grey peak) and day 3 (white peak) post-infection. Data is representative of two independent experiments for infected mice and one experiment for uninfected mice (n=4-6/group). *p<0.05; ***p<0.001 determined by two-tailed unpaired t-test.

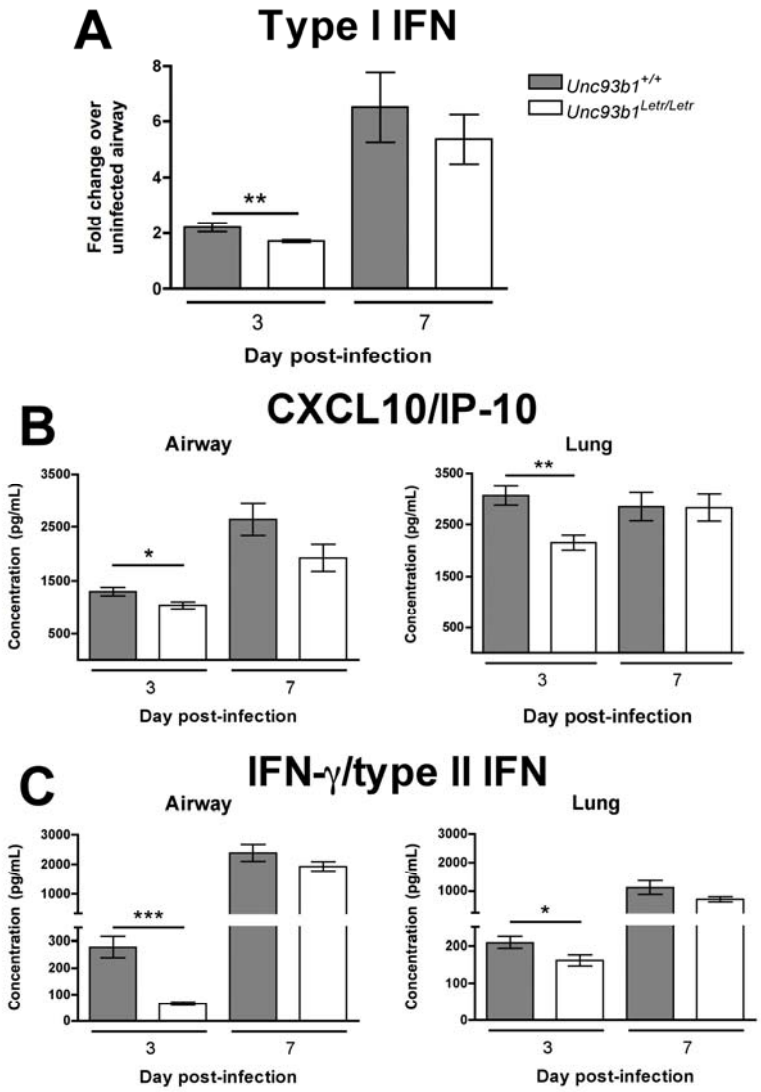
A
Type I IFN
Unc93b1+/+
Unc93b1Letr/Letr
Fold change over uninfected airway
**
Day post-infection
B
CXCL10/IP-10
Airway
Lung
Concentration (pg/mL)
*
**
Day post-infection
C
IFN-γ/type II IFN
Airway
Lung
***
*
Day post-infection

Figure 2.6

Figure 2.6. Defective *Unc93b1*-dependent signaling leads to reduced expression of type I/II IFN and CXCL10.

(A) Relative type I IFN expression in the airways of *Unc93b1*$^{+/+}$ (grey bars) and *Unc93b1*$^{Letr/Letr}$ (white bars) mice at day 3 and 7 following influenza infection. Data is expressed as fold change compared to uninfected samples. Airway and lung expression of (B) CXCL10 and (C) IFN-γ from *Unc93b1*$^{+/+}$ and *Unc93b1*$^{Letr/Letr}$ mice at day 3 and 7 post-infection. Data is pooled from two independent experiments (n≥9/group). *p<0.05; **p<0.01; ***p<0.001 determined by two-tailed unpaired t-test.

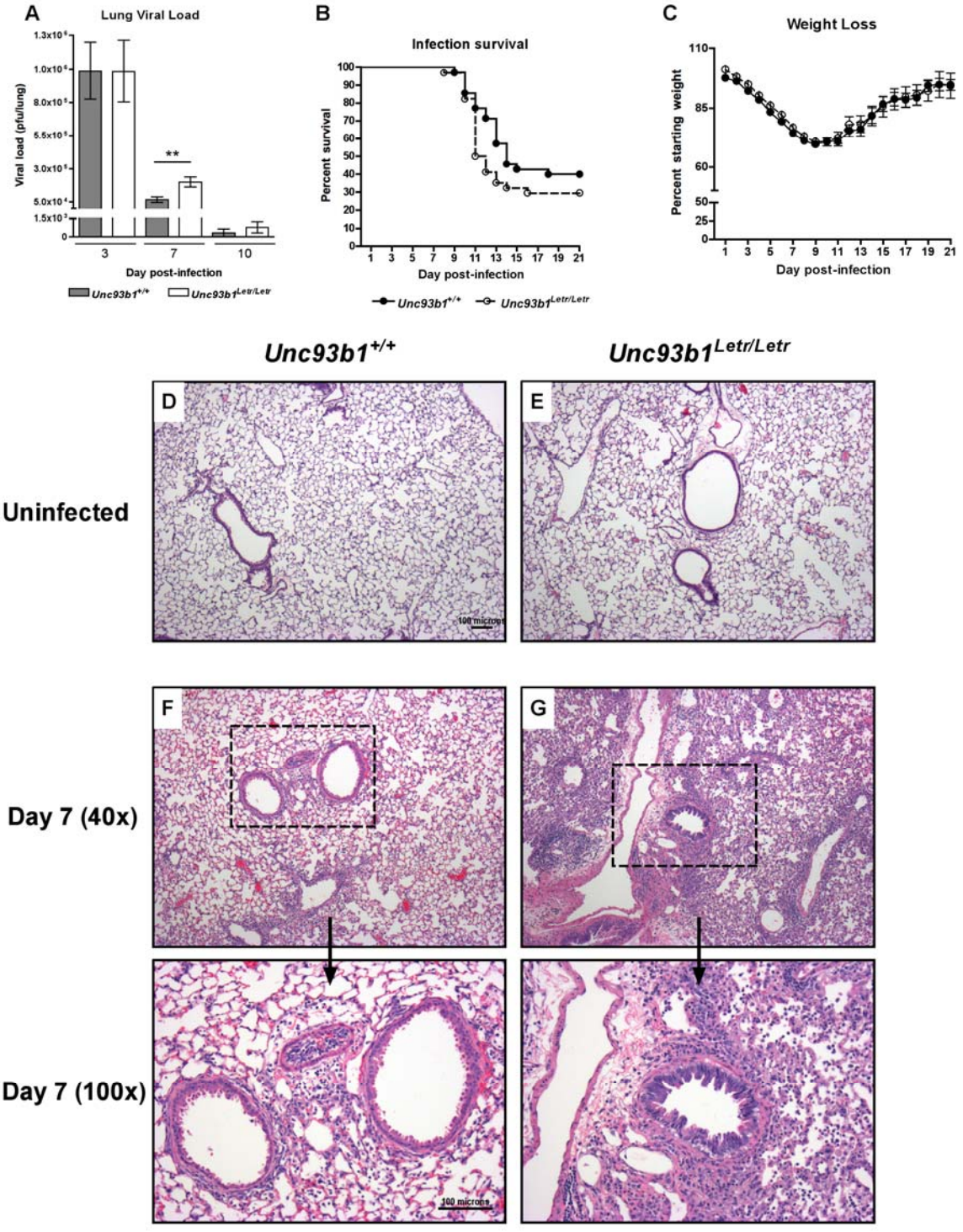
A
Lung Viral Load
Viral load (pfu/lung)
**
Day post-infection
Unc93b1+/+
Unc93b1Letr/Letr
B
Infection survival
Percent survival
Day post-infection
Unc93b1+/+
Unc93b1Letr/Letr
C
Weight Loss
Percent starting weight
Day post-infection
Unc93b1+/+
Unc93b1Letr/Letr
Uninfected
D
E
Day 7 (40x)
F
G
Day 7 (100x)
100 microns

Figure 2.7

Figure 2.7. *Unc93b1* plays a role in mediating viral clearance and tissue inflammation but does not influence survival following influenza A/PR/8/34 (H1N1) infection.

(A) Lung viral load in *Unc93b1*$^{+/+}$ (grey bars) and *Unc93b1*$^{Letr/Letr}$ (white bars) mice at day 3, 7, and 10 following influenza infection. (B) Survival and (C) weight loss of *Unc93b1*$^{+/+}$ (solid line) and *Unc93b1*$^{Letr/Letr}$ (dashed line) mice over a 21-day period following influenza infection. Representative lung sections from (D, E) uninfected or (F, G) infected lungs at day 7 post-infection of (D, F) *Unc93b1*$^{+/+}$ and (E, G) *Unc93b1*$^{Letr/Letr}$ mice. Day 7 post-infection is visualized at 40x and 100x magnification. Data is pooled from independent experiments. (A) n≥10/group, (B) n≥34/group, (C) n≥27/group. **p<0.01 determined by (A) two-tailed unpaired t-test or (B) Logrank test.

Supplementary Figures

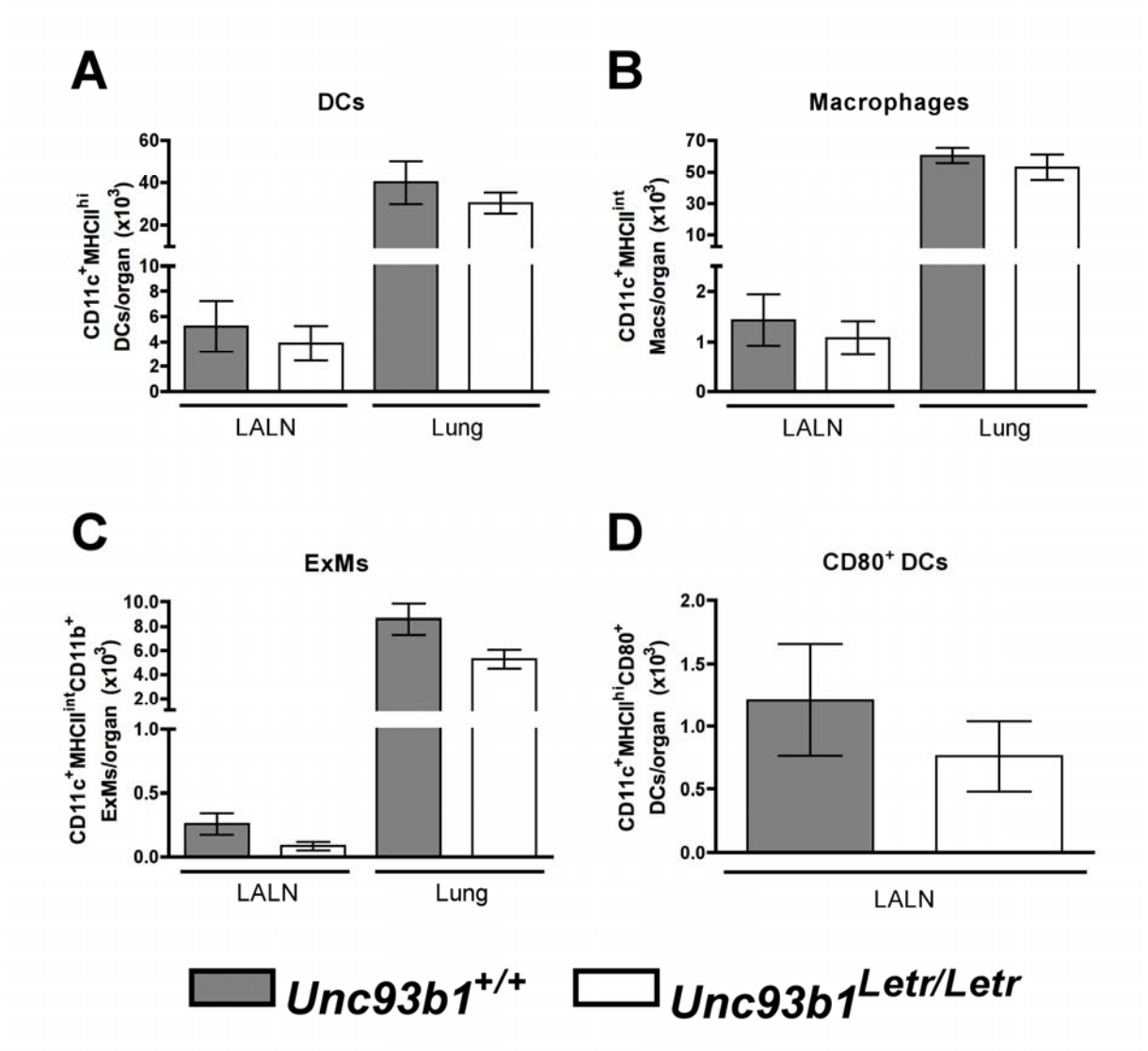

Supplementary Figure 2.1

Supplementary Figure 2.1. Equivalent number of APCs in LALNs and lungs of *Unc93b1*$^{+/+}$ and *Unc93b1*$^{Letr/Letr}$ mice at day 3 post-infection.

Absolute number of LALN and lung (A) CD11c^{+}MHCII^{hi} DCs, (B) CD11c^{+}MHCII^{int} macrophages, (C) CD11c^{+}MHCII^{int}CD11b^{+} ExMs in *Unc93b1*$^{+/+}$ (grey bars) and *Unc93b1*$^{Letr/Letr}$ (white bars) mice. (D) Absolute number of CD80^{+} DCs in the LALNs of *Unc93b1*$^{+/+}$ and *Unc93b1*$^{Letr/Letr}$ mice. Data is representative of two independent experiments (n=6/group).

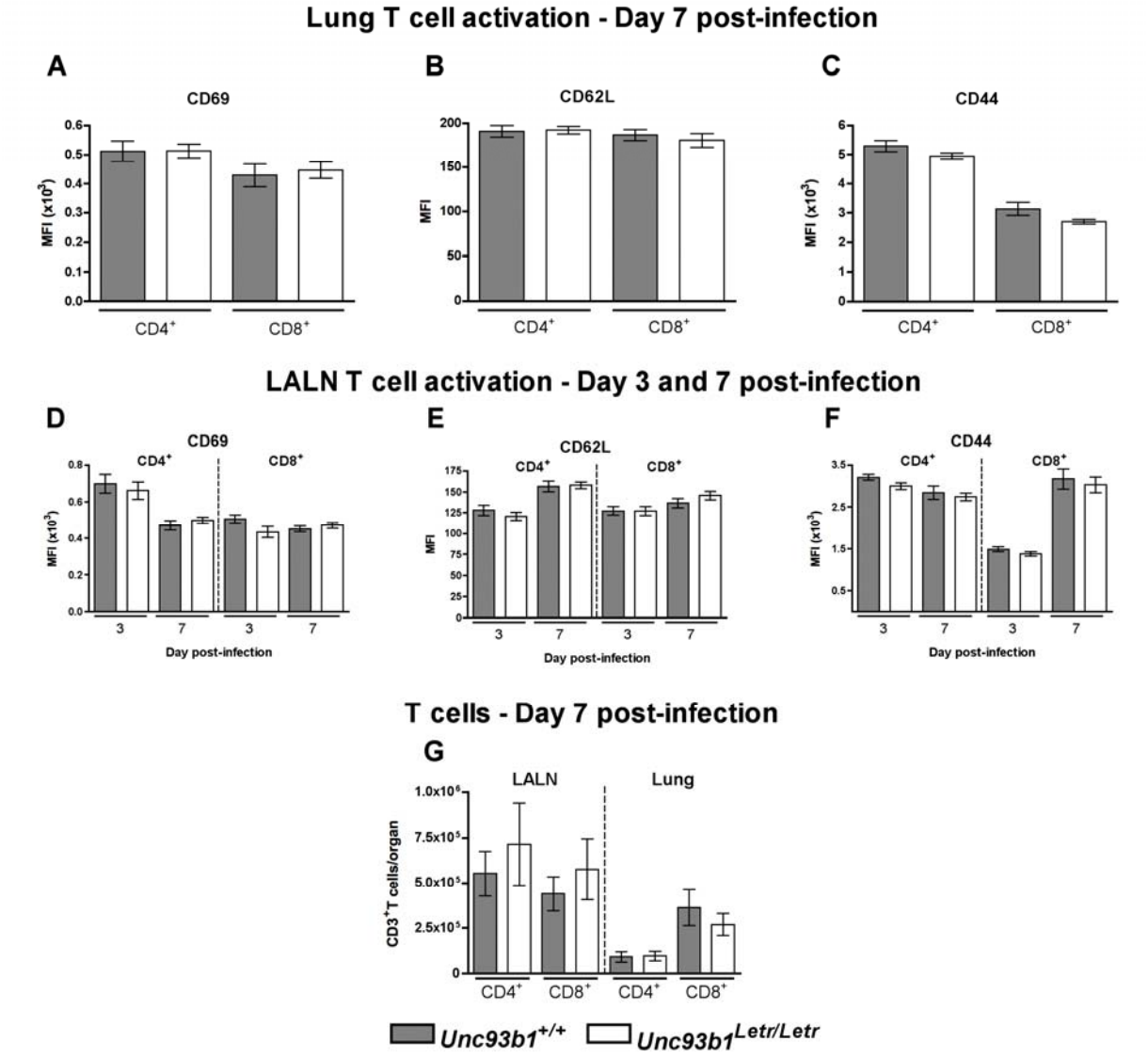

Supplementary Figure 2.2

Supplementary Figure 2.2. Similar activation of T cells in the lungs at day 7 and the LALNs at day 3 and day 7 post-infection between *Unc93b1*$^{+/+}$ and *Unc93b1*$^{Letr/Letr}$ mice.

Expression of (A) CD69, (B) CD62L, and (C) CD44 activation markers on lung CD4^{+} and CD8^{+} T cells at day 7 post-infection from *Unc93b1*$^{+/+}$ (grey bars) and *Unc93b1*$^{Letr/Letr}$ (white bars) mice. Expression of (D) CD69, (E) CD62L, and (F) CD44 activation markers on LALN CD4^{+} and CD8^{+} T cells at day 3 and 7 post-infection. (G) Absolute number of CD4^{+} and CD8^{+} T cells in the LALNs and lungs at day 7 post-infection. Data is representative of two independent experiments (n=5-6/group).

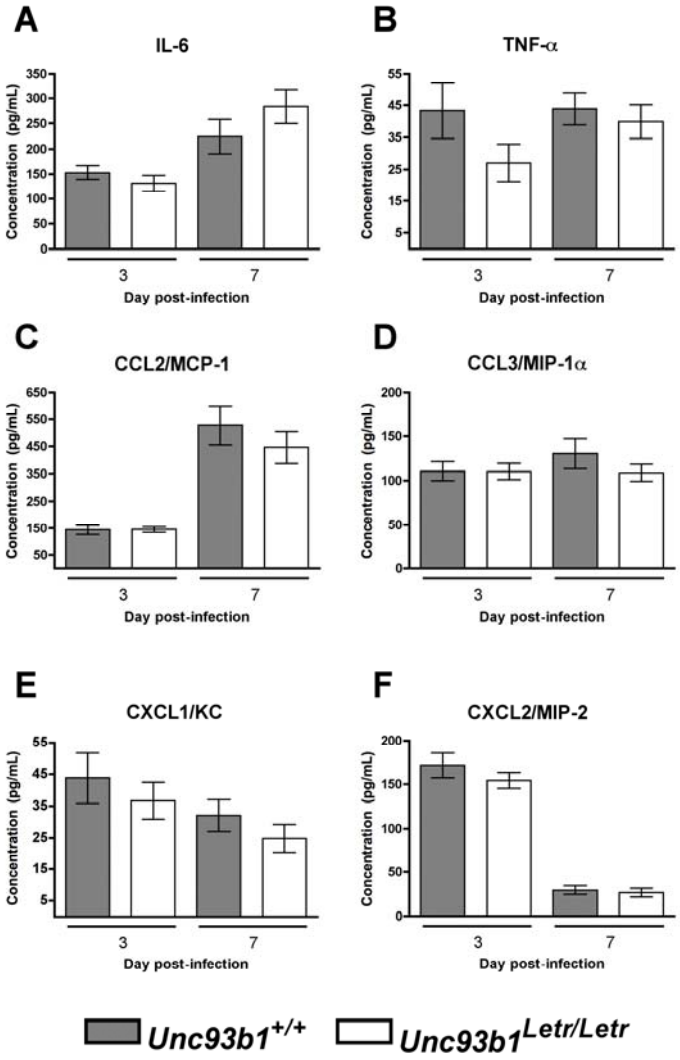

Supplementary Figure 2.3

Supplementary Figure 2.3. Comparable proinflammatory cytokine and chemokine expression in the airways of *Unc93b1*$^{+/+}$ and *Unc93b1*$^{Letr/Letr}$ mice.

(A) IL-6, (B) TNF-α, (C) CCL2, (D) CCL3, (E) CXCL1, and (F) CXCL2 expression in the *Unc93b1*$^{+/+}$ (grey bars) and *Unc93b1*$^{Letr/Letr}$ (white bars) airway at day 3 and 7 post-infection. Data is pooled from two independent experiments (n≥9/group).

CHAPTER 3. *Unc93b1*-dependent endosomal TLR signaling regulates inflammation and mortality during Coxsackievirus B3 infection

Unc93b1-dependent endosomal TLR signaling regulates inflammation and mortality during Coxsackievirus B3 infection

Erin I Lafferty[2,*], Sean A Wiltshire[4,5,*], Silvia M Vidal[3,4,5], and Salman T Qureshi[1,2,3,#]

[1]Department of Critical Care, McGill University Health Centre, Montréal, Québec, Canada

[2]Division of Experimental Medicine, McGill University, Montréal, Québec, Canada

[3]Department of Medicine, McGill University, Montréal, Québec, Canada

[4]Department of Human Genetics, McGill University, Montréal, Québec, Canada

[5]Complex Traits Group of the McGill Life Sciences Complex, McGill University, Montréal, Québec, Canada

*EIL and SAW contributed equally to this work

[#]**Correspondence should be addressed to:**

Dr. Salman T Qureshi

L11-403, 1650 Ave Cedar

Montréal, Québec, Canada

H3G 1A4

Telephone: 514-934-1934 x44626

Email: salman.qureshi@mcgill.ca

Running title: _Unc93b1_-dependent protection in CVB3 infection

Submitted to: _J Innate Immun_**. May 2014**

Preface

The study conducted in chapter two characterized and compared a unique loss-of-function mutation of *Unc93b1*, termed *Letr* for 'loss of endosomal TLR response', to the *3d* mutation of *Unc93b1* at the nucleotide and protein level. Using this model to define the role of *Unc93b1* and endosomal TLRs following influenza infection revealed a modest contribution to early immune activation at the site of infection. This is clearly different from other studies, conducted with the *Unc93b1*$^{3d/3d}$ mice, that demonstrated a significant role for *Unc93b1* and endosomal TLRs to host protection against mortality following infection with diverse microorganisms including MCMV, HSV, NSV, *T. gondii*, and *T. cruzi*.[36, 216, 219, 221, 222]

To determine if a limited role for *Unc93b1* and endosomal TLRs was a more general finding associated with other ssRNA virus infections as well; we characterized the role of *Unc93b1* using another ssRNA virus infection model. The use of another model for the functional characterization of *Unc93b1* is important to the understanding of the specific role of the endosomal TLR signaling pathway during different ssRNA virus infections.

The following study therefore considered the role of *Unc93b1* during acute CVB3-induced myocarditis. Unlike the influenza virus, CVB3 is a positive-sense ssRNA virus that primarily targets the heart. Similar to the influenza virus, CVB3 can activate endosomal TLR3 and TLR7 following infection although a role for the entire endosomal TLR pathway, prior to this study, had not been defined. As TLR3 activation has been demonstrated to be protective while MyD88-mediated immune activation has been shown to be pathogenic in acute CVB3-induced myocarditis, it was challenging to hypothesize how the complete loss of endosomal TLR-mediated immune activation would impact host outcome. To determine this, we examined the impact of defective *Unc93b1* function on survival after acute infection as well as the control of viral load and cardiac tissue damage, markers that represent progressive infection and host pathology, respectively. In addition, we conducted a comprehensive gene expression microarray to define mediators that are regulated through endosomal TLR activation that may be contributing to protection or pathogenesis following CVB3 infection.

Abstract

CVB3-induced myocarditis is an important human disease that causes permanent tissue damage and can lead to death from acute infection or long-term morbidity caused by inflammation and chronic infection. The activation of immune signaling following CVB3 infection can mediate a positive host outcome or increase tissue pathology; depending on the timing and magnitude of immune upregulation and control. To better elucidate the role of endosomal TLR signaling in acute CVB3 infection we studied mice with a loss-of-function mutation, known as *Letr* for 'loss of endosomal TLR response', in *Unc93b1;* a chaperone protein for TLR3, TLR7, and TLR9. Using *Unc93b1*$^{Letr/Letr}$ mice we determined that *Unc93b1*–dependent TLR activation was essential for survival of acute CVB3-induced myocarditis and that a lack of endosomal TLR signaling was associated with a higher viral load in target organs and increased inflammation, necrosis, and repair in cardiac tissue. Loss of *Unc93b1* function was associated with increased cardiac expression of *Ifn-b* and markers of tissue injury and fibrosis including *Lcn2* and *Serpina3n* early after CVB3 infection. These observations establish a significant role for *Unc93b1* in regulation of the host inflammatory response to CVB3 infection and also reveal potential mediators of host tissue damage that merit further investigation in acute viral myocarditis.

Introduction

Myocarditis is described as cardiomyocyte necrosis adjacent to tissue inflammation.[155, 156] In the Western world, coxsackievirus strain B serotype 3 (CVB3) is implicated in 20-40% of viral myocarditis cases.[155, 156] CVB3, a positive-sense single-stranded RNA virus of the *Picornaviridae* family, causes infection via the fecal-oral route and can lead to asymptomatic infection or manifest as a mild febrile or gastrointestinal illness.[155, 156, 164] Infection can also lead to more severe sequelae including meningitis, pancreatitis, and myocarditis; although the true incidence of CVB3-induced myocarditis is unknown due to its variable presentation and a lack of sensitive and specific diagnostic techniques.[156, 164] Patients with viral myocarditis can rapidly succumb to acute heart failure or develop dilated cardiomyopathy (DCM), a chronic inflammatory form of the disease that occurs in 20-30% of cases and frequently requires a heart transplant.[155, 156] Poor outcome following CVB3 infection has been linked to several factors including sex, nutritional status, age, pregnancy, and host immune response.[155, 156]

During the initial phase of infection, replication of the CVB3 virus causes direct virus-mediated cardiomyocyte damage and cell lysis that can contribute to worsening disease.[167, 271] Innate immune cell infiltration, including macrophages, mast cells, neutrophils, and NK cells, occurs 4-5 days post-infection and is followed several days later by an adaptive T and B cell response.[155, 156, 158, 272] Proinflammatory mediators expressed in the heart during CVB3 infection can be produced by both resident cardiac and recruited immune cells and include the chemokines CCL3, CXCL2, and CXCL10 and cytokines tumour necrosis factor (TNF)-α, interleukin (IL)-1β, IL-6, IL-18, interferon (IFN)-γ, IFN-α, and IFN-β.[155, 156, 197, 273, 274] Immune activation in the heart following CVB3 infection has been associated with both protective and pathological features of disease following CVB3 infection.[156] Therefore, a delicate balance in immune timing and magnitude is required to successfully clear the virus from the heart without the induction of severe and permanent immune-mediated tissue damage. Myocardial cell damage and death caused by both viral and immune mechanisms in the heart is particularly deleterious as cardiomyocytes do not regenerate easily.[156, 164] Host sensing of cardiac damage leads to the

stimulation of fibrotic repair mechanisms that cause permanent structural changes to the cardiac architecture, severely affecting cardiac muscle contractility and function.[156, 164]

CVB3 entry into host cells is primarily mediated by decay-accelerating factor (DAF) and coxsackievirus and adenovirus receptors (CAR) on the host cell.[156] The loss of cardiac CAR expression decreases inflammation and tissue remodeling following infection, demonstrating the importance of this receptor for viral entry.[166] Once inside the host cell the CVB3 virus is recognized by multiple pattern recognition receptors (PRRs), including the cytosolic melanoma differentiation-associated protein 5 (MDA5) PRR as well as several toll-like receptors (TLRs).[188-190, 194, 195] CVB3 infection of human cardiomyocytes or TLR-transfected HEK293T cells increased immune activation through TLR4 and, to a greater extent, TLR7 and TLR8.[188] Further, TLR9 expression is upregulated in the wild type heart while the loss of TLR9 reduced cardiac inflammation and immune cell infiltration in a mouse model of acute CVB3-induced myocarditis.[190] Similarly, mice that lack myeloid differentiation primary response gene 88 (MyD88), an adaptor for all TLRs except TLR3, are protected from mortality following CVB3 infection with decreased multi-organ viral load and inflammation, suggesting that immune activation through endosomal TLRs can also contribute to immunopathology.[191] In addition, MyD88-deficient mice had decreased expression of IL-1β, IL-18, IFN-γ, and TNF-α at multiple time points post-infection but increased cardiac IFN-α and IFN-β expression.[191] Conversely, mice lacking TLR3 or TIR-domain-containing adaptor-inducing interferon-β (TRIF), the adaptor for TLR3 and TLR4 signaling, are more susceptible to acute CVB3-induced myocarditis and have increased tissue damage and viral load.[189, 193] Loss of TLR3 diminished expression of IFN-γ, IL-1β, and IL-12p40 but did not affect IFN-β expression at day 3 post-infection while TRIF-deficient mice had increased expression of IL-1β, IL-18, and TNF-α at day 7 post-infection.[189, 193] In addition, studies in a cohort of patients suffering from viral myocarditis revealed a higher-than-expected incidence of *TLR3* polymorphisms compared to controls, supporting a host protective role for TLR3/TRIF-mediated immune signaling.[192] Taken together, these studies seem to indicate a binary role for endosomal TLR signaling in mediating either a host protective or immunopathogenic outcome during CVB3 infection, depending on the degree of immune activation through the TRIF or MyD88 adaptors, respectively.

In an effort to further parse the complex immune signaling mechanisms triggered by CVB3 infection, we have taken advantage of a recently developed loss-of-function mutation of *Unc93b1* to study its role in immune activation following CVB3 infection. UNC93B1 is a transmembrane chaperone protein that trafficks endosomal TLRs (TLR3, TLR7, and TLR9) from the endoplasmic reticulum to the endosome to permit downstream immune signaling.[34-36] Using ENU mutagenesis we created a novel loss-of-function mutation in *Unc93b1* that results in an in-frame deletion of exon 4 following transcript splicing. These mice had a complete lack of immune upregulation via TLR3, TLR7, and TLR9 *in vitro* and *in vivo* following specific agonist stimulation with polyI:C, Imiquimod, and CpG DNA respectively. We termed this mutation *Letr* for 'loss of endosomal TLR response' and, using this model, have recently identified a specific role for *Unc93b1* and endosomal TLRs in early immune activation following influenza A/PR/8/34 (H1N1) infection (Lafferty *et al.,* Accepted to *Genes and Immunity*, April 2014). *Unc93b1* has also been implicated in providing significantly increased protection in other viral infection models including a mouse model of neuroadapted Sindbis virus (NSV), mouse cytomegalovirus (MCMV), and herpes simplex virus (HSV) using a previously derived ENU-induced functional mutation of *Unc93b1* known as *3d.*[36, 215, 216, 219] A role for *UNC93B1* has also been demonstrated in protection against neurological sequelae following human HSV infection.[217]

In the current report, we used our unique model of the loss of *Unc93b1* function to study the consequence of the complete loss of endosomal TLR signaling for the first time in acute CVB3-induced myocarditis. The use of *Unc93b1*$^{Letr/Letr}$ mice allowed us to specifically analyze the role of endosomal TLRs in the presence of functional MyD88 and TRIF adaptors that mediate immune signaling through additional PRRs as well. This demonstrated that the loss of *Unc93b1* function dramatically increased susceptibility to acute CVB3-induced myocarditis and was associated with enhanced viral replication in multiple organs and increased cardiac inflammation and necrosis, leading to greater myocardial fibrosis. Mice are an excellent model system for the study of acute CVB3-induced myocarditis as they present a similar disease progression and pathology to humans.[156, 183] Global cardiac transcriptional profiling determined that the *Unc93b1*$^{Letr/Letr}$ mice have an overall increase in the expression of inflammatory response genes but significantly less expression of genes involved in antigen processing and

presentation of exogenous peptide antigen via major histocompatibility complex (MHC) class II compared to *Unc93b1*$^{+/+}$ mice. Refined analysis of the gene expression array revealed a specific upregulation of *Ifn-b, lipocalin2* (*Lcn2*), and *serine (or cysteine) peptidase inhibitor, clade A, member 3N* (*Serpina3n)* in infected cardiac tissue of *Unc93b1*$^{Letr/Letr}$ mice. This study contributes to an improved understanding of the essential and intricate signaling network triggered by *Unc93b1*- and endosomal TLR-mediated immune activation in response to CVB3 infection in the heart and proposes several interesting mediators that may predict or provoke host pathology during acute CVB3-induced myocarditis.

Results

Loss of *Unc93b1* function increases mortality and delays viral clearance following CVB3 infection

Endosomal TLR signaling via TRIF or MyD88 in acute CVB3-induced myocarditis has been associated with host protection or pathology and disease progression, respectively. To investigate the effect of a complete loss of endosomal TLR signaling on infection outcome, we infected *Unc93b1*$^{+/+}$ and *Unc93b1*$^{Letr/Letr}$ mice with CVB3 and followed the clinical and virological progression of disease. All experiments were conducted using mice on the C57BL/6 genetic background as this strain can effectively clear the virus from the heart following acute infection without developing DCM.[156, 183] After intraperitoneal infection with 400pfu/g of the CVB3-CG strain, *Unc93b1*$^{Letr/Letr}$ mice succumbed more rapidly with an overall mortality of 57%, compared to 4% in *Unc93b1*$^{+/+}$ mice, during a 21-day infection period (Figure 3.1A). The increased susceptibility observed in U*nc93b1*$^{Letr/Letr}$ mice was associated with a significantly elevated cardiac viral load at day 2, 4, and 8 post-infection compared to *Unc93b1*$^{+/+}$ mice (Figure 3.1B). While both genotypes had an elevated viral titer in the liver and spleen at day 2 post-infection, this was sustained in *Unc93b1*$^{Letr/Letr}$ mice at day 4 post-infection compared to controls (Figure 3.1C, D). Detectable virus was fully cleared from the liver and spleen by day 8 post-infection in both the *Unc93b1*$^{+/+}$ and *Unc93b1*$^{Letr/Letr}$ mice (data not shown).

Loss of *Unc93b1* function increases cardiac inflammation and cell necrosis in acute CVB3-induced myocarditis

Following infection, inflammatory cells are recruited to the heart to eliminate the CVB3 virus, often triggering cell necrosis that, along with virus-induced mechanisms of pathology, can lead to permanent structural changes in the heart.[156] This can in turn prolong host recovery time and increase infection-related morbidity and mortality.[164] To determine if a functional deficiency of *Unc93b1* caused increased cardiac damage and inflammation, we analyzed tissue sections stained with hematoxylin and eosin (H&E) at day 8 post-infection, a time point when both necrosis and inflammation can be visualized.[275] *Unc93b1*$^{Letr/Letr}$ mice had significantly

worse myocarditis compared to *Unc93b1*$^{+/+}$ mice when both inflammation and necrosis were quantified using a previously established scoring system[275] (Figure 3.2A). Representative histological sections of heart tissue clearly demonstrate that, following infection, there are more foci of inflammation (clusters of cells that stain blue) and substantially more cell necrosis (areas of clearance) in the hearts of *Unc93b1*$^{Letr/Letr}$ mice compared to *Unc93b1*$^{+/+}$ controls (Figure 3.2B, C).

Loss of *Unc93b1* function causes dysregulated early cardiac gene expression in acute CVB3-induced myocarditis

As *Unc93b1*$^{Letr/Letr}$ mice had greater cardiac damage and were significantly more susceptible to infection, we next sought to determine how the loss of *Unc93b1* function affected cardiac gene expression during the early phase of CVB3 infection to determine if the pattern of early gene activation in the heart could be correlated with host outcome. Accordingly, we performed a global gene transcription analysis in biological replicates of heart tissue from *Unc93b1*$^{+/+}$ mice and *Unc93b1*$^{Letr/Letr}$ mice at day 0 and day 2 post-infection. Day 2 was examined as TLR activation can occur rapidly in primary human aortic muscle cells following infection[188] and early changes in cardiac signaling can predispose the host to a deleterious outcome as the infection progresses.[276] Principal Component Analysis (PCA) of normalized global expression data from the array clustered heart samples based on the experimental factor (factor 1: genotype; factor 2: infection) with only minor variation observed between assayed biological replicates (Figure 3.3A). The PCA further demonstrated that the infection (factor 2) caused a more dramatic change in gene expression in the *Unc93b1*$^{Letr/Letr}$ heart as compared to the *Unc93b1*$^{+/+}$ heart.

FlexArray[277] analysis of gene expression data identified 182 genes with >2-fold differential expression and an adjusted p-value (p_{adj})<0.05 between *Unc93b1*$^{+/+}$ and *Unc93b1*$^{Letr/Letr}$ hearts at day 2 post-infection (Supplementary Table 3.1). Using this gene list, gene ontology (GO) biological process cluster analysis was performed to determine associations with biological process terms that were significantly enriched.[278] Genes within these significantly enriched GO clusters were subsequently segregated based on increased expression

in *Unc93b1*$^{+/+}$ or *Unc93b1*$^{Letr/Letr}$ hearts at day 2 post-infection (Figure 3.3B). This analysis revealed that the differentially expressed genes associated with the term antigen processing and presentation via MHC class II were more highly expressed in *Unc93b1*$^{+/+}$ hearts than *Unc93b1*$^{Letr/Letr}$ hearts. Conversely, the differentially expressed genes associated with the GO terms inflammatory response, cytokine production, positive regulation of TNF production, innate immune response, chemotaxis, and cellular amino acid catabolic process were more highly expressed in *Unc93b1*$^{Letr/Letr}$ as compared to *Unc93b1*$^{+/+}$ hearts at day 2 post-infection.

Of the 182 differentially expressed genes at day 2 post-infection, 49 were more highly expressed in *Unc93b1*$^{+/+}$ hearts while the other 133 genes were more highly expressed in *Unc93b1*$^{Letr/Letr}$ hearts (Supplementary Table 3.1). These gene lists were analyzed separately for significant GO biological process, GO cellular component, and pathway enrichment terms using the Database for Annotation, Visualization, and Integrated Discovery (DAVID).[278, 279] These results confirmed the preliminary GO cluster analysis (Figure 3.3B) and demonstrated that genes involved in the GO biological process term antigen processing and presentation of exogenous peptide antigen via MHC class II and the GO cellular component term MHC class II protein complex were significantly enriched in *Unc93b1*$^{+/+}$ mice at day 2 post-infection while the GO biological process term inflammatory response was significantly enriched in *Unc93b1*$^{Letr/Letr}$ hearts (Table 3.1). Pathway analysis determined that immune genes involved in the toll-like receptor signaling pathway were significantly enriched in *Unc93b1*$^{Letr/Letr}$ hearts while the pathway terms for intestinal immune network for IgA production, asthma, and systemic lupus erythematosus were significantly enriched in the hearts of *Unc93b1*$^{+/+}$ mice (Table 3.1).

Hierarchical clustering of normalized expression data for the 182 differentially expressed genes was performed to order biological replicates (defined at the top of each heat map) based on gene expression similarities (Figure 3.4A). This was successfully done first by infection (day 0 vs. day 2 post-infection), followed by genotype. This cluster analysis demonstrated substantial differences between *Unc93b1*$^{+/+}$ and *Unc93b1*$^{Letr/Letr}$ cardiac gene expression due to the loss of *Unc93b1* function at day 2 post-infection (Figure 3.4A, left two columns) that were not seen between the two genotypes at day 0 post-infection (Figure 3.4A,

right two columns). Further analysis of immune genes only, selected based on their classification under the GO biological process term immune response (GO: 0006955), successfully clustered the biological replicates by infection but was only able to cluster samples by genotype at day 2 post-infection (Figure 3.4B, right two columns). Clustering by genotype in uninfected hearts (day 0) (Figure 3.4B, left two columns) was less precise. This was not surprising, as uninfected *Unc93b1*$^{+/+}$ and *Unc93b1*$^{Letr/Letr}$ hearts were not expected to have baseline differences in immune gene expression. This cluster analysis indicated a greater upregulation of immune genes in *Unc93b1*$^{Letr/Letr}$ compared to *Unc93b1*$^{+/+}$ hearts at day 2 post-infection (Figure 3.4B), which may be related to increased cardiac viral load at this time point.

At day 0 post-infection there were 21 genes that showed >2-fold differential expression and a p_{adj}<0.05 between *Unc93b1*$^{+/+}$ and *Unc93b1*$^{Letr/Letr}$ hearts (Supplementary Table 3.2). Eight of these genes also showed differential expression at day 2 post-infection, of which only one (*c8b*) was significantly clustered in secondary microarray analysis. These findings suggest that basal gene expression did not play a significant role in the expression differences observed following CVB3 infection between *Unc93b1*$^{+/+}$ and *Unc93b1*$^{Letr/Letr}$ hearts.

Loss of *Unc93b1* function increased cardiac expression of *Ifn-b*, *Lcn2,* and *Serpina3n* in acute CVB3-induced myocarditis

To determine genes whose expression could be highly regulated through *Unc93b1* and endosomal TLRs during acute CVB3-induced myocarditis, our microarray analysis was refined to look for genes that had >5-fold differential expression and a p_{adj}<0.05 between *Unc93b1*$^{+/+}$ and *Unc93b1*$^{Letr/Letr}$ hearts at day 2 post-infection. This more rigourous threshold revealed five genes, of which only one (*Dbp*) was more significantly upregulated in *Unc93b1*$^{+/+}$ hearts, while the other four (*Cdo1, Ifn-b, Lcn2, Serpina3n*) were more significantly upregulated in *Unc93b1*$^{Letr/Letr}$ hearts (Table 3.2). A greater number of genes upregulated in *Unc93b1*$^{Letr/Letr}$ compared to *Unc93b1*$^{+/+}$ hearts using the cut-off of >5-fold differential expression mirrors the distribution of upregulated genes observed using the cut-off of >2-fold differential expression (Supplementary Table 3.1).

To confirm expression analysis from the microarray, *Ifn-b, Lcn2*, and *Serpina3n* were analyzed by quantitative reverse transcription PCR (qRT-PCR). These genes were selected based on literature describing their importance in CVB3 infection or a previous association with cardiac pathology (Figure 3.5). We confirmed significantly higher expression of *Ifn-b* and *Lcn2* in *Unc93b1*$^{Letr/Letr}$ hearts compared to *Unc93b1*$^{+/+}$ hearts (Figure 3.5A, B) with a trend towards increased expression of *Serpina3n* visualized in *Unc93b1*$^{Letr/Letr}$ hearts at day 2 post-infection (Figure 3.5C). A previous study demonstrated that the exogenous addition of recombinant Serpin A 3N (rSerpin) increased cardiac remodeling in a mouse model of CVB3-induced autoimmune myocarditis caused by infection with a cocktail of CVB3 virus and cardiac myosin protein,[158, 276] suggesting that elevated expression of *Serpina3n* in the *Unc93b1*$^{Letr/Letr}$ heart may contribute to increased cardiac remodeling in our acute model as well. Therefore, to determine the extent of cardiac remodeling in the *Unc93b1*$^{Letr/Letr}$ mice, we analyzed the degree of fibrosis in heart sections from infected *Unc93b1*$^{+/+}$ and *Unc93b1*$^{Letr/Letr}$ mice at day 8 post-infection using a Masson's trichrome stain. Representative histological sections clearly demonstrate that the degree of cardiac fibrosis, visualized as blue-staining collagen deposition, is much more substantial in *Unc93b1*$^{Letr/Letr}$ hearts (Figure 3.5E) compared to *Unc93b1*$^{+/+}$ hearts (Figure 3.5D), a finding that correlates with increased inflammation and necrosis observed at the same time point.

Discussion

CVB3-induced myocarditis is a serious and often underdiagnosed pathology. The outcome of infection is determined by a complex interaction of host and viral factors that can result in an asymptomatic and self-limiting infection, sudden death during acute myocarditis, or DCM due to persistent inflammation.[155, 156] In this report we used mice with a chemically induced loss-of-function mutation in *Unc93b1* on a resistant C57BL/6 genetic background to study the role of endosomal TLR signaling in acute CVB3-induced myocarditis. While previous studies have examined the role of immune signaling in mice lacking a single TLR or adaptor, this is the first report to examine how the complete loss of endosomal TLR activation affects host outcome following CVB3 infection. We demonstrated that an *Unc93b1* functional deficiency led to increased mortality during acute CVB3-induced myocarditis and that this correlated with significantly elevated viral load in the heart, liver, and spleen as well as increased cardiac inflammation and necrosis. This was accompanied by significantly dysregulated early expression of genes associated with several biological processes including antigen processing and presentation of exogenous peptide antigen via MHC class II and the inflammatory response, with a specific increase in *Ifn-b*, *Lcn2*, and *Serpina3n* expression in *Unc93b1*$^{Letr/Letr}$ hearts. These results suggest that endosomal TLR signaling is crucial for survival and recovery from an acute CVB3 infection in the heart and further reveal potentially interesting mediators that may be associated with pathology in acute CVB3-induced myocarditis.

Increased mortality due to defective *Unc93b1* function is consistent with previous studies of TLR3- or TRIF-deficient mice, both of which have increased mortality, inflammation, and cardiac viral load following CVB3 infection.[189, 193] In addition, a study in patients with viral myocarditis identified an increased frequency of a *TLR3* polymorphism and *in vitro* expression of this variant was associated with diminished responsiveness to CVB3 infection leading to increased viral replication.[192] In contrast to the TLR3/TRIF pathway, signaling via TLR9/MyD88 contributes to disease pathogenesis in acute CVB3-induced myocarditis.[190, 191] Specifically, MyD88 deficiency improved host survival, decreased cardiac and pancreatic tissue damage, and reduced multi-organ viral load in acute CVB3 infection.[191] Interestingly, the current report

demonstrates that the simultaneous loss of protective immune responses through TLR3/TRIF and pathogenic responses through TLR9/MyD88 led to greatly increased susceptibility to acute CVB3-induced myocarditis overall. Our findings further demonstrate that immune activation through MDA5/MAVS, an essential immune activation pathway for host survival following CVB3 infection,[194, 195] and other viral recognition pathways in *Unc93b1*$^{Letr/Letr}$ mice is not sufficient to compensate for the absence of endosomal TLR signaling in acute CVB3-induced myocarditis.

Microarray analysis at day 2 following CVB3 infection revealed an increase in total gene expression as well as expression of genes associated with the GO biological process term inflammatory response in *Unc93b1*$^{Letr/Letr}$ compared to *Unc93b1*$^{+/+}$ hearts. This suggests that the loss of *Unc93b1* and endosomal TLR signaling did not dampen the immune response but instead led to greater immune activation. This has been observed previously in TRIF-deficient mice, which exhibited increased TNF-α and IL-1β with a concomitant increase in activated T cell, B cell, and macrophage infiltration at day 7 post-infection, despite increased susceptibility to CVB3 infection.[193] Uniquely, genes associated with the GO biological process term antigen processing and presentation of exogenous peptide antigen via MHC class II were more highly expressed in *Unc93b1*$^{+/+}$ compared to *Unc93b1*$^{Letr/Letr}$ hearts at day 2 post-infection. Effective antigen presentation via MHC class II is a crucial mechanism for priming $CD4^+$ T lymphocytes that, in turn, facilitate the continued activation of cytotoxic $CD8^+$ T cells and B cell activation to eliminate infected cells and produce strain-specific antibodies, respectively.[65] MHC class II may play an important role in mediating host resistance against the CVB3 virus as infection of MHC class II-deficient mice led to significantly worse disease that manifested as persistent immune cell infiltration to the heart, cardiac fibrosis, and sustained cardiac viral load at day 21 post-infection, although no survival difference was reported.[280] In the original paper by Tabeta *et al.* that determined the function of *Unc93b1* in endosomal TLR activation, a second independent role for *Unc93b1* in antigen presentation via MHC class II as well as antigen cross-presentation was uncovered using OVA stimulation.[36] Based on the GO biological process analysis in our report and these previous findings, it is tempting to hypothesize that there is an independent role for *Unc93b1* in antigen presentation via MHC class II in acute CVB3-induced myocarditis as well. Subsequent studies to the work done by Tabeta *et al.* however, using similar experimental

conditions, suggested that there is no role for *Unc93b1* in antigen presentation via MHC class II or antigen cross-presentation,[228] demonstrating that further experimentation is required to clarify this.

Pathway analysis further revealed that genes involved in the intestinal immune network for IgA production, asthma, and systemic lupus erythematosus were significantly overrepresented in *Unc93b1*$^{+/+}$ compared to *Unc93b1*$^{Letr/Letr}$ hearts. All of these pathways have previously been associated with the upregulation of Th2-mediated immune signaling, which suggests that *Unc93b1*$^{Letr/Letr}$ mice activate an immune response with a Th1/Th2 imbalance following CVB3 infection. Increased Th2-associated genes in the *Unc93b1*$^{+/+}$ hearts may indicate a bias towards Th1-mediated immune activation in the *Unc93b1*$^{Letr/Letr}$ hearts, which could be contributing to immune-mediated cardiac pathology.

Elevated *Ifn-b* expression in the hearts of susceptible *Unc93b1*$^{Letr/Letr}$ mice compared to resistant *Unc93b1*$^{+/+}$ mice was unexpected as IFN-β has been demonstrated, in both experimental and natural studies of acute viral myocarditis and DCM, to be protective. Both IFN-β- and IFN-α/β receptor (IFNAR)-deficient mice are highly susceptible to acute CVB3-induced myocarditis and exhibit increased splenic and hepatic necrosis.[202, 212] Further research has also demonstrated that exogenous addition of IFN-β to human myocardial fibroblasts *in vitro* or mice *in vivo* reduced viral load and cell damage.[179, 281] In a clinical trial it was even demonstrated that IFN-β treatment could improve clinical disease outcome and reduce viral titer in chronically infected DCM patients over a 6-month treatment period.[176] Despite its clearly important role in host defense, elevated IFN-β does not always correlate with protection in acute CVB3-induced myocarditis. For example TLR3 deficiency, despite significantly increasing mortality and serum viral load, did not affect cardiac IFN-β expression at day 3 post-infection.[189] Increased early expression of *Ifn-b* in *Unc93b1*$^{Letr/Letr}$ hearts suggests that an endosomal TLR-independent pathway is mediating *Ifn-b* upregulation in the heart. Indeed, increased MAVS expression *in vitro* is correlated with increased *Ifn-b* expression and decreased viral RNA presence,[196] suggesting that the early upregulation of *Ifn-b* seen in the *Unc93b1*$^{Letr/Letr}$ hearts may occur through the MDA5/MAVS pathway. Despite the protective effect of IFN-β in CVB3 infection, *Unc93b1*$^{Letr/Letr}$ mice still succumbed to infection more dramatically than

Unc93b1$^{+/+}$ mice. This suggests that the observed *Ifn-b* increase may have been transient or that *Ifn-b* expression in *Unc93b1*$^{Letr/Letr}$ hearts, despite being elevated compared to *Unc93b1*$^{+/+}$ hearts, was not sufficient to compensate for the loss of protective immune mechanisms activated by endosomal TLR signaling.

Lcn2, a 25kDa small molecule transporter and a member of the lipocalin family,[282] was also significantly upregulated in *Unc93b1*$^{Letr/Letr}$ hearts at day 2 post-infection. *Lcn2* expression was originally discovered in neutrophils and expression was subsequently observed in epithelial cells, adipocytes, macrophages, and hepatocytes.[282, 283] LCN2 protects the host during bacterial infection by binding and sequestering iron-scavenging bacterial siderophores to limit the iron acquisition required for bacterial growth.[284] Indeed, *Lcn2*-deficient mice are more susceptible to *Escherichia coli*-induced sepsis and *Klebsiella pneumoniae* infection than wild type mice.[285, 286] In a model of West Nile virus-induced encephalitis however, *Lcn2* deficiency did not affect the host's ability to mount an appropriate cellular immune response, clear brain viral load, or survive the disease,[287] suggesting that it may be dispensable for host protection in certain viral infections. *Lcn2* has also been proposed to be a clinical marker of acute kidney injury as it has low basal expression in the host but is significantly elevated in both plasma and urine samples following renal inflammation or injury.[288] Recent work further suggests that *Lcn2* may be a marker of cardiac injury as its expression is elevated in patients with coronary artery disease and heart failure.[283, 289] Studies in a rat model of autoimmune myocarditis have also correlated cardiac expression of *Lcn2* with disease induction.[282] Based on these studies, upregulation of *Lcn2* in *Unc93b1*$^{Letr/Letr}$ hearts at day 2 post-infection may be predictive of the increased cardiac tissue injury observed at day 8 post-infection. Interestingly, differential cardiac expression of *Lcn2* was also previously seen during the acute phase of CVB3-induced autoimmune myocarditis caused by a cocktail of CVB3 virus and cardiac myosin protein.[158, 276] In this study, the expression of *Lcn2* was significantly elevated in the hearts of male Balb/c mice that progressed to DCM following infection but was not elevated in the hearts of female Balb/c mice that did not develop DCM, suggesting that elevated *Lcn2* in the acute phase may predict progression to chronic DCM.[276] Therefore, our report of an early increase in cardiac *Lcn2* expression in a model of acute CVB3-induced myocarditis complements this study in

autoimmune myocarditis and suggests that there is a potential utility for *Lcn2* to act as an informative biomarker of tissue damage in acute, in addition to chronic, myocarditis.

Serpina3n is one of 14 mouse genes that, in humans, is coded for by a single gene known as *α1-antichymotrypsin*.[290] At day 2 post-infection we observed a trend towards increased expression of *Serpina3n* in *Unc93b1*$^{Letr/Letr}$ hearts by qRT-PCR. *Serpina3n* is a serine protease inhibitor that can bind and inactivate serine proteases including granzyme B, chymotrypsin, trypsin, cathepsin G, and elastase, which normally degrade the extracellular matrix.[291, 292] Patients with atherosclerosis had significantly increased cardiac expression of *Serpina3n* compared to healthy controls[293] while elevated *Serpina3n* expression has also been seen in patients with heart failure, supporting an association between *Serpina3n* expression and increased cardiac damage and repair.[294] A recent study in a mouse model of CVB3-induced autoimmune myocarditis correlated elevated expression of *Serpina3n* in the acute phase of the disease with an increased propensity to progress to chronic DCM.[276] Similar to our findings, this study demonstrated elevated cardiac *Serpina3n* in susceptible mice beginning at day 2 post-infection and this was sustained until day 10 post-infection.[276] They also demonstrated that *Serpina3n* expression was elicited from non-CD11b^{+} cells, suggesting that cardiac resident cells as opposed to immune cells predominantly produce it.[276] Further, the exogenous addition of rSerpin in mice infected with CVB3-induced autoimmune myocarditis significantly increased fibrosis compared to infected mice that received phosphate-buffered saline (PBS), therefore specifically implicating *Serpina3n* expression in cardiac remodeling.[276] This suggests that the substantial cardiac remodeling and fibrosis that we observed in the *Unc93b1*$^{Letr/Letr}$ hearts at day 8 post-infection may be associated with an increase in early *Serpina3n* expression. Though elevated *Serpina3n* was linked to increased pathology in susceptible male Balb/c mice, this study conducted in CVB3-induced autoimmune myocarditis did not observe a difference in viral load between resistant female and susceptible male Balb/c mice.[276] This is distinct from the results of the current study that demonstrated that *Unc93b1*$^{Letr/Letr}$ mice had significantly elevated multi-organ viral load compared to *Unc93b1*$^{+/+}$ mice. This suggests that, in our model of acute CVB3-induced myocarditis, there may be additional virus-mediated mechanisms that are contributing to significantly worse pathogenesis and mortality in the *Unc93b1*$^{Letr/Letr}$ mice.

In summary, our studies using mice with a complete loss-of-function mutation of *Unc93b1* have shown that endosomal TLR signaling is essential for survival of acute CVB3-induced myocarditis and that compensatory immune signaling via MDA5/MAVS or an additional immune activation pathway in *Unc93b1*$^{Letr/Letr}$ mice is insufficient for host recovery. This finding extends the results of previous studies in MCMV, HSV, and NSV infection that also demonstrated an essential role for *Unc93b1*-mediated immune activation in infection survival.[36, 215, 216, 219] Our studies confirm the indispensable role for TLR3-mediated immune activation in host protection during CVB3 infection and further demonstrate that, even the loss of pathological immune activation mediated by MyD88 activation does not protect the *Unc93b1*$^{Letr/Letr}$ mice against infection. It is currently unknown whether the protection attributed to MyD88 deficiency in acute CVB3-induced myocarditis[191] is due the loss of IL-1 receptor (IL-1R)-mediated immune activation; which also signals through the MyD88 adaptor,[110] or is related to the loss of endosomal TLR7- and TLR9-mediated immune activation. This is an important distinction to make as the exogenous addition of IL-1β can induce or worsen inflammation in experimental models of CVB3-induced autoimmune myocarditis[208] while inhibiting IL-1-mediated immune activation using an IL-1R antagonist (IL-1Ra) significantly decreases mortality, cardiac viral load, and tissue damage in a model of acute CVB3-induced myocarditis.[209] Further, studies in patients with DCM revealed significantly less IL-1Ra expression in the heart compared to healthy controls.[295] This suggests that IL-1R-mediated immune activation can lead to a worse outcome in the heart and therefore the absence of this immune activation pathway in MyD88-deficient mice may have been the predominant factor mediating enhanced host protection in that study. As no *in vivo* studies of the role of TLR7 following CVB3 infection have been conducted to date, it is challenging to predict the relative contribution of this pathway to host pathology or protection. The use of *Unc93b1*$^{Letr/Letr}$ mice, which maintain intact MyD88 and TRIF adaptors, in this study allowed us to circumvent this issue and define the role of endosomal TLRs for the first time in acute CVB3-induced myocarditis without the confounding effects of the loss of immune activation through other signaling pathways. In addition, our finding of significantly elevated *Lcn2* expression and a trend towards increased *Serpina3n* expression in the *Unc93b1*$^{Letr/Letr}$ hearts suggests that the

continued investigation of these genes as potential markers of cardiac damage during acute as well as chronic viral myocarditis may significantly improve the current diagnostic and therapeutic landscape that exists for this disease.

Materials and Methods

Ethics statement

All experiments using animals were conducted following the guidelines of the Canadian Council on Animal Care and approved by the McGill University Animal Care Committee (Montréal, Canada).

Mice, virus, and infection

Eight-week old wild type mice and *Unc93b1*$^{Letr/Letr}$ mice on a C57BL/6 background were housed in a specific pathogen-free facility and used for all experiments. The CVB3-CG virus[183] was administered intraperitoneally at a dose of 400pfu/g in sterile PBS (Wisent, St-Bruno, Canada). Mice were monitored daily for signs of illness and humanely sacrificed if they appeared moribund.

Viral quantification by plaque assay

HeLa cells were grown at 37°C, 5% CO_2 in DMEM (Wisent) supplemented with 10% fetal bovine serum (FBS) (Wisent) and 1% penicillin/streptomycin (Life Technologies, Burlington, Canada). Infected mice were humanely sacrificed at day 2, 4, and 8 post-infection and hearts were perfused with 10mL of PBS. The apex of the heart, a single liver lobe, and half of the spleen were placed in separate 1mL aliquots of incomplete DMEM in Lysing Matrix D tubes (MP Biomedicals, Solon, OH) and frozen at -80°C until further analysis. For viral quantification samples were thawed, homogenized at 7000rpm for 40 seconds using a MagNA Lyser (Roche Applied Science, Laval, Canada), and subjected to three freeze/thaw cycles. Following 10-fold serial dilutions in incomplete DMEM, 200µL of tissue supernatant was added in triplicate to a confluent monolayer of HeLa cells on a 12-well plate (Greiner Bio One, Germany) and incubated for 1 hour at 37°C, 5% CO_2. Following incubation, 1.5mL of a 50:50 mixture of 0.5% agarose (Life Technologies) and DMEM supplemented with 20% FBS and 2% penicillin/streptomycin was added and plates were incubated at 37°C, 5% CO_2. Forty-eight hours later, 1mL of 10% phosphate-buffered formalin (Fisher Scientific, Toronto, Canada) was added and incubated at

room temperature overnight. Agarose plugs and formalin were then removed and plaques were stained with 100µL of a 0.5% crystal violet solution (Sigma-Aldrich, Oakville, Canada) in 70% ethanol (Commercial Alcohols, Brampton, Canada).

Histology

Mice were humanely sacrificed at day 8 post-infection and hearts were cut in the sagittal plane, embedded in optimal cutting temperature compound (Tissue-Tek, VWR, Ville Mont-Royal, Canada) and frozen in liquid nitrogen-chilled isopentane. 5µm tissue sections were stained with H&E at the Histology Facility of the University of Ottawa (Ottawa, Canada) or with Masson's trichrome at the Histology Facility of the Goodman Cancer Research Centre (McGill University, Montréal, Canada). Representative photographs of heart sections were visualized at 40x and 100x magnification on a BX51 microscope (Olympus, Richmond Hill, Canada) with a QICAM Fast 1394 digital CCD camera (QImaging, Surrey, Canada), and Image-Pro Plus, version 7.0.1.658 (Media Cybernetics, Rockville, MD). To determine the degree of myocarditis, slides were blindly scored by two independent observers using a previously published scoring system that quantified myocarditis as a composite of inflammation and necrosis.[275] Independent reviewer scoring was in agreement.

RNA extraction and reverse transcription

Hearts from female *Unc93b1*$^{+/+}$ and *Unc93b1*$^{Letr/Letr}$ mice at day 0 and day 2 post-infection were aseptically removed and the apex was snap-frozen in RNAlater (Life Technologies). RNA was extracted using the RNeasy Fibrous Tissue Mini Kit (Qiagen, Toronto, Canada) following the manufacturer's instructions, quantified with a NanoDrop (Fisher Scientific), and stored at -80°C. Reverse transcription was performed using the ABI High Capacity cDNA Reverse Transcription Kit with RNase Inhibitor following the manufacturer's instructions (Life Technologies).

Microarray

Gene expression analyses of total RNA from cardiac tissue were performed using the Mouse WG-6 Expression BeadChips (Illumina, San Diego, CA) at the McGill University and Genome Quebec Innovation Centre (Montréal, Canada). For the microarray, three separate biological replicates were analyzed for each genotype at day 0 and day 2 post-infection. The expression data from the microarray was analyzed using FlexArray, version 1.6.2.[277] Data was normalized using the robust spline normalization of the lumi algorithm. To obtain lists of differentially expressed genes between wild type and *Unc93b1*$^{Letr/Letr}$ hearts at day 2 post-infection, the cyber-T (Baldi & Long) test was used with a Benjamini-Hochberg false discovery rate correction to account for multiple testing. Genes with >2-fold differential expression and a p_{adj}<0.05 were used for further pathway and ontology analysis while a cut-off of >5-fold differential expression and a p_{adj} <0.05 was used to select genes for confirmation of array expression data by qRT-PCR.

Analysis of differentially expressed genes

A PCA plot was used to visualize changes in total normalized gene expression. The Mouse Genome Informatics (MGI) database, version 5.15[296] (The Jackson Laboratory, Bar Harbor, ME) was used to annotate the unassigned targets representing transcripts in the gene expression microarray. Additional analysis of gene expression array data including pathway, GO biological process, and GO cellular component analyses was conducted using DAVID, version 6.7[278, 279] (http://david.abcc.ncifcrf.gov; National Institute of Allergy and Infectious Diseases, National Institutes of Health, Frederick, MD). Differentially expressed genes that were not recognized by either the MGI or DAVID annotation databases were excluded from further analysis as the role of these genes in CVB3 infection could not be inferred. Hierarchical clustering with complete linkage was conducted using MultiExperiment Viewer, version 4.9[297, 298] (http://www.tm4.org/mev.html; Dana-Farber Cancer Institute, Boston, MA). The AmiGO database, version 1.8[299, 300] and the GO biological process term for immune response (0006955) (http://amigo.geneontology.org/cgi-bin/amigo/go.cgi; the Gene Ontology Consortium) were used to define the immune genes on the gene expression array.

Quantitative reverse transcription PCR

To confirm differential gene expression, qRT-PCR was conducted using the ABI 7500 Real-Time PCR System and accompanying software, version 2.0.3 (Life Technologies). TaqMan probes were used for *Gapdh* (Mm99999915_g1), *Ifn-b* (Mm00439552_s1), *Lcn2* (Mm01324470_m1), and *Serpina3n* (Mm00776439_m1) (Life Technologies). Each reaction consisted of 10µl of TaqMan Genotyping Master Mix (Life Technologies), 5µl of water (Wisent), 1µl of TaqMan probe (Life Technologies), and 80ng of cDNA in 4µl of water. The PCR cycling conditions were 95°C for 10 minutes followed by 40 cycles of 95°C for 15 seconds/60°C for 1 minute. Analysis was performed using the comparative C_t method ($2^{-\Delta\Delta Ct}$).[301] *Gapdh* was used as an endogenous control and gene expression at day 2 is relative to gene expression in uninfected hearts.

Statistical analysis

All statistical analyses, excluding the analysis of microarray data, were conducted using GraphPad Prism, version 4 (GraphPad Software, La Jolla, CA). Survival analysis was performed using the logrank test. An unpaired t-test was used for comparisons of viral load, myocarditis score, and relative gene expression measured by qRT-PCR.

Acknowledgements

The authors would like to acknowledge the technical support of Jennifer Marton, Isabelle Angers, Patricia D'Arcy, and Geneviève Perrault. In addition, the authors would like to thank Dr. Patricia Tonin and François Lefebvre for guidance conducting microarray analysis. Funding was provided by a CIHR Team grant (CTP-87520), a Canada Research Chair in Host Resistance to Respiratory Infections (STQ), and Fonds de Recherche du Québec – Santé.

Conflict of Interest Statement

The authors of this manuscript declare no current or potential conflict of interest.

Figures and Tables

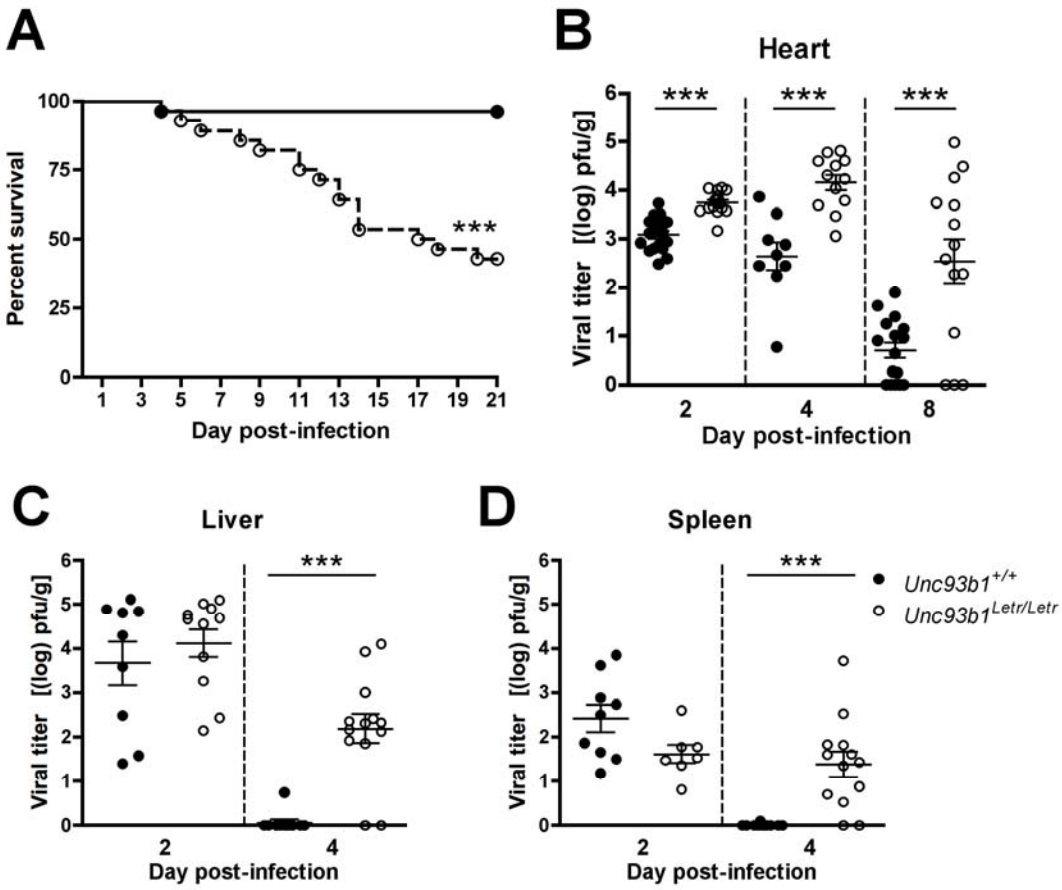

Figure 3.1

Figure 3.1. *Unc93b1*-mediated immune activation improves survival and viral clearance during acute CVB3 infection.

(A) Survival of *Unc93b1*$^{+/+}$ (black circles, solid line) and *Unc93b1*$^{Letr/Letr}$ (white circles, dashed line) mice following intraperitoneal infection with 400pfu/g of CVB3-CG virus. Viral load in (B) heart, (C) liver, and (D) spleen was determined at day 2, 4, and 8 following CVB3 infection in *Unc93b1*$^{+/+}$ (black circles) and *Unc93b1*$^{Letr/Letr}$ (white circles) mice. (A) n≥27/group (B-D) n≥7/group. Data is representative of two independent experiments. ***p<0.001 determined by (A) logrank test or (B-D) two-tailed unpaired t-test.

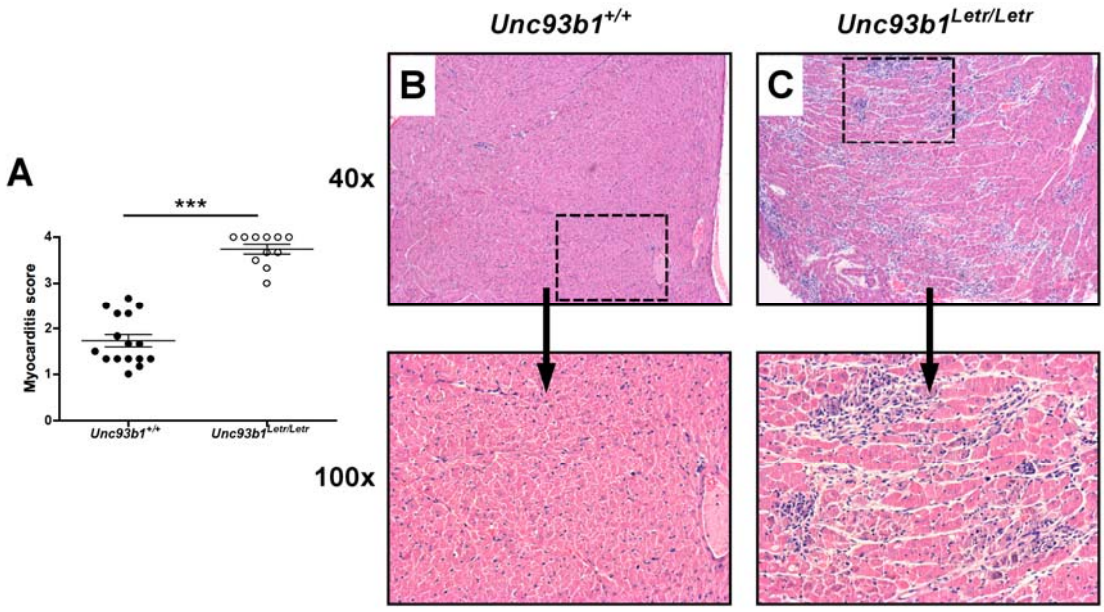
A
***
Myocarditis score
0
1
2
3
4
Unc93b1+/+
Unc93b1Letr/Letr
Unc93b1+/+
Unc93b1Letr/Letr
B
C
40x
100x

Figure 3.2

Figure 3.2. Loss of *Unc93b1* function increases cardiac damage and inflammation during acute CVB3 infection.

(A) Myocarditis score, a composite of cardiac inflammation and necrosis, in *Unc93b1*$^{+/+}$ (black circles) and *Unc93b1*$^{Letr/Letr}$ (white circles) at day 8 post-infection. (B, C) Representative histological sections stained with H&E and displayed at 40x (top panel) or 100x (bottom panel) from (B) *Unc93b1*$^{+/+}$ and (C) *Unc93b1*$^{Letr/Letr}$ hearts. Inflammation is visualized as condensed areas of nucleated cells (stained blue) while necrosis causes the appearance of areas of clearance within the normal heart tissue (stained red). Histological sections were scored by two independent and blinded observers (n≥11/group). ***p<0.001 determined by two-tailed unpaired t-test.

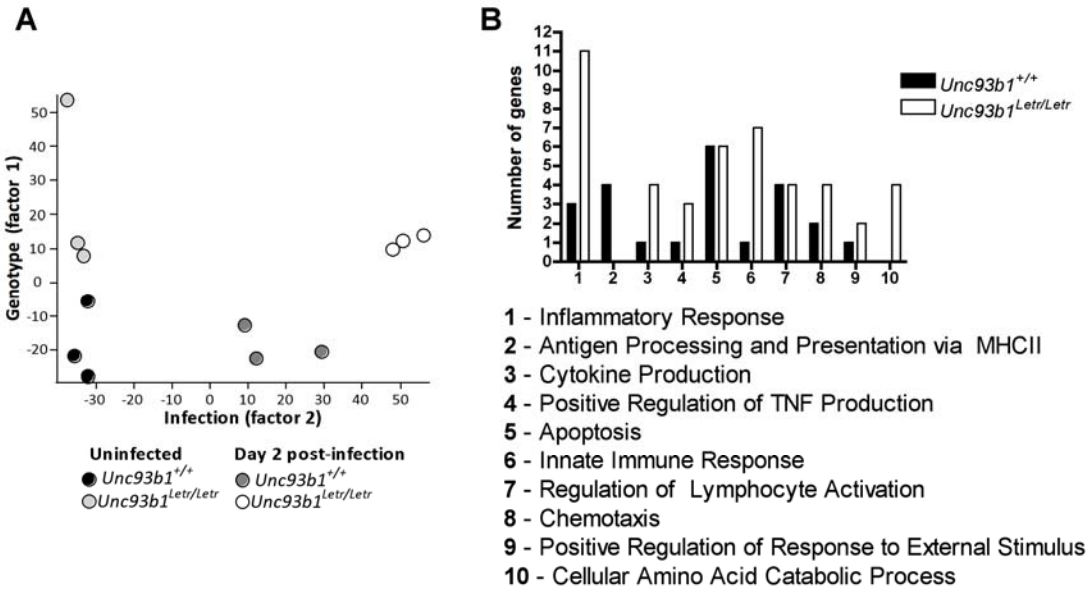
A
Genotype (factor 1)
Infection (factor 2)
Uninfected
Unc93b1+/+
Unc93b1Letr/Letr
Day 2 post-infection
Unc93b1+/+
Unc93b1Letr/Letr
B
Numnber of genes
Unc93b1+/+
Unc93b1Letr/Letr
1 - Inflammatory Response
2 - Antigen Processing and Presentation via MHCII
3 - Cytokine Production
4 - Positive Regulation of TNF Production
5 - Apoptosis
6 - Innate Immune Response
7 - Regulation of Lymphocyte Activation
8 - Chemotaxis
9 - Positive Regulation of Response to External Stimulus
10 - Cellular Amino Acid Catabolic Process

Figure 3.3

Figure 3.3. Loss of *Unc93b1* function causes dysregulated cardiac gene expression in CVB3 infection.

(A) PCA plot of normalized gene expression from *Unc93b1*$^{+/+}$ (black, dark grey) and *Unc93b1*$^{Letr/Letr}$ (light grey, white) hearts at day 0 (black, light grey) and day 2 (dark grey, white) post-infection. (B) Significantly enriched GO biological process clusters of differentially expressed genes at day 2 post-infection, stratified based on significantly increased gene expression in *Unc93b1*$^{+/+}$ (black bars) or *Unc93b1*$^{Letr/Letr}$ hearts (white bars).

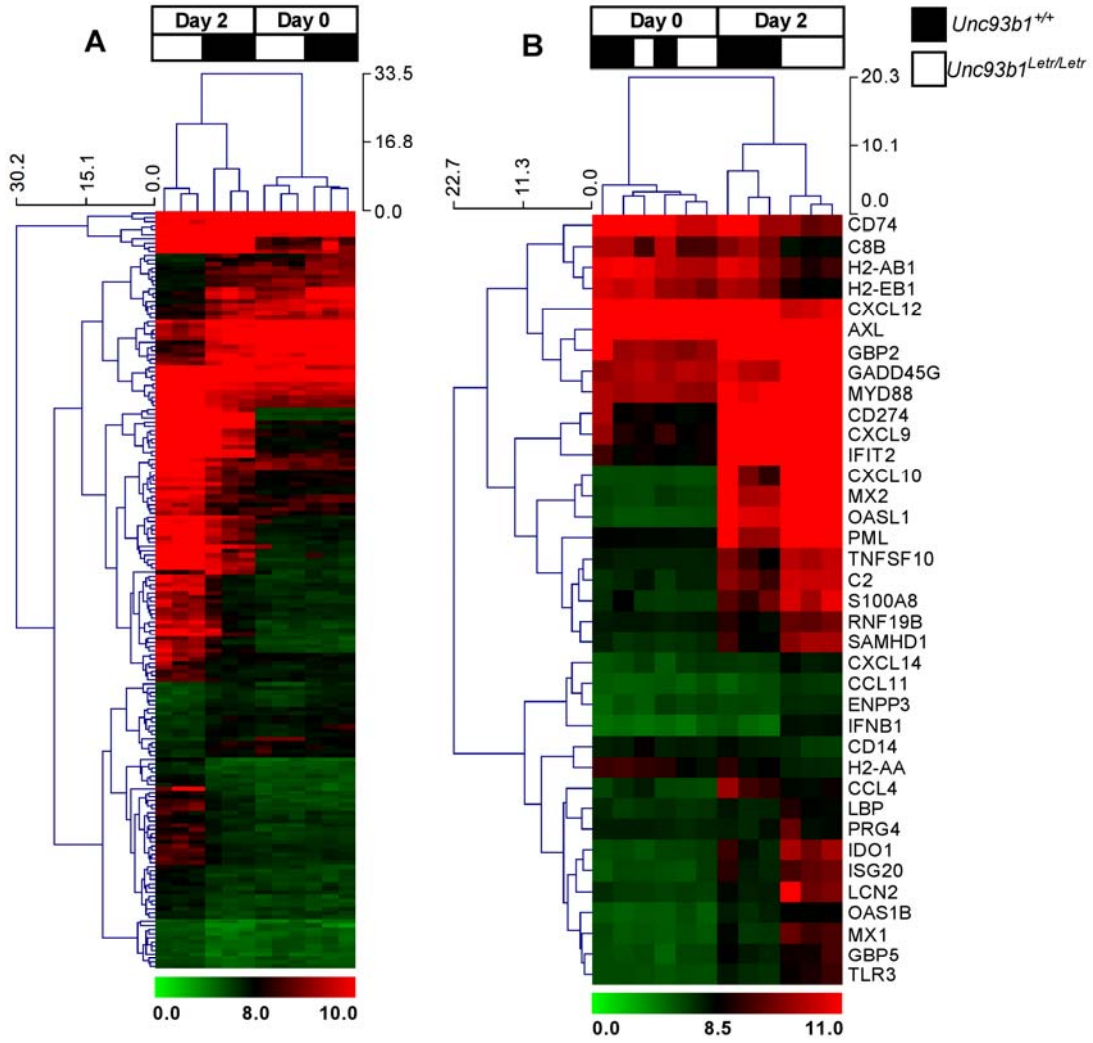
A
Day 2
Day 0
33.5
16.8
0.0
30.2
15.1
0.0
0.0
8.0
10.0
B
Day 0
Day 2
Unc93b1+/+
Unc93b1Letr/Letr
20.3
10.1
0.0
22.7
11.3
0.0
CD74
C8B
H2-AB1
H2-EB1
CXCL12
AXL
GBP2
GADD45G
MYD88
CD274
CXCL9
IFIT2
CXCL10
MX2
OASL1
PML
TNFSF10
C2
S100A8
RNF19B
SAMHD1
CXCL14
CCL11
ENPP3
IFNB1
CD14
H2-AA
CCL4
LBP
PRG4
IDO1
ISG20
LCN2
OAS1B
MX1
GBP5
TLR3
0.0
8.5
11.0

Figure 3.4

Figure 3.4. Differential gene expression clustering in *Unc93b1*$^{+/+}$ and *Unc93b1*$^{Letr/Letr}$ hearts following CVB3 infection.

Hierarchical clustering of normalized gene expression data from (A) all differentially expressed genes or (B) differentially expressed immune response genes at day 0 and day 2 post-infection in *Unc93b1*$^{+/+}$ and *Unc93b1*$^{Letr/Letr}$ hearts. The day post-infection and genotype are indicated at the top of each heat map for *Unc93b1*$^{+/+}$ (black) and *Unc93b1*$^{Letr/Letr}$ (white) hearts.

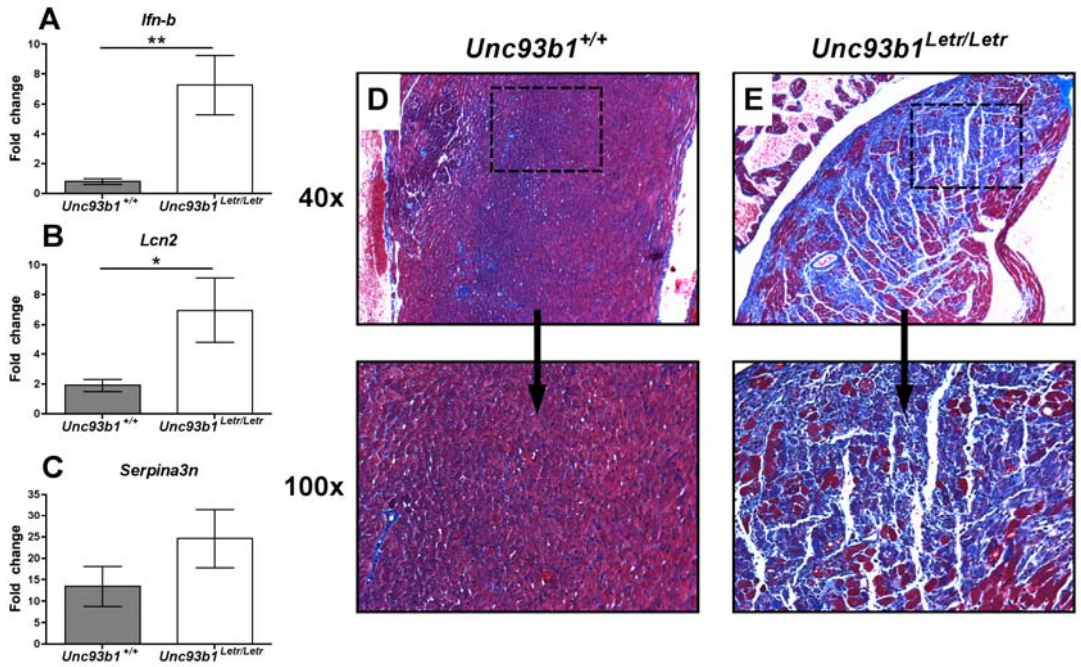
A
Ifn-b
**
Fold change
Unc93b1 +/+
Unc93b1 Letr/Letr
B
Lcn2
*
C
Serpina3n
Unc93b1+/+
Unc93b1Letr/Letr
40x
100x
D
E

Figure 3.5

Figure 3.5. Functional deficiency of *Unc93b1* increases *Ifn-b, Lcn2,* and *Serpina3n* expression during CVB3 infection.

qRT-PCR analysis of (A) *Ifn-b*, (B) *Lcn2*, and (C) *Serpina3n* expression at day 2 post-infection in *Unc93b1*$^{+/+}$ (grey) and *Unc93b1*$^{Letr/Letr}$ (white) hearts. Target gene expression was normalized to endogenous *Gapdh* gene expression and is presented as gene expression at day 2 post-infection relative to gene expression in uninfected mice. (D, E) Representative histological sections were stained with Masson's trichrome as an indicator of fibrosis (blue) in (D) *Unc93b1*$^{+/+}$ and (E) *Unc93b1*$^{Letr/Letr}$ hearts at day 8 post-infection. (A-C) n≥5/group. *p<0.05; **P<0.01 determined by one-tailed unpaired t-test.

Table 3.1. Significant term enrichment following CVB3 infection in the heart

Term	Genes	Fold Enrichment	P_{adj} value
Significantly enriched terms in Unc93b1$^{+/+}$ mice at day 2 post-infection			
Antigen processing and presentation of exogenous peptide antigen via MHC class II			
GO:0019886	H2-EB1, H2-AA, H2-AB1, CD74	92.3	3.43E-03
MHC class II protein complex			
GO:0042613	H2-EB1, H2-AA, H2-AB1	125.23	1.39E-02
Intestinal immune network for IgA production			
mmu04672	H2-EB1, H2-AA, H2-AB1, CXCL12	21.18	2.56E-02
Asthma			
mmu05310	H2-EB1, H2-AA, H2-AB1	27.38	4.27E-02
Systemic lupus erythematosus			
mmu05322	C8B, H2-EB1, H2-AA, H2-AB1	11.64	4.77E-02
Significantly enriched terms in Unc93b1$^{Letr/Letr}$ mice at day 2 post-infection			
Inflammatory response			
GO:0006954	CCL11, SERPINA3N, MYD88, SAA1, SPHK1, CXCL9, TLR3, C2, IDO1, LBP, CXCL10	6.70	1.06E-03
Toll-like receptor signaling pathway			
mmu04620	FOS, MYD88, IFNB1, CXCL9, TLR3, LBP, CXCL10	8.93	7.23E-03

Table 3.2. Genes differentially expressed >5-fold at day 2 post-infection

Gene	Gene name	Fold Enrichment	P_{adj} value
Upregulated gene expression in Unc93b1$^{+/+}$ hearts at day 2 post-infection			
DBP	D site albumin promoter binding protein	5.22	5.02E-8
Upregulated gene expression in Unc93b1$^{Letr/Letr}$ hearts at day 2 post-infection			
CDO1	cysteine dioxygenase 1, cytosolic	0.109	7.22E-8
IFN-B1	interferon beta 1, fibroblast	0.143	3.77E-7
LCN2	lipocalin 2	0.198	1.53E-5
SERPINA3N	serine (or cysteine) peptidase inhibitor, clade A, member 3N	0.157	3.09E-5

Supplementary Tables

Supplementary Table 3.1. Genes differentially expressed at day 2 following CVB3 infection^

Gene	Gene name (determined from the MGI database)	Fold enrichment	P_{adj} value
Upregulated gene expression in Unc93b1$^{+/+}$ hearts at day 2 post-infection			
3300002I08 RIK	RIKEN cDNA 3300002I08 gene	2.36	1.07E-03
ACIN1	apoptotic chromatin condensation inducer 1	3.93	3.77E-07
ACTA2	actin, alpha 2, smooth muscle, aorta	2.22	5.39E-04
ACTC1	actin, alpha, cardiac muscle 1	2.38	2.02E-07
AK3	adenylate kinase 3	2.13	7.63E-05
AQP7	aquaporin 7	2.31	6.63E-05
BCL2L12	BCL2-like 12 (proline rich)	3.07	1.95E-05
C8B	complement component 8, beta polypeptide	3.26	5.81E-07
CCL4	chemokine (C-C motif) ligand 4	2.04	4.96E-03
CD14	CD14 antigen	2.00	7.90E-03
CD74	CD74 antigen (invariant polypeptide of major histocompatibility complex, class II antigen-associated)	2.09	5.86E-03
CD83	CD83 antigen	2.07	9.57E-04
COL15A1	collagen, type XV, alpha 1	2.41	2.98E-05
COL5A1	Collagen, type V, alpha 1	2.02	3.01E-04
COL6A2	collagen, type VI, alpha 2	2.32	2.72E-05
COL6A3	collagen, type VI, alpha 3	2.34	2.55E-05
CXCL12	chemokine (C-X-C motif) ligand 12	2.15	3.27E-05
D0H4S114	Neuronal regeneration related protein	4.32	6.17E-07
D8ERTD82E	DNA segment, Chr 8, ERATO Doi 82, expressed	2.05	8.75E-04
DBP	D site albumin promoter binding protein	5.22	5.02E-08
DDX3Y	DEAD (Asp-Glu-Ala-Asp) box polypeptide 3, Y-linked	2.08	7.37E-03
EGLN3	EGL nine homolog 3 (C. elegans)	2.32	1.08E-04
FBXL22	F-box and leucine-rich repeat protein 22	2.30	1.97E-03
FFAR3	free fatty acid receptor 3	3.34	6.05E-07
GM129	predicted gene 129	2.04	8.00E-03
GM14378	predicted gene 14378	2.06	1.42E-03
GPR22	G protein-coupled receptor 22	2.18	8.12E-04
GRB14	growth factor receptor bound protein 14	2.10	1.79E-04
H2-AA	histocompatibility 2, class II antigen A, alpha	2.24	6.29E-04
H2-AB1	histocompatibility 2, class II antigen A, beta 1	2.57	1.01E-04
H2-EB1	histocompatibility 2, class II antigen E beta	2.76	1.56E-05
HERC1	hect (homologous to the E6-AP (UBE3A) carboxyl terminus) domain and RCC1 (CHC1)-like domain (RLD) 1	2.40	3.49E-04
IP6K3	inositol hexaphosphate kinase 3	2.04	3.54E-03
ITGA9	Integrin alpha 9	2.41	2.69E-05
ITPRIPL1	inositol 1,4,5-triphosphate receptor interacting protein-like 1	2.27	2.55E-04
KLHL3	Kelch-like 3	2.01	1.16E-03
KY	kyphoscoliosis peptidase	2.23	1.30E-04
LINGO4	leucine rich repeat and Ig domain containing 4	2.09	9.02E-03
MMP15	matrix metallopeptidase 15	2.02	8.90E-05
NDRG4	N-myc downstream regulated gene 4	2.22	4.67E-04
PAWR	PRKC, apoptosis, WT1, regulator	2.00	8.84E-03
PISD-PS3	phosphatidylserine decarboxylase, pseudogene 3	2.53	5.56E-04

PTPRS	protein tyrosine phosphatase, receptor type, S	2.12	1.48E-04
RGMA	RGM domain family, member A	2.00	2.31E-03
RNF207	ring finger protein 207	2.42	4.52E-05
RPTN	repetin	2.33	2.23E-04
STK16	serine/threonine kinase 16	2.36	6.63E-05
TNFRSF10B	tumor necrosis factor receptor superfamily, member 10b	2.01	1.13E-03
TUBA4A	tubulin, alpha 4A	2.24	8.74E-04
Upregulated gene expression in UNc93b1$^{Letr/Letr}$ hearts at day 2 post-infection			
1500012F01 RIK	RIKEN cDNA 1500012F01 gene	0.489	4.14E-05
AA467197	expressed sequence AA467197	0.314	4.66E-05
ACE	angiotensin I converting enzyme (peptidyl-dipeptidase A) 1	0.435	3.52E-05
ADAMTS15	a disintegrin-like and metallopeptidase (reprolysin type) with thrombospondin type 1 motif, 15	0.417	1.43E-04
ADAMTS4	a disintegrin-like and metallopeptidase (reprolysin type) with thrombospondin type 1 motif, 4	0.371	8.30E-04
ADH1	alcohol dehydrogenase 1 (class I)	0.345	1.45E-04
AI607873	expressed sequence AI607873	0.453	2.15E-03
ANGPTL7	angiopoietin-like 7	0.446	1.20E-02
ARHGAP8	Rho GTPase activating protein 8	0.361	1.30E-04
ARNTL	aryl hydrocarbon receptor nuclear translocator-like	0.418	1.45E-04
ATF3	activating transcription factor 3	0.342	1.30E-04
AW011738	expressed sequence AW011738	0.497	5.79E-03
AXL	AXL receptor tyrosine kinase	0.464	2.26E-05
BTC	betacellulin, epidermal growth factor family member	0.465	3.31E-03
C2	complement component 2 (within H-2S)	0.493	4.44E-04
C330006P03 RIK	RIKEN cDNA C330006P03 gene	0.438	5.15E-04
CASK	calcium/calmodulin-dependent serine protein kinase (MAGUK family)	0.459	2.72E-05
CCL11	chemokine (C-C motif) ligand 11	0.493	8.81E-03
CCRL2	chemokine (C-C motif) receptor-like 2	0.479	2.86E-03
CD274	CD274 antigen	0.377	1.28E-04
CDKN1A	cyclin-dependent kinase inhibitor 1A (P21)	0.245	8.03E-05
CDO1	cysteine dioxygenase 1, cytosolic	0.109	7.22E-08
CDS1	CDP-diacylglycerol synthase 1	0.434	5.39E-04
CNKSR1	connector enhancer of kinase suppressor of Ras 1	0.274	9.32E-06
CNTN5	contactin 5	0.270	8.10E-07
CRELD2	cysteine-rich with EGF-like domains 2	0.402	1.00E-05
CSRNP1	cysteine-serine-rich nuclear protein 1	0.475	8.56E-04
CXCL10	chemokine (C-X-C motif) ligand 10	0.313	1.66E-02
CXCL14	chemokine (C-X-C motif) ligand 14	0.437	3.71E-04
CXCL9	chemokine (C-X-C motif) ligand 9	0.474	2.61E-04
DAXX	Fas death domain-associated protein	0.382	4.26E-04
DDIT4	DNA-damage-inducible transcript 4	0.335	2.23E-04
DEFA1	defensin, alpha 1	0.427	4.27E-02
DUSP28	dual specificity phosphatase 28	0.446	4.61E-05
ECE2	endothelin converting enzyme 2	0.392	3.05E-04
EIF1A	eukaryotic translation initiation factor 1A	0.496	3.77E-04
ENPP3	ectonucleotide pyrophosphatase/phosphodiesterase 3	0.498	1.28E-03
ERRFI1	ERBB receptor feedback inhibitor 1	0.450	1.47E-05
FAM107A	family with sequence similarity 107, member A	0.417	2.58E-04
FAM46A	family with sequence similarity 46, member A	0.430	3.28E-04

FBXW17	F-box and WD-40 domain protein 17	0.433	3.12E-05
FCGR4	Fc receptor, IgG, low affinity IV	0.443	1.02E-04
FKBP5	FK506 binding protein 5	0.350	2.72E-05
FOS	FBJ osteosarcoma oncogene	0.430	4.76E-04
FXYD6	FXYD domain-containing ion transport regulator 6	0.376	3.60E-07
GADD45G	growth arrest and DNA-damage-inducible 45 gamma	0.456	1.48E-05
GBP2	guanylate binding protein 2	0.475	1.17E-04
GBP5	guanylate binding protein 5	0.495	9.05E-03
GCNT1	glucosaminyl (N-acetyl) transferase 1, core 2	0.425	3.14E-04
GLDC	glycine decarboxylase	0.396	1.17E-04
GM14446	predicted gene 14446	0.169	7.75E-07
GM694	predicted gene 694	0.483	4.86E-03
GRRP1	glycine/arginine rich protein 1	0.442	1.43E-04
HAP1	huntingtin-associated protein 1	0.378	1.72E-06
HBB-BH1	hemoglobin Z, beta-like embryonic chain	0.489	4.97E-02
HDC	histidine decarboxylase	0.424	1.72E-05
HECA	headcase homolog (Drosophila)	0.400	1.24E-04
HOXB5	homeobox B5	0.399	1.43E-04
HSD11B1	hydroxysteroid 11-beta dehydrogenase 1	0.431	9.75E-06
HSPA1A	heat shock protein 1A	0.373	9.37E-05
IDO1	indoleamine 2,3-dioxygenase 1	0.276	5.39E-04
IFI205	interferon activated gene 205	0.428	2.56E-02
IFI35	interferon-induced protein 35	0.494	1.62E-05
IFIT2	interferon-induced protein with tetratricopeptide repeats 2	0.386	1.45E-04
IFNB1	interferon beta 1, fibroblast	0.143	3.77E-07
IL3RA	interleukin 3 receptor, alpha chain	0.494	5.33E-04
ISG20	interferon-stimulated protein	0.361	1.51E-03
ITIH4	inter alpha-trypsin inhibitor, heavy chain 4	0.491	4.44E-03
KRT75	keratin 75	0.498	2.46E-02
LAMP2	lysosomal-associated membrane protein 2	0.491	4.50E-05
LBP	lipopolysaccharide binding protein	0.492	2.41E-03
LCN2	lipocalin 2	0.198	1.53E-05
LMO2	LIM domain only 2	0.467	7.06E-05
LYPD6B	LY6/PLAUR domain containing 6B	0.378	5.94E-05
MAP3K6	mitogen-activated protein kinase kinase kinase 6	0.399	4.76E-04
MARCH5	membrane-associated ring finger (C3HC4) 5	0.418	2.07E-04
MCM6	minichromosome maintenance deficient 6 (MIS5 homolog, *S. pombe*) (*S. cerevisiae*)	0.445	1.72E-04
MITD1	MIT, microtubule interacting and transport, domain containing 1	0.480	2.48E-04
MMP3	matrix metallopeptidase 3	0.353	2.98E-05
MS4A6D	membrane-spanning 4-domains, subfamily A, member 6D	0.474	8.42E-04
MTAP1B	microtubule-associated protein 1B	0.312	7.43E-03
MUSTN1	musculoskeletal, embryonic nuclear protein 1	0.411	6.63E-05
MX1	myxovirus (influenza virus) resistance 1	0.248	9.61E-05
MX2	myxovirus (influenza virus) resistance 2	0.463	5.06E-04
MYD88	myeloid differentiation primary response gene 88	0.460	4.89E-05
N4BP1	NEDD4 binding protein 1	0.418	6.63E-05
NMRAL1	NmrA-like family domain containing 1	0.444	3.28E-04
NSMAF	neutral sphingomyelinase (N-SMase) activation associated factor	0.435	1.60E-05
OAS1B	2'-5' oligoadenylate synthetase 1B	0.479	5.71E-04
OAS1G	2'-5' oligoadenylate synthetase 1G	0.458	6.63E-05

OASL1	2'-5' oligoadenylate synthetase-like 1	0.303	5.39E-04
OSMR	oncostatin M receptor	0.362	5.80E-05
PARP14	poly (ADP-ribose) polymerase family, member 14	0.494	3.98E-03
PFPL	pore forming protein-like	0.462	3.38E-02
PHF11	PHD finger protein 11	0.401	2.84E-04
PLAC8	placenta-specific 8	0.316	3.88E-06
PML	promyelocytic leukemia	0.470	1.16E-03
POU3F1	POU domain, class 3, transcription factor 1	0.275	3.14E-06
PRG4	proteoglycan 4 (megakaryocyte stimulating factor, articular superficial zone protein)	0.497	4.63E-02
PROKR1	prokineticin receptor 1	0.498	1.46E-02
RBM43	RNA binding motif protein 43	0.304	9.32E-06
RCAN1	regulator of calcineurin 1	0.461	1.36E-02
RHOU	ras homolog gene family, member U	0.497	1.53E-02
RNF19B	ring finger protein 19B	0.484	6.75E-04
S100A8	S100 calcium binding protein A8 (calgranulin A)	0.429	1.75E-04
SAA1	serum amyloid A 1	0.424	1.57E-03
SAMHD1	SAM domain and HD domain, 1	0.381	5.59E-05
SCN2B	sodium channel, voltage-gated, type II, beta	0.466	8.34E-03
SDF2L1	stromal cell-derived factor 2-like 1	0.468	8.18E-04
SERPINA3N	serine (or cysteine) peptidase inhibitor, clade A, member 3N	0.157	3.09E-05
SETDB2	SET domain, bifurcated 2	0.365	1.21E-03
SIPA1L1	signal-induced proliferation-associated 1 like 1	0.492	1.86E-03
SLC10A6	solute carrier family 10 (sodium/bile acid cotransporter family), member 6	0.307	3.82E-04
SLC16A1	solute carrier family 16 (monocarboxylic acid transporters), member 1	0.495	2.43E-02
SOCS3	suppressor of cytokine signaling 3	0.370	4.76E-04
SPHK1	sphingosine kinase 1	0.489	1.66E-03
ST6GALNAC 4	ST6 (alpha-N-acetyl-neuraminyl-2,3-beta-galactosyl-1,3)-N-acetylgalactosaminide alpha-2,6-sialyltransferase 4	0.477	4.73E-03
TAPBPL	TAP binding protein-like	0.481	7.09E-04
TBRG1	transforming growth factor beta regulated gene 1	0.466	1.81E-05
TCP10A	t-complex protein 10a	0.418	3.14E-02
TLR3	toll-like receptor 3	0.340	5.61E-05
TMEM106A	transmembrane protein 106A	0.438	1.72E-04
TNFSF10	tumor necrosis factor (ligand) superfamily, member 10	0.431	7.16E-04
TNRC6A	trinucleotide repeat containing 6a	0.496	2.46E-02
TOR3A	torsin family 3, member A	0.399	6.09E-04
TREX1	three prime repair exonuclease 1	0.419	2.58E-04
TRIM30	tripartite motif-containing 30	0.484	2.81E-04
TTPAL	tocopherol (alpha) transfer protein-like	0.416	5.57E-04
USP34	ubiquitin specific peptidase 34	0.446	4.67E-02
VWA5A	von Willebrand factor A domain containing 5A	0.487	2.90E-04
WHAMM	WAS protein homolog associated with actin, golgi membranes and microtubules	0.4999	2.61E-03
XDH	xanthine dehydrogenase	0.423	2.69E-05
ZBTB26	zinc finger and BTB domain containing 26	0.420	2.96E-03

^Genes not recognized by MGI or DAVID were excluded from the list for the purpose of analysis

Supplementary Table 3.2. Genes differentially expressed between uninfected *Unc93b1*$^{+/+}$ and *Unc93b1*$^{Letr/Letr}$ mice^

Gene	Gene name (determined from the MGI database)	Fold enrichment	P_{adj} value
	Upregulated genes in uninfected Unc93b1$^{+/+}$ *hearts*		
ACIN1	apoptotic chromatin condensation inducer 1	2.642783	8.97E-06
BCL2L12	BCL2-like 12 (proline rich)	2.595062	3.99E-05
C8B	complement component 8, beta polypeptide	2.218415	1.09E-05
DCT	similar to Dopachrome tautomerase; dopachrome tautomerase	2.459963	6.06E-03
FFAR3	free fatty acid receptor 3	2.232266	2.46E-04
HTR2B	5-hydroxytryptamine (serotonin) receptor 2B	2.075865	6.67E-03
ITPRIPL1	inositol 1,4,5-triphosphate receptor interacting protein-like 1	2.067725	2.43E-02
PAWR	PRKC, apoptosis, WT1, regulator	2.217154	3.23E-03
PISD-PS3	phosphatidylserine decarboxylase, pseudogene 3	2.650547	7.56E-03
PTGDS	prostaglandin D2 synthase (brain)	2.091451	9.42E-05
RETNLA	resistin like alpha	2.191398	9.51E-03
RPTN	repetin	2.386672	1.62E-03
SPON2	spondin 2, extracellular matrix protein	2.025142	3.29E-03
TFRC	transferrin receptor	2.288894	4.09E-04
XIST	inactive X specific transcripts	2.194107	3.40E-02
	Upregulated genes in uninfected Unc93b1$^{Letr/Letr}$ *hearts*		
INMT	indolethylamine N-methyltransferase	0.4108694	4.28E-04
MELA	melanoma antigen	0.01526786	1.20E-08
PHLDA1	pleckstrin homology-like domain, family A, member 1	0.4902517	2.21E-04
RAB4A	RAB4A, member RAS oncogene family	0.246438	1.33E-05
SCD2	stearoyl-Coenzyme A desaturase 2	0.3108119	2.75E-02
WDFY1	WD repeat and FYVE domain containing 1	0.1974565	3.17E-08

^Genes not recognized by MGI or DAVID were excluded from the list for the purpose of analysis

CHAPTER 4. Discussion

Thesis summary

The fundamental goal of this thesis was to characterize a novel mouse model with an ENU-induced loss-of-function mutation in *Unc93b1* and use this to determine the contribution of endosomal TLR-mediated signaling to immune activation and host outcome during severe infection. As endosomal TLR3, TLR7, and TLR9 recognize nucleic acid-associated PAMPs that are particularly important for immune activation against viruses we focused our studies on the role of *Unc93b1*-mediated immunity during viral infection. When we began this project in 2008, a protective role for *Unc93b1* had been identified following experimental MCMV infection[36] while a human study had determined that *UNC93B1* activation provided protection against HSV encephalitis.[217] Therefore, *Unc93b1*-mediated activation of endosomal TLRs appeared to be important for host outcome following viral infection. Importantly, both MCMV and HSV are DNA viruses with no studies exploring the role of *Unc93b1* in ssRNA viral infection published at that time. Based on this knowledge gap, we decided to study the role of *Unc93b1* in host protection and immune activation during infection with two clinically relevant and highly prevalent ssRNA viruses:

1. Influenza A H1N1, which causes yearly seasonal outbreaks as well as sporadic pandemics that are responsible for significant morbidity and mortality globally.[71]
2. Acute CVB3-induced myocarditis, which can cause severe and irreversible cardiac damage in infected patients who can rapidly succumb to the infection or develop chronic DCM and may require a heart transplant.[156]

Previous studies have demonstrated that endosomal TLR3 and TLR7 are activated following infection with influenza or CVB3 virus;[31, 99, 101, 102, 105, 188, 189] however, no detailed studies have investigated how the complete loss of endosomal TLR-mediated immune activation impacts the host during either infection. By defining the contribution of *Unc93b1* and endosomal TLR-mediated viral recognition to host resistance or susceptibility, our aim was to provide novel and pathogen-specific insights to inform further experimental and clinical studies in influenza and CVB3 infection that may improve human health and reduce the global burden of disease caused by these viruses.

Major findings and unanswered questions

A novel mouse model to study the loss of Unc93b1 function

Using ENU mutagenesis we created a novel allele of *Unc93b1,* named *Letr* for 'loss of endosomal TLR response'*,* consisting of a single bp mutation at a 5' intronic donor site that results in a splicing defect and eliminates the 3rd and 4th transmembrane domains of the protein. Previous work, also using ENU mutagenesis, created a missense mutation of *Unc93b1* that caused a single amino acid change (H412R) in the 9th transmembrane domain of the protein and abrogated its chaperone function.[36] It was through this mutant that the role of mammalian *Unc93b1* in trafficking TLR3, TLR7, and TLR9 from the ER to the endosome to activate innate immune signaling was discovered.[34-36] Interestingly, unlike the D34A N-terminal mutation of *Unc93b1* that predisposed mice to autoimmunity,[230, 233] our mutation caused the same hyporesponsive phenotype to PAMP stimulation that was observed with the *3d* mutation. This suggests that individual domains of UNC93B1 have specific functions such that biased immune activation can occur through a particular mutation at the N-terminus while alteration of one or more transmembrane domains eliminates protein function.

As we found a similar functional defect between *Unc93b1*$^{3d/3d}$ and *Unc93b1*$^{Letr/Letr}$ mice *in vitro*, it is valid to hypothesize that the *Letr* mutation also causes the same alteration in protein binding and trafficking as the *3d* mutation. *In vitro* studies in bone marrow-derived DCs determined that protein from *Unc93b1*$^{3d/3d}$ mice was still able to localize to the ER but failed to bind TLRs and traffic to the endosome following PAMP stimulation.[34, 35] To test this in *Unc93b1*$^{Letr/Letr}$ mice, a combination of co-immunoprecipitation experiments for protein binding partners as well as immunofluorescence detection of intracellular protein localization before and after stimulation could be applied.[34, 35] Alternatively, the multi-transmembrane domain deletion caused by the *Letr* mutation may not allow for proper protein folding following translation and the truncated amino acid sequence may instead be targeted for degradation. Therefore it will be important to determine if the UNC93B1 protein is present in naïve cells from *Unc93b1*$^{Letr/Letr}$ mice prior to more detailed protein binding and trafficking studies.

An early role for Unc93b1 in immune activation during influenza infection

Using our novel ENU-induced model for the loss of *Unc93b1* function we demonstrated a subtle but significant role for *Unc93b1* in early immune activation in the lungs and airway during influenza infection. These observations included decreased activated macrophage recruitment, decreased activation of lung-specific T cells and significantly less type I IFN, CXCL10, and IFN-γ expression in the *Unc93b1*$^{Letr/Letr}$ mice at day 3 post-infection. While this diminished immune activation caused a subsequent delay in viral clearance and led to increased airway inflammation, the loss of *Unc93b1* did not significantly increase mortality. Therefore this study demonstrates that *Unc93b1* and endosomal TLRs are not essential for host survival following influenza infection. Our findings are in agreement with studies done by Allen *et al.* and Le Goffic *et al.* who demonstrated that immune activation through MyD88 is redundant for infection survival;[99, 107] however, they contradict studies by Seo *et al.* that revealed a significant requirement for MyD88 in infection survival.[104] It is challenging to compare our findings to those conducted with MyD88-deficient mice as the loss of this adaptor causes a defect in TLR7-mediated as well as IL-1R-mediated immune activation during influenza infection.[110] Earlier studies by Schmitz *et al.* revealed an important role for IL-1R during influenza infection as IL-1R-deficient mice had increased mortality despite substantially decreased lung pathology.[117] Furthermore, recent studies by Pang *et al.* demonstrated an essential role for IL-1R-mediated activation in dendritic cells to elicit an antigen-specific $CD8^+$ T cell response following influenza infection.[118]

Research conducted by Le Goffic *et al.* revealed that TLR3 deficiency improved host survival following infection, despite an elevated viral load, suggesting that TLR3 activation is detrimental to the host during an influenza infection.[99] As the *Unc93b1*$^{Letr/Letr}$ mice are functionally deficient in both TLR7- and TLR3-mediated immune activation and no studies of the effect of TLR7 deficiency on host survival following influenza infection have been published, it is difficult to determine whether the results of Le Goffic *et al*. are particular to their model or if the additional loss of TLR7-mediated immune signaling in the *Unc93b1*$^{Letr/Letr}$ model eliminated the protective effect induced by TLR3 deficiency.

The discovery of a subtle role for *Unc93b1* in immune activation following influenza infection is in line with studies of human *UNC93B1*. Specifically, two pediatric patients from consanguineous families with distinct mutations in *UNC93B1* progressed to HSE following HSV infection yet their clinical history did not indicate that they were prone to increased infection or disease caused by other pathogens.[217] Despite this narrow clinical susceptibility, *in vitro* stimulation of cells from these patients with ten other viruses resulted in significantly less type I IFN expression than stimulation of cells from healthy children.[217] This data implies that *UNC93B1* and endosomal TLRs can respond to diverse viral infections but the role of this pathway in humans, similar to our study in *Unc93b1*$^{Letr/Letr}$ mice during influenza infection, is limited.

In the discussion section of chapter two we proposed two possible mechanisms through which *Unc93b1*-mediated endosomal TLR activation may contribute to immune activation following influenza infection. One proposed function for *Unc93b1* and endosomal TLRs was ExM activation through type I IFN activation. Once activated, ExMs can induce IFN-γ expression from NK cells, which in turn activates CXCL10 expression at the site of infection. In previous influenza studies we found no difference in the total number of NK cells in the lungs between *Unc93b1*$^{+/+}$ and *Unc93b1*$^{Letr/Letr}$ mice (E.I Lafferty, unpublished observations); however, we did not determine their activation status or cytokine secreting capacity. Therefore, to determine the cellular source of proinflammatory cytokine expression that is affected in *Unc93b1*$^{Letr/Letr}$ mice, intracellular cytokine staining studies could be conducted at multiple time points post-infection in the lungs and airway. Due to their established role in IFN-γ production,[64, 66] NK cells may be the predominant source of this cytokine at the site of infection at early time points. Another possibility that would be interesting to look at is the activation of ILC1s, a recently described innate immune population that are similar to NK cells in their ability to produce IFN-γ but lack cytotoxic capacity.[66] The activation of ILC1s may therefore be dysregulated due to the *Letr* mutation in influenza infection.

The second potential function of *Unc93b1*-mediated immune activation in influenza infection that we described in chapter two is a direct role in T cell activation, as previously demonstrated in several infection models. For example, during experimental infection with

lymphocytic choriomeningitis virus, T cell-specific MyD88 expression was required for $CD8^+$ T cell survival while infection with *T. gondii* revealed a T cell-specific role for MyD88 in IFN-γ production and the prevention of severe infection-induced sequelae and mortality.[260, 261] One way to study this would be to generate mice that exclusively carry the *Letr* mutation in the T cell compartment[260] and study their lung T cell activation phenotype *in vivo* following infection. If the *Unc93b1*-mutant T cells exhibited a defective phenotype, this would suggest that endosomal TLRs are indeed directly required for T cell activation at the site of infection. Further *in vivo* analysis could determine if this T cell defect was the cause of the delayed viral clearance and increased airway pathology seen in the *Unc93b1*$^{Letr/Letr}$ mice.

An essential role for Unc93b1 in controlling cardiac damage and infection outcome in acute CVB3-induced myocarditis

Interestingly, the role of *Unc93b1* in CVB3 infection was dramatically different from the observations made in the influenza model. In acute CVB3-induced myocarditis the loss of *Unc93b1*-dependent endosomal TLR signaling led to a significant increase in multi-organ viral titer, cardiac damage, remodeling and necrosis, and mortality. The data we obtained in CVB3 infection clearly demonstrate a requirement for immune signaling through the *Unc93b1* pathway. Other studies have also investigated the contribution of endosomal TLR-related immune mediators during CVB3 infection. Specifically, Negishi *et al.* demonstrated that the loss of TLR3 significantly increased mortality and serum viral load,[189] while Fuse *et al.* demonstrated that MyD88-deficient animals had improved survival that correlated with reduced cardiac tissue damage and viral load.[191] In trying to reconcile these publications with our findings, it may be that the loss of potentially pathogenic immune activation through MyD88-specific endosomal TLRs does not compensate for the loss of TLR3-mediated protection in the *Unc93b1*$^{Letr/Letr}$ mice, leading to the increased pathology and susceptibility that we observed.

We further demonstrated that the *Unc93b1*$^{Letr/Letr}$ mice had a significantly different cardiac gene expression profile at day 2 post-infection compared to *Unc93b1*$^{+/+}$ mice. In particular, the loss of *Unc93b1* and endosomal TLR-mediated immune activation led to a significant increase in the expression of genes that are classified under the GO biological

process term inflammatory response as well as increased expression of *Ifn-b, Lcn2*, and *Serpina3n* in the heart. Similar to our study, increased cardiac *Ifn-b* was observed in MyD88-deficient mice, though it was measured at day 4 and day 7 post-infection with levels reduced to the detection limit in both MyD88-deficient and wild type mice by day 10 post-infection.[191] Therefore it will be important in future studies to measure cardiac *Ifn-b* expression at additional time points to determine if increased expression in the *Unc93b1*$^{Letr/Letr}$ hearts is sustained as the infection progresses. Despite this similarity in *Ifn-b* expression between our findings and the currently published literature on MyD88 deficiency, the *Unc93b1*$^{Letr/Letr}$ mice were significantly more susceptible to CVB3 infection with no correlation observed between elevated *Ifn-b* expression and increased host protection as was seen in MyD88-deficient mice.[191] As previous research on the role of IFN-β in acute CVB3-induced myocarditis and DCM clearly indicates a protective function for IFN-β expression,[176, 179, 202, 212] this suggests that increased early *Ifn-b* expression in our model does not contribute to the observed increase in cardiac pathology in the *Unc93b1*$^{Letr/Letr}$ hearts. Instead, elevated *Ifn-b* in the *Unc93b1*$^{Letr/Letr}$ heart may not be sufficient to provide the enhanced immune protection required to overcome the dramatic increase in cardiac viral load that occurred. It would therefore be interesting to determine if the exogenous addition of IFN-β to *Unc93b1*$^{Letr/Letr}$ mice during infection could improve infection outcome by allowing for better control of cardiac damage and viral load.

Our discovery of a trend towards increased *Serpina3n* and significantly increased *Lcn2* expression in the heart of *Unc93b1*$^{Letr/Letr}$ mice at day 2 post-infection suggests a potential role for one or both of these genes in mediating pathology during infection and is supported by findings from other studies. For example, LCN2 expression is significantly increased in patients with atherosclerosis or cardiac inflammation[282, 283, 289] while significantly elevated expression of plasma LCN2 has been observed at multiple time points post-infection during experimental autoimmune myocarditis in rats.[282] Elevated *Serpina3n* expression has been demonstrated in mice using a CVB3-induced model of autoimmune myocarditis.[276] Rather interestingly, the same study also revealed a significant increase in *Lcn2* expression in the hearts of susceptible male mice at day 10 post-infection using a gene expression array.[276] These findings, in addition to the data on *Lcn2* and *Serpina3n* expression from our own gene array, warrant further study on the

role of these genes in acute as well as chronic CVB3-induced myocarditis. It would be interesting to determine the expression pattern of *Serpina3n* and *Lcn2* in the heart at additional time points in the *Unc93b1*$^{Letr/Letr}$ mice, particularly at day 8 post-infection when increased cardiac damage and remodeling were observed. Though there was only a trend towards increased expression of *Serpina3n* in the *Unc93b1*$^{Letr/Letr}$ mice, further study of this gene in acute CVB3-induced myocarditis is justifiable based on previous work that specifically demonstrated its ability to induce cardiac pathology in wild type mice following exogenous addition of rSerpin during CVB3-induced autoimmune myocarditis.[276] To determine the role of *Lcn2* and *Serpina3n* in mediating tissue damage and infection severity in *Unc93b1*$^{Letr/Letr}$ mice, experiments studying the effect on mortality, viral load, and cardiac tissue damage and repair could be conducted in *Unc93b1*$^{Letr/Letr}$ mice after the expression of *Lcn2* or *Serpina3n* was knocked down. If these genes mediate pathology in our model, one would expect to see some improvement in infection outcome following their knockdown in *Unc93b1*$^{Letr/Letr}$ mice. Further to this, it would be interesting to determine if the addition of recombinant Lcn2 to wild type mice prior to infection led to a similar increase in tissue pathology as was seen with the addition of recombinant Serpina3n. Finally, studies of acute CVB3-induced myocarditis in *Lcn2*- or *Serpina3n*-deficient mice would allow us to determine if decreased expression of these genes is sufficient to protect the host against cardiac damage during infection. Results from these studies could inform clinical decisions for acute CVB3-induced myocarditis in humans. In particular, the expression of *LCN2* or *SERPINA3N* could be explored as markers of pathology and disease progression in patients. Ideally, their detection in a blood sample could assist in tracking myocarditis severity, thereby reducing the need for repeated and invasive biopsies to determine the degree of cardiac inflammation and necrosis in patients. The expression of LCN2 may be particularly relevant as it has already been demonstrated to be a relatively accurate prognostic marker of acute kidney injury[288] and has been proposed to be a useful biomarker of cardiac damage and disease, though further studies are required.[289] Therefore, following extensive additional experimentation, the use of LCN2 as a marker of disease progression and severity in acute CVB3-induced myocarditis in the clinic may be a realistic goal.

Broad research implications

Perspective on phenotype-driven ENU mutagenesis

This thesis emphasizes the value of ENU mutagenesis as a tool to create novel loss-of-function mutations. The *Letr* mutation is a novel allele of *Unc93b1* and provides an alternative model to the *3d* mutation for functional studies. We used PAMP stimulation to screen for an ENU-induced mutation in the immune response because the readouts were sensitive, reliable, easy to perform, and had the potential to uncover potentially relevant mutations for multiple infection models. We discovered a mutant with a dramatic phenotype following *in vitro* and *in vivo* PAMP stimulation; however, this did not translate to a comparably dramatic *in vivo* phenotype during influenza infection. This difference highlights the advantage, as well as the limitation, of our non pathogen-specific PAMP-based approach to screening. If we had conducted a screen following influenza infection, it is highly unlikely that we would have picked up this novel mutation in *Unc93b1* due to the subtle nature of the phenotype. On the other hand, one could argue that screening with a particular pathogen is a proven and highly successful approach,[266, 302] despite the fact that it can be biased towards more dramatic and therefore easily detectable and quantifiable phenotypes.[13] From our experience it would seem that the exclusive use of phenotype-driven screening may limit the utility of ENU mutagenesis in the discovery and characterization of genes with a modest role in host resistance.[13] To address this concern, some ENU-based studies are conducting screening using a gene-driven approach.[303, 304] In these studies, a large cryopreservation library of ENU-mutagenized gDNA and sperm from heterozygous G1 male mice is first established.[303, 304] Primers are then designed and used to screen all gDNA samples to detect a mutation in a gene-of-interest.[303, 304] Once a relevant mutation has been discovered, the corresponding sperm is used to rederive the mutant strain that is then utilized for subsequent hypothesis-based experimental studies.[303, 304]

There are several advantages to gene-driven screening following ENU mutagenesis. As samples are frozen at the G1 generation, the cost of housing and husbandry is significantly reduced and animal rederivation can occur in a short period of time.[303, 305] Another advantage is that all rederived progeny will be viable, as dominant lethal mutations could not have produced

the G1 mice that the samples for cryopreservation were originally derived from.[305] In addition, as samples are cryopreserved, screening with a gene-driven approach is not time sensitive and allows for multiple screens to be performed on the same samples. Compared to phenotype-driven approaches to screening, once a mutant is discovered through a gene-driven approach, secondary phenotyping can be more extensive as it is conducted on fewer mice and is therefore not required to be as high-throughput. Finally, as current libraries of ENU-mutagenized G1 samples range from 4000 to greater than 15 000 specimens, there is the potential to discover mice that carry distinct mutations in the same gene which can allow for the elucidation of structure-function relationships during an infection or disease.[305-307]

One disadvantage of the gene-driven approach is that the selection of a gene for screening within a gDNA library and the subsequent rederivation of a model for secondary phenotyping shifts the approach from a forward genetic to a reverse genetic strategy. Therefore, the disadvantages inherent to reverse genetic approaches, including a bias towards what is already known in the literature and a dependence on the validity of previous conclusions, may limit the power of gene-driven screens.[4, 7] Nonetheless, as the cost of genetic sequencing continues to be reduced, the ability to sequence the entire genome of all cryopreserved gDNA samples, rather than selecting and screening for changes in a single gene at a time, will allow for a more unbiased approach to the discovery of novel ENU-induced mutations.[304, 308]

Infection-specific susceptibility to ssRNA viral infection

One interesting finding that we noted in our studies is that the similar mortality between *Unc93b1*$^{Letr/Letr}$ and *Unc93b1*$^{+/+}$ mice following influenza infection was in sharp contrast to the significant increase in death observed during acute CVB3-induced myocarditis in *Unc93b1*$^{Letr/Letr}$ mice. This suggests that the same protein and immune signaling pathway can have a non-essential and an essential role in host protection following infection with influenza or CVB3 ssRNA viruses, respectively. Perhaps the most obvious factor that may be contributing to this difference is that influenza and CVB3 are simply different viruses and therefore their effect on the host is not directly comparable. One major difference between the viruses is their

genome structure; specifically, the influenza virus has a segmented genome, arranged into eight discrete fragments while CVB3 has a single unsegmented genome.[71, 73, 74] Another notable difference between the viruses is seen during replication. Influenza is a negative-sense RNA virus, which means that it cannot make functional viral proteins until its genome is transcribed and thus converted to positive-sense RNA. The CVB3 virus, on the other hand, already has a positive-sense genome and can therefore be directly translated into proteins following uncoating. A further distinction is that the model used to induce each infection is different. While influenza directly infects mucosal cells that line the respiratory tract following intranasal instillation of the virus, the CVB3 virus infects multiple tissues after experimental intraperitoneal injection and systemic transit via the bloodstream.

A further potential explanation for the differential susceptibility observed between these two infections is that influenza may activate additional complementary mechanisms for viral recognition and immune activation compared to the CVB3 virus, meaning that the loss of the endosomal TLR pathway would have a less significant impact on infection outcome in the former infection. In addition to endosomal TLRs the cytosolic RLRs, RIG-I and MDA5, are activated and play a role in host immune signaling and defense following influenza and CVB3 infection, respectively.[111, 194, 195] The NLRP3-dependent inflammasome is also activated by the influenza M2 protein and is required for the activation and secretion of IL-1β and IL-18 into the airway following infection.[107, 113, 114, 116] Along with the expression of the other inflammasome components, including the ASC adaptor and caspase-1, NLRP3 is essential for survival following influenza infection.[107, 116] To date, no specific role for the inflammasome in viral recognition or immune activation has been elucidated following CVB3 infection, suggesting that it may not play a significant role in host protection or pathology. In an animal model of myocardial infarction, NLRP3-dependent inflammasome activation has been observed in cardiac fibroblasts, demonstrating that this immune signaling pathway is functional in the heart.[309] In this model of severe non-infectious cardiac disease, NLRP3-mediated immune activation increased cardiac pathology, which suggests that it could contribute to increased immune-mediated pathology if activated by the CVB3 virus.[309]

Controlling interstudy variability when examining gene function following infection

The studies conducted in this thesis provide interesting insights into the role of *Unc93b1* and the endosomal TLR pathway in viral recognition and immune activation following infection with influenza and CVB3. While these findings raise exciting questions for future experimental inquiry, attempts to reconcile them with conclusions from previous infection studies into a unified model of gene function following infection are challenging. The existence of contradictory findings in the current literature is often attributed to interstudy differences in experimentation.[104, 107] Such variation may arise through the use of different host genetic backgrounds, differences in the age of the mice when infected, the viral strain and dose, the time points and organs analyzed, and the environmental conditions under which studies are conducted. An important question that arises from this is how to resolve these experimental differences so that studies that examine the role of different genes during infection are truly comparable?

One resource that may assist in answering this question is the large pool of knockout mice created by the International Knockout Mouse Consortium (IKMC).[310, 311] The goal of this large-scale mouse mutagenesis program is to create a knockout mouse model for every gene.[310, 311] As a complement to this collaboration, large-scale phenotyping initiatives have also been created in order to take advantage of this experimental resource and improve our knowledge of gene function.[312] The premise behind large-scale phenotyping collaborations is to use a hypothesis-free approach to analyze multiple organs and biological systems of knockout mice in a controlled environment to assign a phenotype or function to every gene in the mouse genome.[312-315] Information from these studies will be collected into a database of easily accessible information that can guide further hypothesis-based experimental and clinical studies.[312-315]

The largest phenotyping collaboration currently operating is the International Mouse Phenotyping Consortium (IMPC). Established in 2011 with a ten year outlook, the goal of the IMPC is to use the knockout mice created by the IKMC to systematically assign function to 20 000 genes.[313, 314] This large-scale approach to phenotyping will examine diverse body systems

including the brain, nerves, heart, lungs, reproductive organs, bone, muscle, and immune system in unchallenged mice.[313, 314] It is likely that this strategy will provide unique insights into gene function in normal mice; however, a lack of consistently derived findings on gene function following host challenge, such as infection, will remain. Challenge studies were most likely excluded from this phenotyping platform since a comprehensive analysis of the role of every gene in different infections would be a massive undertaking.[313, 314] Despite this hurdle, the availability of standardized phenotype data from different knockout or mutant mice following infection would be an invaluable resource for both experimental and human research.

Perhaps the biggest advantage of creating a standardized library of gene-phenotype associations among knockout mice during an infection is that disparities among experimental variables in currently published host-pathogen interaction studies such as mouse background, mouse age, viral strain or dose used, housing conditions, food source, exposure to other microbes during breeding and infection, and the flora populating the intestinal microbiome would be consistent between strains and therefore not confound the interpretation of research findings. In addition, conducting the same tests at the same time points in the same organs would allow for clearer interstrain comparison than what is currently available in the literature.

Therefore, I propose that a consortium could be created which applied the ideals of systemic phenotyping proposed by the IMPC to the focused study of mice that are missing immune genes such as PRRs, adaptors, and TFs during an infection. Research from labs such as ours has defined some of the key immune mediators involved in diverse infections and these findings could contribute to the selection of relevant knockout models to be used for further phenotyping. For practical reasons it would be important to prioritize the pathogens and models used for study based on factors such as relevance to global human health, areas of uncertainty in the literature, and validity of the available mouse model to human infection.

Mouse models are heavily used in biomedical research as the genetic and environmental variation that makes studies in humans challenging to interpret can be minimized.[4] As we learn more about the multiple host, pathogen, and environmental factors that can impact the outcome of infection studies in mice however, it will be important to revise how these studies are conducted to better control for the additional factors that may confound

research conclusions. A standardized, large-scale phenotyping collaboration for the study of gene function during infection would provide us with more consistent and higher quality data that would allow for easier interstrain comparison and improve the knowledge of host-pathogen interactions.

Conclusion

For the host to overcome an infection, multiple signaling pathways and mediators must be activated in a controlled and balanced manner. To better dissect these complicated mechanisms of host protection we used an ENU-induced loss-of-function model to study the role of *Unc93b1* and endosomal TLR activation during infection with two clinically relevant ssRNA viruses. The functional characterization of *Unc93b1* in influenza infection and acute CVB3-induced myocarditis in this thesis contributes new knowledge on the role of innate immunity during host-pathogen interactions. Future studies will allow us to refine our understanding of how the intricate immune signaling network of the host is activated and controlled during diverse infections. It is only through an improved understanding of immune activation and interaction that we will be able to design more effective and specific diagnostic, treatment, and prophylactic options against these debilitating human diseases.

CHAPTER 5. Bibliography

1. WHO. The top 10 causes of death. Fact sheet No. 310. In, 2013.

2. Casanova JL, Abel L. The human model: a genetic dissection of immunity to infection in natural conditions. *Nat Rev Immunol* 2004; **4**(1)**:** 55-66.

3. Acevedo-Arozena A, Wells S, Potter P, Kelly M, Cox RD, Brown SD. ENU mutagenesis, a way forward to understand gene function. *Annu Rev Genomics Hum Genet* 2008; **9:** 49-69.

4. Vidal SM, Malo D, Marquis JF, Gros P. Forward genetic dissection of immunity to infection in the mouse. *Annu Rev Immunol* 2008; **26:** 81-132.

5. Waterston RH, Lindblad-Toh K, Birney E, Rogers J, Abril JF, Agarwal P *et al.* Initial sequencing and comparative analysis of the mouse genome. *Nature* 2002; **420**(6915)**:** 520-62.

6. Beck JA, Lloyd S, Hafezparast M, Lennon-Pierce M, Eppig JT, Festing MF *et al.* Genealogies of mouse inbred strains. *Nat Genet* 2000; **24**(1)**:** 23-5.

7. Hoebe K, Beutler B. Unraveling innate immunity using large scale N-ethyl-N-nitrosourea mutagenesis. *Tissue Antigens* 2005; **65**(5)**:** 395-401.

8. van der Weyden L, White JK, Adams DJ, Logan DW. The mouse genetics toolkit: revealing function and mechanism. *Genome biology* 2011; **12**(6)**:** 224.

9. Brehm MA, Jouvet N, Greiner DL, Shultz LD. Humanized mice for the study of infectious diseases. *Curr Opin Immunol* 2013; **25**(4)**:** 428-35.

10. Shultz LD, Brehm MA, Garcia-Martinez JV, Greiner DL. Humanized mice for immune system investigation: progress, promise and challenges. *Nat Rev Immunol* 2012; **12**(11)**:** 786-98.

11. Beutler B, Jiang Z, Georgel P, Crozat K, Croker B, Rutschmann S *et al.* Genetic analysis of host resistance: Toll-like receptor signaling and immunity at large. *Annu Rev Immunol* 2006; **24:** 353-89.

12. Rogner UC, Avner P. Congenic mice: cutting tools for complex immune disorders. *Nat Rev Immunol* 2003; **3**(3)**:** 243-52.

13. Nelms KA, Goodnow CC. Genome-wide ENU mutagenesis to reveal immune regulators. *Immunity* 2001; **15**(3)**:** 409-18.

14. Russell LB, Hunsicker PR, Cacheiro NL, Bangham JW, Russell WL, Shelby MD. Chlorambucil effectively induces deletion mutations in mouse germ cells. *Proc Natl Acad Sci U S A* 1989; **86**(10)**:** 3704-8.

15. Russell WL, Kelly EM, Hunsicker PR, Bangham JW, Maddux SC, Phipps EL. Specific-locus test shows ethylnitrosourea to be the most potent mutagen in the mouse. *Proc Natl Acad Sci U S A* 1979; **76**(11)**:** 5818-9.

16. Richer E, Qureshi ST, Vidal SM, Malo D. Chemical mutagenesis: a new strategy against the global threat of infectious diseases. *Mamm Genome* 2008; **19**(5)**:** 309-17.

17. Hoyne GF, Goodnow CC. The use of genomewide ENU mutagenesis screens to unravel complex mammalian traits: identifying genes that regulate organ-specific and systemic autoimmunity. *Immunol Rev* 2006; **210:** 27-39.

18. Justice MJ, Noveroske JK, Weber JS, Zheng B, Bradley A. Mouse ENU mutagenesis. *Hum Mol Genet* 1999; **8**(10)**:** 1955-63.

19. Concepcion D, Seburn KL, Wen G, Frankel WN, Hamilton BA. Mutation rate and predicted phenotypic target sizes in ethylnitrosourea-treated mice. *Genetics* 2004; **168**(2)**:** 953-9.

20. Barbaric I, Wells S, Russ A, Dear TN. Spectrum of ENU-induced mutations in phenotype-driven and gene-driven screens in the mouse. *Environ Mol Mutagen* 2007; **48**(2)**:** 124-42.

21. Caspary T. Phenotype-driven mouse ENU mutagenesis screens. *Methods in enzymology* 2010; **477:** 313-27.

22. Papathanasiou P, Goodnow CC. Connecting mammalian genome with phenome by ENU mouse mutagenesis: gene combinations specifying the immune system. *Annual review of genetics* 2005; **39:** 241-62.

23. Nolan PM, Peters J, Strivens M, Rogers D, Hagan J, Spurr N *et al.* A systematic, genome-wide, phenotype-driven mutagenesis programme for gene function studies in the mouse. *Nat Genet* 2000; **25**(4)**:** 440-3.

24. Broz P, Monack DM. Newly described pattern recognition receptors team up against intracellular pathogens. *Nat Rev Immunol* 2013; **13**(8)**:** 551-65.

25. Ishii KJ, Koyama S, Nakagawa A, Coban C, Akira S. Host innate immune receptors and beyond: making sense of microbial infections. *Cell Host Microbe* 2008; **3**(6)**:** 352-63.

26. Anderson KV, Bokla L, Nusslein-Volhard C. Establishment of dorsal-ventral polarity in the Drosophila embryo: the induction of polarity by the Toll gene product. *Cell* 1985; **42**(3)**:** 791-8.

27. Lemaitre B, Nicolas E, Michaut L, Reichhart JM, Hoffmann JA. The dorsoventral regulatory gene cassette spatzle/Toll/cactus controls the potent antifungal response in Drosophila adults. *Cell* 1996; **86**(6)**:** 973-83.

28. Kawai T, Akira S. Toll-like receptors and their crosstalk with other innate receptors in infection and immunity. *Immunity* 2011; **34**(5)**:** 637-50.

29. Medzhitov R, Preston-Hurlburt P, Janeway CA, Jr. A human homologue of the Drosophila Toll protein signals activation of adaptive immunity. *Nature* 1997; **388**(6640)**:** 394-7.

30. Alexopoulou L, Holt AC, Medzhitov R, Flavell RA. Recognition of double-stranded RNA and activation of NF-kappaB by Toll-like receptor 3. *Nature* 2001; **413**(6857)**:** 732-8.

31. Diebold SS, Kaisho T, Hemmi H, Akira S, Reis e Sousa C. Innate antiviral responses by means of TLR7-mediated recognition of single-stranded RNA. *Science* 2004; **303**(5663)**:** 1529-31.

32. Hemmi H, Kaisho T, Takeuchi O, Sato S, Sanjo H, Hoshino K *et al.* Small anti-viral compounds activate immune cells via the TLR7 MyD88-dependent signaling pathway. *Nat Immunol* 2002; **3**(2)**:** 196-200.

33. Hemmi H, Takeuchi O, Kawai T, Kaisho T, Sato S, Sanjo H *et al.* A Toll-like receptor recognizes bacterial DNA. *Nature* 2000; **408**(6813)**:** 740-5.

34. Brinkmann MM, Spooner E, Hoebe K, Beutler B, Ploegh HL, Kim YM. The interaction between the ER membrane protein UNC93B and TLR3, 7, and 9 is crucial for TLR signaling. *J Cell Biol* 2007; **177**(2)**:** 265-75.

35. Kim YM, Brinkmann MM, Paquet ME, Ploegh HL. UNC93B1 delivers nucleotide-sensing toll-like receptors to endolysosomes. *Nature* 2008; **452**(7184)**:** 234-8.

36. Tabeta K, Hoebe K, Janssen EM, Du X, Georgel P, Crozat K *et al.* The Unc93b1 mutation 3d disrupts exogenous antigen presentation and signaling via Toll-like receptors 3, 7 and 9. *Nat Immunol* 2006; **7**(2)**:** 156-64.

37. Kawai T, Akira S. TLR signaling. *Cell death and differentiation* 2006; **13**(5)**:** 816-25.

38. Dixit E, Kagan JC. Intracellular pathogen detection by RIG-I-like receptors. *Adv Immunol* 2013; **117:** 99-125.

39. Loo YM, Gale M, Jr. Immune signaling by RIG-I-like receptors. *Immunity* 2011; **34**(5)**:** 680-92.

40. Elinav E, Strowig T, Henao-Mejia J, Flavell RA. Regulation of the antimicrobial response by NLR proteins. *Immunity* 2011; **34**(5)**:** 665-79.

41. Kato H, Sato S, Yoneyama M, Yamamoto M, Uematsu S, Matsui K *et al.* Cell type-specific involvement of RIG-I in antiviral response. *Immunity* 2005; **23**(1)**:** 19-28.

42. Saito T, Hirai R, Loo YM, Owen D, Johnson CL, Sinha SC *et al.* Regulation of innate antiviral defenses through a shared repressor domain in RIG-I and LGP2. *Proc Natl Acad Sci U S A* 2007; **104**(2)**:** 582-7.

43. Venkataraman T, Valdes M, Elsby R, Kakuta S, Caceres G, Saijo S *et al.* Loss of DExD/H box RNA helicase LGP2 manifests disparate antiviral responses. *J Immunol* 2007; **178**(10)**:** 6444-55.

44. Yoneyama M, Kikuchi M, Matsumoto K, Imaizumi T, Miyagishi M, Taira K *et al.* Shared and unique functions of the DExD/H-box helicases RIG-I, MDA5, and LGP2 in antiviral innate immunity. *J Immunol* 2005; **175**(5)**:** 2851-8.

45. Yoneyama M, Kikuchi M, Natsukawa T, Shinobu N, Imaizumi T, Miyagishi M *et al.* The RNA helicase RIG-I has an essential function in double-stranded RNA-induced innate antiviral responses. *Nat Immunol* 2004; **5**(7)**:** 730-7.

46. Hornung V, Ellegast J, Kim S, Brzozka K, Jung A, Kato H *et al.* 5'-Triphosphate RNA is the ligand for RIG-I. *Science* 2006; **314**(5801)**:** 994-7.

47. Pichlmair A, Schulz O, Tan CP, Naslund TI, Liljestrom P, Weber F *et al.* RIG-I-mediated antiviral responses to single-stranded RNA bearing 5'-phosphates. *Science* 2006; **314**(5801)**:** 997-1001.

48. Schlee M, Roth A, Hornung V, Hagmann CA, Wimmenauer V, Barchet W *et al.* Recognition of 5' triphosphate by RIG-I helicase requires short blunt double-stranded RNA as contained in panhandle of negative-strand virus. *Immunity* 2009; **31**(1)**:** 25-34.

49. Gack MU, Shin YC, Joo CH, Urano T, Liang C, Sun L *et al.* TRIM25 RING-finger E3 ubiquitin ligase is essential for RIG-I-mediated antiviral activity. *Nature* 2007; **446**(7138)**:** 916-920.

50. Kawai T, Takahashi K, Sato S, Coban C, Kumar H, Kato H *et al.* IPS-1, an adaptor triggering RIG-I- and Mda5-mediated type I interferon induction. *Nat Immunol* 2005; **6**(10)**:** 981-8.

51. Meylan E, Curran J, Hofmann K, Moradpour D, Binder M, Bartenschlager R *et al.* Cardif is an adaptor protein in the RIG-I antiviral pathway and is targeted by hepatitis C virus. *Nature* 2005; **437**(7062)**:** 1167-72.

52. Seth RB, Sun L, Ea CK, Chen ZJ. Identification and characterization of MAVS, a mitochondrial antiviral signaling protein that activates NF-kappaB and IRF 3. *Cell* 2005; **122**(5)**:** 669-82.

53. Xu LG, Wang YY, Han KJ, Li LY, Zhai Z, Shu HB. VISA is an adapter protein required for virus-triggered IFN-beta signaling. *Molecular cell* 2005; **19**(6)**:** 727-40.

54. Gitlin L, Barchet W, Gilfillan S, Cella M, Beutler B, Flavell RA *et al.* Essential role of mda-5 in type I IFN responses to polyriboinosinic:polyribocytidylic acid and encephalomyocarditis picornavirus. *Proc Natl Acad Sci U S A* 2006; **103**(22)**:** 8459-64.

55. Kato H, Takeuchi O, Sato S, Yoneyama M, Yamamoto M, Matsui K *et al.* Differential roles of MDA5 and RIG-I helicases in the recognition of RNA viruses. *Nature* 2006; **441**(7089)**:** 101-5.

56. Jiang X, Kinch LN, Brautigam CA, Chen X, Du F, Grishin NV *et al.* Ubiquitin-induced oligomerization of the RNA sensors RIG-I and MDA5 activates antiviral innate immune response. *Immunity* 2012; **36**(6)**:** 959-73.

57. Schroder K, Tschopp J. The inflammasomes. *Cell* 2010; **140**(6)**:** 821-32.

58. Sabbah A, Chang TH, Harnack R, Frohlich V, Tominaga K, Dube PH *et al.* Activation of innate immune antiviral responses by Nod2. *Nat Immunol* 2009; **10**(10)**:** 1073-80.

59. Davis BK, Wen H, Ting JP. The inflammasome NLRs in immunity, inflammation, and associated diseases. *Annu Rev Immunol* 2011; **29:** 707-35.

60. Srinivasula SM, Poyet JL, Razmara M, Datta P, Zhang Z, Alnemri ES. The PYRIN-CARD protein ASC is an activating adaptor for caspase-1. *J Biol Chem* 2002; **277**(24)**:** 21119-22.

61. Miao EA, Leaf IA, Treuting PM, Mao DP, Dors M, Sarkar A *et al.* Caspase-1-induced pyroptosis is an innate immune effector mechanism against intracellular bacteria. *Nat Immunol* 2010; **11**(12)**:** 1136-42.

62. Iwasaki A, Medzhitov R. Regulation of adaptive immunity by the innate immune system. *Science* 2010; **327**(5963)**:** 291-5.

63. Kreijtz JH, Fouchier RA, Rimmelzwaan GF. Immune responses to influenza virus infection. *Virus research* 2011; **162**(1-2)**:** 19-30.

64. Kohlmeier JE, Woodland DL. Immunity to respiratory viruses. *Annu Rev Immunol* 2009; **27:** 61-82.

65. Rouse BT, Sehrawat S. Immunity and immunopathology to viruses: what decides the outcome? *Nat Rev Immunol* 2010; **10**(7)**:** 514-26.

66. Spits H, Artis D, Colonna M, Diefenbach A, Di Santo JP, Eberl G *et al.* Innate lymphoid cells--a proposal for uniform nomenclature. *Nat Rev Immunol* 2013; **13**(2)**:** 145-9.

67. Mocsai A. Diverse novel functions of neutrophils in immunity, inflammation, and beyond. *J Exp Med* 2013; **210**(7)**:** 1283-99.

68. Murray PJ, Wynn TA. Protective and pathogenic functions of macrophage subsets. *Nat Rev Immunol* 2011; **11**(11)**:** 723-37.

69. Braciale TJ, Sun J, Kim TS. Regulating the adaptive immune response to respiratory virus infection. *Nat Rev Immunol* 2012; **12**(4)**:** 295-305.

70. Satpathy AT, Wu X, Albring JC, Murphy KM. Re(de)fining the dendritic cell lineage. *Nat Immunol* 2012; **13**(12)**:** 1145-54.

71. Taubenberger JK, Morens DM. The pathology of influenza virus infections. *Annual review of pathology* 2008; **3:** 499-522.

72. WHO. Influenza Fact Sheet No.211. In, 2009.

73. Brown EG. Influenza virus genetics. *Biomedicine & pharmacotherapy = Biomedecine & pharmacotherapie* 2000; **54**(4)**:** 196-209.

74. Tscherne DM, Garcia-Sastre A. Virulence determinants of pandemic influenza viruses. *J Clin Invest* 2011; **121**(1)**:** 6-13.

75. Johnson NP, Mueller J. Updating the accounts: global mortality of the 1918-1920 "Spanish" influenza pandemic. *Bulletin of the history of medicine* 2002; **76**(1)**:** 105-15.

76. Taubenberger JK, Morens DM. 1918 Influenza: the mother of all pandemics. *Emerg Infect Dis* 2006; **12**(1)**:** 15-22.

77. Perrone LA, Plowden JK, Garcia-Sastre A, Katz JM, Tumpey TM. H5N1 and 1918 pandemic influenza virus infection results in early and excessive infiltration of macrophages and neutrophils in the lungs of mice. *PLoS Pathog* 2008; **4**(8)**:** e1000115.

78. Didierlaurent A, Goulding J, Patel S, Snelgrove R, Low L, Bebien M *et al.* Sustained desensitization to bacterial Toll-like receptor ligands after resolution of respiratory influenza infection. *J Exp Med* 2008; **205**(2)**:** 323-9.

79. Morens DM, Taubenberger JK, Fauci AS. Predominant role of bacterial pneumonia as a cause of death in pandemic influenza: implications for pandemic influenza preparedness. *J Infect Dis* 2008; **198**(7)**:** 962-70.

80. Pittet LA, Hall-Stoodley L, Rutkowski MR, Harmsen AG. Influenza virus infection decreases tracheal mucociliary velocity and clearance of Streptococcus pneumoniae. *Am J Respir Cell Mol Biol* 2010; **42**(4)**:** 450-60.

81. Shahangian A, Chow EK, Tian X, Kang JR, Ghaffari A, Liu SY *et al.* Type I IFNs mediate development of postinfluenza bacterial pneumonia in mice. *J Clin Invest* 2009; **119**(7)**:** 1910-20.

82. Sun K, Metzger DW. Inhibition of pulmonary antibacterial defense by interferon-gamma during recovery from influenza infection. *Nat Med* 2008; **14**(5)**:** 558-64.

83. Yang Y, Halloran ME, Sugimoto JD, Longini IM, Jr. Detecting human-to-human transmission of avian influenza A (H5N1). *Emerg Infect Dis* 2007; **13**(9)**:** 1348-53.

84. WHO. Cumulative number of confirmed human cases of avian influenza A(H5N1) reported to WHO. In, 2014.

85. Toapanta FR, Ross TM. Impaired immune responses in the lungs of aged mice following influenza infection. *Respir Res* 2009; **10:** 112.

86. Subbarao K, Matsuoka Y. The prospects and challenges of universal vaccines for influenza. *Trends in microbiology* 2013; **21**(7)**:** 350-8.

87. Darwish I, Mubareka S, Liles WC. Immunomodulatory therapy for severe influenza. *Expert review of anti-infective therapy* 2011; **9**(7)**:** 807-22.

88. Diebold SS, Montoya M, Unger H, Alexopoulou L, Roy P, Haswell LE *et al.* Viral infection switches non-plasmacytoid dendritic cells into high interferon producers. *Nature* 2003; **424**(6946)**:** 324-8.

89. Kallfass C, Lienenklaus S, Weiss S, Staeheli P. Visualizing the beta interferon response in mice during infection with influenza A viruses expressing or lacking nonstructural protein 1. *J Virol* 2013; **87**(12)**:** 6925-30.

90. Gack MU, Albrecht RA, Urano T, Inn KS, Huang IC, Carnero E *et al.* Influenza A virus NS1 targets the ubiquitin ligase TRIM25 to evade recognition by the host viral RNA sensor RIG-I. *Cell Host Microbe* 2009; **5**(5)**:** 439-49.

91. Guo Z, Chen LM, Zeng H, Gomez JA, Plowden J, Fujita T *et al.* NS1 protein of influenza A virus inhibits the function of intracytoplasmic pathogen sensor, RIG-I. *Am J Respir Cell Mol Biol* 2007; **36**(3)**:** 263-9.

92. Labella AM, Merel SE. Influenza. *The Medical clinics of North America* 2013; **97**(4)**:** 621-45, x.

93. Harper SA, Bradley JS, Englund JA, File TM, Gravenstein S, Hayden FG *et al.* Seasonal influenza in adults and children--diagnosis, treatment, chemoprophylaxis, and institutional outbreak management: clinical practice guidelines of the Infectious Diseases Society of America. *Clinical infectious diseases : an official publication of the Infectious Diseases Society of America* 2009; **48**(8)**:** 1003-32.

94. Deyde VM, Xu X, Bright RA, Shaw M, Smith CB, Zhang Y *et al.* Surveillance of resistance to adamantanes among influenza A(H3N2) and A(H1N1) viruses isolated worldwide. *J Infect Dis* 2007; **196**(2)**:** 249-57.

95. Kreijtz JH, Osterhaus AD, Rimmelzwaan GF. Vaccination strategies and vaccine formulations for epidemic and pandemic influenza control. *Human vaccines* 2009; **5**(3)**:** 126-35.

96. Osterholm MT, Kelley NS, Sommer A, Belongia EA. Efficacy and effectiveness of influenza vaccines: a systematic review and meta-analysis. *The Lancet infectious diseases* 2012; **12**(1)**:** 36-44.

97. Barnard DL. Animal models for the study of influenza pathogenesis and therapy. *Antiviral research* 2009; **82**(2)**:** A110-22.

98. Brown EG. Increased virulence of a mouse-adapted variant of influenza A/FM/1/47 virus is controlled by mutations in genome segments 4, 5, 7, and 8. *J Virol* 1990; **64**(9)**:** 4523-33.

99. Le Goffic R, Balloy V, Lagranderie M, Alexopoulou L, Escriou N, Flavell R *et al.* Detrimental contribution of the Toll-like receptor (TLR)3 to influenza A virus-induced acute pneumonia. *PLoS Pathog* 2006; **2**(6)**:** e53.

100. Lee N, Wong CK, Hui DS, Lee SK, Wong RY, Ngai KL *et al.* Role of human Toll-like receptors in naturally occurring influenza A infections. *Influenza and other respiratory viruses* 2013; **7**(5)**:** 666-75.

101. Lund JM, Alexopoulou L, Sato A, Karow M, Adams NC, Gale NW *et al.* Recognition of single-stranded RNA viruses by Toll-like receptor 7. *Proc Natl Acad Sci U S A* 2004; **101**(15)**:** 5598-603.

102. Guillot L, Le Goffic R, Bloch S, Escriou N, Akira S, Chignard M *et al.* Involvement of toll-like receptor 3 in the immune response of lung epithelial cells to double-stranded RNA and influenza A virus. *J Biol Chem* 2005; **280**(7)**:** 5571-80.

103. Hidaka F, Matsuo S, Muta T, Takeshige K, Mizukami T, Nunoi H. A missense mutation of the Toll-like receptor 3 gene in a patient with influenza-associated encephalopathy. *Clin Immunol* 2006; **119**(2)**:** 188-94.

104. Seo SU, Kwon HJ, Song JH, Byun YH, Seong BL, Kawai T *et al.* MyD88 signaling is indispensable for primary influenza A virus infection but dispensable for secondary infection. *J Virol* 2010; **84**(24)**:** 12713-22.

105. Heer AK, Shamshiev A, Donda A, Uematsu S, Akira S, Kopf M *et al.* TLR signaling fine-tunes anti-influenza B cell responses without regulating effector T cell responses. *J Immunol* 2007; **178**(4)**:** 2182-91.

106. Weber F, Wagner V, Rasmussen SB, Hartmann R, Paludan SR. Double-stranded RNA is produced by positive-strand RNA viruses and DNA viruses but not in detectable amounts by negative-strand RNA viruses. *J Virol* 2006; **80**(10)**:** 5059-64.

107. Allen IC, Scull MA, Moore CB, Holl EK, McElvania-TeKippe E, Taxman DJ *et al.* The NLRP3 inflammasome mediates in vivo innate immunity to influenza A virus through recognition of viral RNA. *Immunity* 2009; **30**(4)**:** 556-65.

108. Koyama S, Ishii KJ, Kumar H, Tanimoto T, Coban C, Uematsu S *et al.* Differential role of TLR- and RLR-signaling in the immune responses to influenza A virus infection and vaccination. *J Immunol* 2007; **179**(7)**:** 4711-20.

109. Lopez CB, Moltedo B, Alexopoulou L, Bonifaz L, Flavell RA, Moran TM. TLR-independent induction of dendritic cell maturation and adaptive immunity by negative-strand RNA viruses. *J Immunol* 2004; **173**(11)**:** 6882-9.

110. Adachi O, Kawai T, Takeda K, Matsumoto M, Tsutsui H, Sakagami M *et al.* Targeted disruption of the MyD88 gene results in loss of IL-1- and IL-18-mediated function. *Immunity* 1998; **9**(1)**:** 143-50.

111. Le Goffic R, Pothlichet J, Vitour D, Fujita T, Meurs E, Chignard M *et al.* Cutting Edge: Influenza A virus activates TLR3-dependent inflammatory and RIG-I-dependent antiviral responses in human lung epithelial cells. *J Immunol* 2007; **178**(6)**:** 3368-72.

112. Goulet ML, Olagnier D, Xu Z, Paz S, Belgnaoui SM, Lafferty EI *et al.* Systems analysis of a RIG-I agonist inducing broad spectrum inhibition of virus infectivity. *PLoS Pathog* 2013; **9**(4)**:** e1003298.

113. Ichinohe T, Pang IK, Iwasaki A. Influenza virus activates inflammasomes via its intracellular M2 ion channel. *Nat Immunol* 2010; **11**(5)**:** 404-10.

114. Ichinohe T, Lee HK, Ogura Y, Flavell R, Iwasaki A. Inflammasome recognition of influenza virus is essential for adaptive immune responses. *J Exp Med* 2009; **206**(1)**:** 79-87.

115. Pothlichet J, Meunier I, Davis BK, Ting JP, Skamene E, von Messling V *et al.* Type I IFN triggers RIG-I/TLR3/NLRP3-dependent inflammasome activation in influenza A virus infected cells. *PLoS Pathog* 2013; **9**(4)**:** e1003256.

116. Thomas PG, Dash P, Aldridge JR, Jr., Ellebedy AH, Reynolds C, Funk AJ *et al.* The intracellular sensor NLRP3 mediates key innate and healing responses to influenza A virus via the regulation of caspase-1. *Immunity* 2009; **30**(4)**:** 566-75.

117. Schmitz N, Kurrer M, Bachmann MF, Kopf M. Interleukin-1 is responsible for acute lung immunopathology but increases survival of respiratory influenza virus infection. *J Virol* 2005; **79**(10)**:** 6441-8.

118. Pang IK, Ichinohe T, Iwasaki A. IL-1R signaling in dendritic cells replaces pattern-recognition receptors in promoting CD8(+) T cell responses to influenza A virus. *Nat Immunol* 2013; **14**(3)**:** 246-53.

119. Pang IK, Pillai PS, Iwasaki A. Efficient influenza A virus replication in the respiratory tract requires signals from TLR7 and RIG-I. *Proc Natl Acad Sci U S A* 2013; **110**(34)**:** 13910-5.

120. Damjanovic D, Small CL, Jeyanathan M, McCormick S, Xing Z. Immunopathology in influenza virus infection: uncoupling the friend from foe. *Clin Immunol* 2012; **144**(1)**:** 57-69.

121. Buchweitz JP, Harkema JR, Kaminski NE. Time-dependent airway epithelial and inflammatory cell responses induced by influenza virus A/PR/8/34 in C57BL/6 mice. *Toxicol Pathol* 2007; **35**(3)**:** 424-35.

122. Wareing MD, Lyon AB, Lu B, Gerard C, Sarawar SR. Chemokine expression during the development and resolution of a pulmonary leukocyte response to influenza A virus infection in mice. *J Leukoc Biol* 2004; **76**(4)**:** 886-95.

123. McGill J, Heusel JW, Legge KL. Innate immune control and regulation of influenza virus infections. *J Leukoc Biol* 2009; **86**(4)**:** 803-12.

124. Lin KL, Suzuki Y, Nakano H, Ramsburg E, Gunn MD. CCR2+ monocyte-derived dendritic cells and exudate macrophages produce influenza-induced pulmonary immune pathology and mortality. *J Immunol* 2008; **180**(4)**:** 2562-72.

125. Jayasekera JP, Vinuesa CG, Karupiah G, King NJ. Enhanced antiviral antibody secretion and attenuated immunopathology during influenza virus infection in nitric oxide synthase-2-deficient mice. *J Gen Virol* 2006; **87**(Pt 11)**:** 3361-71.

126. Peper RL, Van Campen H. Tumor necrosis factor as a mediator of inflammation in influenza A viral pneumonia. *Microb Pathog* 1995; **19**(3)**:** 175-83.

127. Dawson TC, Beck MA, Kuziel WA, Henderson F, Maeda N. Contrasting effects of CCR5 and CCR2 deficiency in the pulmonary inflammatory response to influenza A virus. *Am J Pathol* 2000; **156**(6)**:** 1951-9.

128. Herold S, Steinmueller M, von Wulffen W, Cakarova L, Pinto R, Pleschka S *et al.* Lung epithelial apoptosis in influenza virus pneumonia: the role of macrophage-expressed TNF-related apoptosis-inducing ligand. *J Exp Med* 2008; **205**(13)**:** 3065-77.

129. Narasaraju T, Ng HH, Phoon MC, Chow VT. MCP-1 antibody treatment enhances damage and impedes repair of the alveolar epithelium in influenza pneumonitis. *Am J Respir Cell Mol Biol* 2010; **42**(6)**:** 732-43.

130. Piqueras B, Connolly J, Freitas H, Palucka AK, Banchereau J. Upon viral exposure, myeloid and plasmacytoid dendritic cells produce 3 waves of distinct chemokines to recruit immune effectors. *Blood* 2006; **107**(7)**:** 2613-8.

131. Ingulli E, Funatake C, Jacovetty EL, Zanetti M. Cutting edge: antigen presentation to CD8 T cells after influenza A virus infection. *J Immunol* 2009; **182**(1)**:** 29-33.

132. GeurtsvanKessel CH, Lambrecht BN. Division of labor between dendritic cell subsets of the lung. *Mucosal Immunol* 2008; **1**(6)**:** 442-50.

133. Sung SS, Fu SM, Rose CE, Jr., Gaskin F, Ju ST, Beaty SR. A major lung CD103 (alphaE)-beta7 integrin-positive epithelial dendritic cell population expressing Langerin and tight junction proteins. *J Immunol* 2006; **176**(4)**:** 2161-72.

134. Ballesteros-Tato A, Leon B, Lund FE, Randall TD. Temporal changes in dendritic cell subsets, cross-priming and costimulation via CD70 control CD8(+) T cell responses to influenza. *Nat Immunol* 2010; **11**(3)**:** 216-24.

135. GeurtsvanKessel CH, Willart MA, van Rijt LS, Muskens F, Kool M, Baas C *et al.* Clearance of influenza virus from the lung depends on migratory langerin+CD11b- but not plasmacytoid dendritic cells. *J Exp Med* 2008; **205**(7)**:** 1621-34.

136. Helft J, Manicassamy B, Guermonprez P, Hashimoto D, Silvin A, Agudo J *et al.* Cross-presenting CD103+ dendritic cells are protected from influenza virus infection. *J Clin Invest* 2012; **122**(11)**:** 4037-47.

137. Kim TS, Braciale TJ. Respiratory dendritic cell subsets differ in their capacity to support the induction of virus-specific cytotoxic CD8+ T cell responses. *PLoS One* 2009; **4**(1)**:** e4204.

138. Ho AW, Prabhu N, Betts RJ, Ge MQ, Dai X, Hutchinson PE *et al.* Lung CD103+ dendritic cells efficiently transport influenza virus to the lymph node and load viral antigen onto MHC class I for presentation to CD8 T cells. *J Immunol* 2011; **187**(11)**:** 6011-21.

139. Belz GT, Smith CM, Kleinert L, Reading P, Brooks A, Shortman K *et al.* Distinct migrating and nonmigrating dendritic cell populations are involved in MHC class I-restricted antigen presentation after lung infection with virus. *Proc Natl Acad Sci U S A* 2004; **101**(23)**:** 8670-5.

140. Wolf AI, Buehler D, Hensley SE, Cavanagh LL, Wherry EJ, Kastner P *et al.* Plasmacytoid dendritic cells are dispensable during primary influenza virus infection. *J Immunol* 2009; **182**(2)**:** 871-9.

141. Yoon H, Legge KL, Sung SS, Braciale TJ. Sequential activation of CD8+ T cells in the draining lymph nodes in response to pulmonary virus infection. *J Immunol* 2007; **179**(1)**:** 391-9.

142. Lawrence CW, Braciale TJ. Activation, differentiation, and migration of naive virus-specific CD8+ T cells during pulmonary influenza virus infection. *J Immunol* 2004; **173**(2)**:** 1209-18.

143. Roman E, Miller E, Harmsen A, Wiley J, Von Andrian UH, Huston G *et al.* CD4 effector T cell subsets in the response to influenza: heterogeneity, migration, and function. *J Exp Med* 2002; **196**(7)**:** 957-68.

144. Baaten BJ, Li CR, Bradley LM. Multifaceted regulation of T cells by CD44. *Communicative & integrative biology* 2010; **3**(6)**:** 508-12.

145. Swain SL, Dutton RW, Woodland DL. T cell responses to influenza virus infection: effector and memory cells. *Viral Immunol* 2004; **17**(2)**:** 197-209.

146. Arbones ML, Ord DC, Ley K, Ratech H, Maynard-Curry C, Otten G *et al.* Lymphocyte homing and leukocyte rolling and migration are impaired in L-selectin-deficient mice. *Immunity* 1994; **1**(4)**:** 247-60.

147. Dolfi DV, Duttagupta PA, Boesteanu AC, Mueller YM, Oliai CH, Borowski AB *et al.* Dendritic cells and CD28 costimulation are required to sustain virus-specific CD8+ T cell responses during the effector phase in vivo. *J Immunol* 2011; **186**(8)**:** 4599-608.

148. McGill J, Van Rooijen N, Legge KL. Protective influenza-specific CD8 T cell responses require interactions with dendritic cells in the lungs. *J Exp Med* 2008; **205**(7)**:** 1635-46.

149. McGill J, Legge KL. Cutting edge: contribution of lung-resident T cell proliferation to the overall magnitude of the antigen-specific CD8 T cell response in the lungs following murine influenza virus infection. *J Immunol* 2009; **183**(7)**:** 4177-81.

150. Kim TS, Sun J, Braciale TJ. T cell responses during influenza infection: getting and keeping control. *Trends in immunology* 2011; **32**(5)**:** 225-31.

151. Brown DM, Dilzer AM, Meents DL, Swain SL. CD4 T cell-mediated protection from lethal influenza: perforin and antibody-mediated mechanisms give a one-two punch. *J Immunol* 2006; **177**(5)**:** 2888-98.

152. Graham MB, Braciale VL, Braciale TJ. Influenza virus-specific CD4+ T helper type 2 T lymphocytes do not promote recovery from experimental virus infection. *J Exp Med* 1994; **180**(4)**:** 1273-82.

153. Sun J, Madan R, Karp CL, Braciale TJ. Effector T cells control lung inflammation during acute influenza virus infection by producing IL-10. *Nat Med* 2009; **15**(3)**:** 277-84.

154. Sun J, Dodd H, Moser EK, Sharma R, Braciale TJ. CD4+ T cell help and innate-derived IL-27 induce Blimp-1-dependent IL-10 production by antiviral CTLs. *Nat Immunol* 2011; **12**(4)**:** 327-34.

155. Corsten MF, Schroen B, Heymans S. Inflammation in viral myocarditis: friend or foe? *Trends Mol Med* 2012; **18**(7)**:** 426-37.

156. Esfandiarei M, McManus BM. Molecular biology and pathogenesis of viral myocarditis. *Annual review of pathology* 2008; **3:** 127-55.

157. Drory Y, Turetz Y, Hiss Y, Lev B, Fisman EZ, Pines A *et al.* Sudden unexpected death in persons less than 40 years of age. *The American journal of cardiology* 1991; **68**(13)**:** 1388-92.

158. Fairweather D, Stafford KA, Sung YK. Update on coxsackievirus B3 myocarditis. *Curr Opin Rheumatol* 2012; **24**(4)**:** 401-7.

159. Fairley CK, Ryan M, Wall PG, Weinberg J. The organisms reported to cause infective myocarditis and pericarditis in England and Wales. *The Journal of infection* 1996; **32**(3)**:** 223-5.

160. Morris SA, Tanowitz HB, Wittner M, Bilezikian JP. Pathophysiological insights into the cardiomyopathy of Chagas' disease. *Circulation* 1990; **82**(6)**:** 1900-9.

161. Grist NR, Reid D. Organisms in myocarditis/endocarditis viruses. *The Journal of infection* 1997; **34**(2)**:** 155.

162. Kim KS, Hufnagel G, Chapman NM, Tracy S. The group B coxsackieviruses and myocarditis. *Rev Med Virol* 2001; **11**(6)**:** 355-68.

163. Bowles NE, Vallejo J. Viral causes of cardiac inflammation. *Current opinion in cardiology* 2003; **18**(3)**:** 182-8.

164. Tam PE. Coxsackievirus myocarditis: interplay between virus and host in the pathogenesis of heart disease. *Viral Immunol* 2006; **19**(2)**:** 133-46.

165. Bergelson JM, Cunningham JA, Droguett G, Kurt-Jones EA, Krithivas A, Hong JS *et al.* Isolation of a common receptor for Coxsackie B viruses and adenoviruses 2 and 5. *Science* 1997; **275**(5304)**:** 1320-3.

166. Shi Y, Chen C, Lisewski U, Wrackmeyer U, Radke M, Westermann D *et al.* Cardiac deletion of the Coxsackievirus-adenovirus receptor abolishes Coxsackievirus B3 infection and prevents myocarditis in vivo. *J Am Coll Cardiol* 2009; **53**(14)**:** 1219-26.

167. McManus BM, Chow LH, Wilson JE, Anderson DR, Gulizia JM, Gauntt CJ *et al.* Direct myocardial injury by enterovirus: a central role in the evolution of murine myocarditis. *Clin Immunol Immunopathol* 1993; **68**(2)**:** 159-69.

168. Badorff C, Lee GH, Lamphear BJ, Martone ME, Campbell KP, Rhoads RE *et al.* Enteroviral protease 2A cleaves dystrophin: evidence of cytoskeletal disruption in an acquired cardiomyopathy. *Nat Med* 1999; **5**(3)**:** 320-6.

169. Cornell CT, Kiosses WB, Harkins S, Whitton JL. Coxsackievirus B3 proteins directionally complement each other to downregulate surface major histocompatibility complex class I. *J Virol* 2007; **81**(13)**:** 6785-97.

170. Kemball CC, Harkins S, Whitmire JK, Flynn CT, Feuer R, Whitton JL. Coxsackievirus B3 inhibits antigen presentation in vivo, exerting a profound and selective effect on the MHC class I pathway. *PLoS Pathog* 2009; **5**(10)**:** e1000618.

171. Mukherjee A, Morosky SA, Delorme-Axford E, Dybdahl-Sissoko N, Oberste MS, Wang T *et al.* The coxsackievirus B 3C protease cleaves MAVS and TRIF to attenuate host type I interferon and apoptotic signaling. *PLoS Pathog* 2011; **7**(3)**:** e1001311.

172. Aretz HT. Myocarditis: the Dallas criteria. *Human pathology* 1987; **18**(6)**:** 619-24.

173. Schultheiss HP, Kuhl U. Why is diagnosis of infectious myocarditis such a challenge? *Expert review of anti-infective therapy* 2011; **9**(12)**:** 1093-5.

174. Jin O, Sole MJ, Butany JW, Chia WK, McLaughlin PR, Liu P *et al.* Detection of enterovirus RNA in myocardial biopsies from patients with myocarditis and cardiomyopathy using gene amplification by polymerase chain reaction. *Circulation* 1990; **82**(1)**:** 8-16.

175. Papageorgiou AP, Heymans S. Interactions between the extracellular matrix and inflammation during viral myocarditis. *Immunobiology* 2012; **217**(5)**:** 503-10.

176. Kuhl U, Pauschinger M, Schwimmbeck PL, Seeberg B, Lober C, Noutsias M *et al.* Interferon-beta treatment eliminates cardiotropic viruses and improves left ventricular function in patients with myocardial persistence of viral genomes and left ventricular dysfunction. *Circulation* 2003; **107**(22)**:** 2793-8.

177. Hahn EA, Hartz VL, Moon TE, O'Connell JB, Herskowitz A, McManus BM *et al.* The Myocarditis Treatment Trial: design, methods and patients enrollment. *Eur Heart J* 1995; **16 Suppl O:** 162-7.

178. Mason JW, O'Connell JB, Herskowitz A, Rose NR, McManus BM, Billingham ME *et al.* A clinical trial of immunosuppressive therapy for myocarditis. The Myocarditis Treatment Trial Investigators. *The New England journal of medicine* 1995; **333**(5)**:** 269-75.

179. Wang YX, da Cunha V, Vincelette J, White K, Velichko S, Xu Y *et al.* Antiviral and myocyte protective effects of murine interferon-beta and -{alpha}2 in coxsackievirus B3-induced myocarditis and epicarditis in Balb/c mice. *Am J Physiol Heart Circ Physiol* 2007; **293**(1)**:** H69-76.

180. Walther EU, Hohlfeld R. Multiple sclerosis: side effects of interferon beta therapy and their management. *Neurology* 1999; **53**(8)**:** 1622-7.

181. Leipner C, Grun K, Schneider I, Gluck B, Sigusch HH, Stelzner A. Coxsackievirus B3-induced myocarditis: differences in the immune response of C57BL/6 and Balb/c mice. *Med Microbiol Immunol* 2004; **193**(2-3)**:** 141-7.

182. Tomko RP, Xu R, Philipson L. HCAR and MCAR: the human and mouse cellular receptors for subgroup C adenoviruses and group B coxsackieviruses. *Proc Natl Acad Sci U S A* 1997; **94**(7)**:** 3352-6.

183. Chow LH, Gauntt CJ, McManus BM. Differential effects of myocarditic variants of Coxsackievirus B3 in inbred mice. A pathologic characterization of heart tissue damage. *Lab Invest* 1991; **64**(1)**:** 55-64.

184. Fairweather D, Kaya Z, Shellam GR, Lawson CM, Rose NR. From infection to autoimmunity. *Journal of autoimmunity* 2001; **16**(3)**:** 175-86.

185. Woodruff JF, Woodruff JJ. Involvement of T lymphocytes in the pathogenesis of coxsackie virus B3 heart disease. *J Immunol* 1974; **113**(6)**:** 1726-34.

186. Neu N, Rose NR, Beisel KW, Herskowitz A, Gurri-Glass G, Craig SW. Cardiac myosin induces myocarditis in genetically predisposed mice. *J Immunol* 1987; **139**(11)**:** 3630-6.

187. Fairweather D, Rose NR. Coxsackievirus-induced myocarditis in mice: a model of autoimmune disease for studying immunotoxicity. *Methods* 2007; **41**(1)**:** 118-22.

188. Triantafilou K, Orthopoulos G, Vakakis E, Ahmed MA, Golenbock DT, Lepper PM *et al.* Human cardiac inflammatory responses triggered by Coxsackie B viruses are mainly Toll-like receptor (TLR) 8-dependent. *Cell Microbiol* 2005; **7**(8)**:** 1117-26.

189. Negishi H, Osawa T, Ogami K, Ouyang X, Sakaguchi S, Koshiba R *et al.* A critical link between Toll-like receptor 3 and type II interferon signaling pathways in antiviral innate immunity. *Proc Natl Acad Sci U S A* 2008; **105**(51)**:** 20446-51.

190. Riad A, Westermann D, Escher F, Becher PM, Savvatis K, Lettau O *et al.* Myeloid differentiation factor-88 contributes to TLR9-mediated modulation of acute coxsackievirus B3-induced myocarditis in vivo. *Am J Physiol Heart Circ Physiol* 2010; **298**(6)**:** H2024-31.

191. Fuse K, Chan G, Liu Y, Gudgeon P, Husain M, Chen M *et al.* Myeloid differentiation factor-88 plays a crucial role in the pathogenesis of Coxsackievirus B3-induced myocarditis and influences type I interferon production. *Circulation* 2005; **112**(15)**:** 2276-85.

192. Gorbea C, Makar KA, Pauschinger M, Pratt G, Bersola JL, Varela J *et al.* A role for Toll-like receptor 3 variants in host susceptibility to enteroviral myocarditis and dilated cardiomyopathy. *J Biol Chem* 2010; **285**(30)**:** 23208-23.

193. Riad A, Westermann D, Zietsch C, Savvatis K, Becher PM, Bereswill S *et al.* TRIF is a critical survival factor in viral cardiomyopathy. *J Immunol* 2011; **186**(4)**:** 2561-70.

194. Huhn MH, McCartney SA, Lind K, Svedin E, Colonna M, Flodstrom-Tullberg M. Melanoma differentiation-associated protein-5 (MDA-5) limits early viral replication but is not

essential for the induction of type 1 interferons after Coxsackievirus infection. *Virology* 2010; **401**(1)**:** 42-8.

195. Wang JP, Cerny A, Asher DR, Kurt-Jones EA, Bronson RT, Finberg RW. MDA5 and MAVS mediate type I interferon responses to coxsackie B virus. *J Virol* 2010; **84**(1)**:** 254-60.

196. Zhang QM, Song WQ, Li YJ, Qian J, Zhai AX, Wu J *et al.* Over-expression of mitochondrial antiviral signaling protein inhibits coxsackievirus B3 infection by enhancing type-I interferons production. *Virol J* 2012; **9:** 312.

197. Yuan J, Liu Z, Lim T, Zhang H, He J, Walker E *et al.* CXCL10 inhibits viral replication through recruitment of natural killer cells in coxsackievirus B3-induced myocarditis. *Circ Res* 2009; **104**(5)**:** 628-38.

198. Godeny EK, Gauntt CJ. Involvement of natural killer cells in coxsackievirus B3-induced murine myocarditis. *J Immunol* 1986; **137**(5)**:** 1695-702.

199. Godeny EK, Gauntt CJ. Murine natural killer cells limit coxsackievirus B3 replication. *J Immunol* 1987; **139**(3)**:** 913-8.

200. Huhn MH, Hultcrantz M, Lind K, Ljunggren HG, Malmberg KJ, Flodstrom-Tullberg M. IFN-gamma production dominates the early human natural killer cell response to Coxsackievirus infection. *Cell Microbiol* 2008; **10**(2)**:** 426-36.

201. Henke A, Zell R, Martin U, Stelzner A. Direct interferon-gamma-mediated protection caused by a recombinant coxsackievirus B3. *Virology* 2003; **315**(2)**:** 335-44.

202. Wessely R, Klingel K, Knowlton KU, Kandolf R. Cardioselective infection with coxsackievirus B3 requires intact type I interferon signaling: implications for mortality and early viral replication. *Circulation* 2001; **103**(5)**:** 756-61.

203. Huber SA, Job LP. Cellular immune mechanisms in Coxsackievirus group B, type 3 induced myocarditis in Balb/C mice. *Advances in experimental medicine and biology* 1983; **161:** 491-508.

204. Henke A, Huber S, Stelzner A, Whitton JL. The role of CD8+ T lymphocytes in coxsackievirus B3-induced myocarditis. *J Virol* 1995; **69**(11)**:** 6720-8.

205. Opavsky MA, Penninger J, Aitken K, Wen WH, Dawood F, Mak T *et al.* Susceptibility to myocarditis is dependent on the response of alphabeta T lymphocytes to coxsackieviral infection. *Circ Res* 1999; **85**(6)**:** 551-8.

206. Okuno M, Nakagawa M, Shimada M, Saito M, Hishinuma S, Yamauchi-Takihara K. Expressional patterns of cytokines in a murine model of acute myocarditis: early expression of cardiotrophin-1. *Lab Invest* 2000; **80**(3)**:** 433-40.

207. Shioi T, Matsumori A, Sasayama S. Persistent expression of cytokine in the chronic stage of viral myocarditis in mice. *Circulation* 1996; **94**(11)**:** 2930-7.

208. Lane JR, Neumann DA, Lafond-Walker A, Herskowitz A, Rose NR. Interleukin 1 or tumor necrosis factor can promote Coxsackie B3-induced myocarditis in resistant B10.A mice. *J Exp Med* 1992; **175**(4)**:** 1123-9.

209. Lim BK, Choe SC, Shin JO, Ho SH, Kim JM, Yu SS *et al.* Local expression of interleukin-1 receptor antagonist by plasmid DNA improves mortality and decreases myocardial inflammation in experimental coxsackieviral myocarditis. *Circulation* 2002; **105**(11)**:** 1278-81.

210. Matsumori A, Yamada T, Suzuki H, Matoba Y, Sasayama S. Increased circulating cytokines in patients with myocarditis and cardiomyopathy. *Br Heart J* 1994; **72**(6)**:** 561-6.

211. Torre-Amione G, Kapadia S, Lee J, Durand JB, Bies RD, Young JB *et al.* Tumor necrosis factor-alpha and tumor necrosis factor receptors in the failing human heart. *Circulation* 1996; **93**(4)**:** 704-11.

212. Deonarain R, Cerullo D, Fuse K, Liu PP, Fish EN. Protective role for interferon-beta in coxsackievirus B3 infection. *Circulation* 2004; **110**(23)**:** 3540-3.

213. Kashuba VI, Protopopov AI, Kvasha SM, Gizatullin RZ, Wahlestedt C, Kisselev LL *et al.* hUNC93B1: a novel human gene representing a new gene family and encoding an unc-93-like protein. *Gene* 2002; **283**(1-2)**:** 209-17.

214. Levin JZ, Horvitz HR. The Caenorhabditis elegans unc-93 gene encodes a putative transmembrane protein that regulates muscle contraction. *J Cell Biol* 1992; **117**(1)**:** 143-55.

215. Crane MJ, Gaddi PJ, Salazar-Mather TP. UNC93B1 mediates innate inflammation and antiviral defense in the liver during acute murine cytomegalovirus infection. *PLoS One* 2012; **7**(6)**:** e39161.

216. Wang JP, Bowen GN, Zhou S, Cerny A, Zacharia A, Knipe DM *et al.* Role of specific innate immune responses in herpes simplex virus infection of the central nervous system. *J Virol* 2012; **86**(4)**:** 2273-81.

217. Casrouge A, Zhang SY, Eidenschenk C, Jouanguy E, Puel A, Yang K *et al.* Herpes simplex virus encephalitis in human UNC-93B deficiency. *Science* 2006; **314**(5797)**:** 308-12.

218. Lafaille FG, Pessach IM, Zhang SY, Ciancanelli MJ, Herman M, Abhyankar A *et al.* Impaired intrinsic immunity to HSV-1 in human iPSC-derived TLR3-deficient CNS cells. *Nature* 2012; **491**(7426)**:** 769-73.

219. Esen N, Blakely PK, Rainey-Barger EK, Irani DN. Complexity of the microglial activation pathways that drive innate host responses during lethal alphavirus encephalitis in mice. *ASN Neuro* 2012; **4**(4)**:** 207-21.

220. Schamber-Reis BL, Petritus PM, Caetano BC, Martinez ER, Okuda K, Golenbock D *et al.* UNC93B1 and nucleic acid-sensing Toll-like receptors mediate host resistance to infection with Leishmania major. *J Biol Chem* 2013; **288**(10)**:** 7127-36.

221. Caetano BC, Carmo BB, Melo MB, Cerny A, dos Santos SL, Bartholomeu DC *et al.* Requirement of UNC93B1 reveals a critical role for TLR7 in host resistance to primary infection with Trypanosoma cruzi. *J Immunol* 2011; **187**(4)**:** 1903-11.

222. Melo MB, Kasperkovitz P, Cerny A, Konen-Waisman S, Kurt-Jones EA, Lien E *et al.* UNC93B1 mediates host resistance to infection with Toxoplasma gondii. *PLoS Pathog* 2010; **6**(8)**:** e1001071.

223. Andrade WA, Souza Mdo C, Ramos-Martinez E, Nagpal K, Dutra MS, Melo MB *et al.* Combined action of nucleic acid-sensing Toll-like receptors and TLR11/TLR12 heterodimers imparts resistance to Toxoplasma gondii in mice. *Cell Host Microbe* 2013; **13**(1)**:** 42-53.

224. Pifer R, Benson A, Sturge CR, Yarovinsky F. UNC93B1 is essential for TLR11 activation and IL-12-dependent host resistance to Toxoplasma gondii. *J Biol Chem* 2011; **286**(5)**:** 3307-14.

225. Raetz M, Kibardin A, Sturge CR, Pifer R, Li H, Burstein E *et al.* Cooperation of TLR12 and TLR11 in the IRF8-dependent IL-12 response to Toxoplasma gondii profilin. *J Immunol* 2013; **191**(9)**:** 4818-27.

226. Zhang D, Zhang G, Hayden MS, Greenblatt MB, Bussey C, Flavell RA *et al.* A toll-like receptor that prevents infection by uropathogenic bacteria. *Science* 2004; **303**(5663)**:** 1522-6.

227. Koehn J, Huesken D, Jaritz M, Rot A, Zurini M, Dwertmann A *et al.* Assessing the function of human UNC-93B in Toll-like receptor signaling and major histocompatibility complex II response. *Hum Immunol* 2007; **68**(11)**:** 871-8.

228. Deguine J, Lee BL, Newman ZR, Barton GM. No antigen-presentation defect in Unc93b1(3d/3d) (3d) mice. *Nat Immunol* 2013; **14**(11)**:** 1101-2.

229. Tabeta K, Hoebe K, Janssen EM, Xia Y, Beutler B. Respond to "No antigen-presentation defect in Unc93b1(3d/3d) (3d) mice". *Nat Immunol* 2013; **14**(11)**:** 1102-3.

230. Fukui R, Saitoh S, Matsumoto F, Kozuka-Hata H, Oyama M, Tabeta K *et al.* Unc93B1 biases Toll-like receptor responses to nucleic acid in dendritic cells toward DNA- but against RNA-sensing. *J Exp Med* 2009; **206**(6)**:** 1339-50.

231. Christensen SR, Shupe J, Nickerson K, Kashgarian M, Flavell RA, Shlomchik MJ. Toll-like receptor 7 and TLR9 dictate autoantibody specificity and have opposing inflammatory and regulatory roles in a murine model of lupus. *Immunity* 2006; **25**(3)**:** 417-28.

232. Deane JA, Pisitkun P, Barrett RS, Feigenbaum L, Town T, Ward JM *et al.* Control of toll-like receptor 7 expression is essential to restrict autoimmunity and dendritic cell proliferation. *Immunity* 2007; **27**(5)**:** 801-10.

233. Fukui R, Saitoh S, Kanno A, Onji M, Shibata T, Ito A *et al.* Unc93B1 restricts systemic lethal inflammation by orchestrating Toll-like receptor 7 and 9 trafficking. *Immunity* 2011; **35**(1)**:** 69-81.

234. Kono DH, Haraldsson MK, Lawson BR, Pollard KM, Koh YT, Du X *et al.* Endosomal TLR signaling is required for anti-nucleic acid and rheumatoid factor autoantibodies in lupus. *Proc Natl Acad Sci U S A* 2009; **106**(29)**:** 12061-6.

235. Fauci AS. Seasonal and pandemic influenza preparedness: science and countermeasures. *J Infect Dis* 2006; **194 Suppl 2:** S73-6.

236. Fraser C, Donnelly CA, Cauchemez S, Hanage WP, Van Kerkhove MD, Hollingsworth TD *et al.* Pandemic potential of a strain of influenza A (H1N1): early findings. *Science* 2009; **324**(5934)**:** 1557-61.

237. Neumann G, Noda T, Kawaoka Y. Emergence and pandemic potential of swine-origin H1N1 influenza virus. *Nature* 2009; **459**(7249)**:** 931-9.

238. Barker WH, Mullooly JP. Impact of epidemic type A influenza in a defined adult population. *Am J Epidemiol* 1980; **112**(6)**:** 798-811.

239. Webster RG. Immunity to influenza in the elderly. *Vaccine* 2000; **18**(16)**:** 1686-9.

240. Vermaelen KY, Carro-Muino I, Lambrecht BN, Pauwels RA. Specific migratory dendritic cells rapidly transport antigen from the airways to the thoracic lymph nodes. *J Exp Med* 2001; **193**(1)**:** 51-60.

241. Waithman J, Mintern JD. Dendritic cells and influenza A virus infection. *Virulence* 2012; **3**(7)**:** 603-8.

242. Oshiumi H, Matsumoto M, Funami K, Akazawa T, Seya T. TICAM-1, an adaptor molecule that participates in Toll-like receptor 3-mediated interferon-beta induction. *Nat Immunol* 2003; **4**(2)**:** 161-7.

243. Horby P, Nguyen NY, Dunstan SJ, Baillie JK. The role of host genetics in susceptibility to influenza: a systematic review. *PLoS One* 2012; **7**(3)**:** e33180.

244. Buer J, Balling R. Mice, microbes and models of infection. *Nat Rev Genet* 2003; **4**(3)**:** 195-205.

245. Takeuchi O, Hoshino K, Kawai T, Sanjo H, Takada H, Ogawa T *et al.* Differential roles of TLR2 and TLR4 in recognition of gram-negative and gram-positive bacterial cell wall components. *Immunity* 1999; **11**(4)**:** 443-51.

246. Short KR, Brooks AG, Reading PC, Londrigan SL. The fate of influenza A virus after infection of human macrophages and dendritic cells. *J Gen Virol* 2012; **93**(Pt 11)**:** 2315-25.

247. Brown DM, Lee S, Garcia-Hernandez Mde L, Swain SL. Multifunctional CD4 cells expressing gamma interferon and perforin mediate protection against lethal influenza virus infection. *J Virol* 2012; **86**(12)**:** 6792-803.

248. Hufford MM, Kim TS, Sun J, Braciale TJ. Antiviral CD8+ T cell effector activities in situ are regulated by target cell type. *J Exp Med* 2011; **208**(1)**:** 167-80.

249. Mykkanen J, Torrents D, Pineda M, Camps M, Yoldi ME, Horelli-Kuitunen N *et al.* Functional analysis of novel mutations in y(+)LAT-1 amino acid transporter gene causing lysinuric protein intolerance (LPI). *Hum Mol Genet* 2000; **9**(3)**:** 431-8.

250. Chen LY, Lin B, Pan CJ, Hiraiwa H, Chou JY. Structural requirements for the stability and microsomal transport activity of the human glucose 6-phosphate transporter. *J Biol Chem* 2000; **275**(44)**:** 34280-6.

251. Herold S, von Wulffen W, Steinmueller M, Pleschka S, Kuziel WA, Mack M *et al.* Alveolar epithelial cells direct monocyte transepithelial migration upon influenza virus infection: impact of chemokines and adhesion molecules. *J Immunol* 2006; **177**(3)**:** 1817-24.

252. Delamarre L, Pack M, Chang H, Mellman I, Trombetta ES. Differential lysosomal proteolysis in antigen-presenting cells determines antigen fate. *Science* 2005; **307**(5715)**:** 1630-4.

253. Caron G, Duluc D, Fremaux I, Jeannin P, David C, Gascan H *et al.* Direct stimulation of human T cells via TLR5 and TLR7/8: flagellin and R-848 up-regulate proliferation and IFN-gamma production by memory CD4+ T cells. *J Immunol* 2005; **175**(3)**:** 1551-7.

254. Gelman AE, Zhang J, Choi Y, Turka LA. Toll-like receptor ligands directly promote activated CD4+ T cell survival. *J Immunol* 2004; **172**(10)**:** 6065-73.

255. Hornung V, Rothenfusser S, Britsch S, Krug A, Jahrsdorfer B, Giese T *et al.* Quantitative expression of toll-like receptor 1-10 mRNA in cellular subsets of human peripheral blood mononuclear cells and sensitivity to CpG oligodeoxynucleotides. *J Immunol* 2002; **168**(9)**:** 4531-7.

256. Kabelitz D. Expression and function of Toll-like receptors in T lymphocytes. *Curr Opin Immunol* 2007; **19**(1)**:** 39-45.

257. Kulkarni R, Behboudi S, Sharif S. Insights into the role of Toll-like receptors in modulation of T cell responses. *Cell Tissue Res* 2011; **343**(1)**:** 141-52.

258. Funderburg N, Luciano AA, Jiang W, Rodriguez B, Sieg SF, Lederman MM. Toll-like receptor ligands induce human T cell activation and death, a model for HIV pathogenesis. *PLoS One* 2008; **3**(4)**:** e1915.

259. Tabiasco J, Devevre E, Rufer N, Salaun B, Cerottini JC, Speiser D *et al.* Human effector CD8+ T lymphocytes express TLR3 as a functional coreceptor. *J Immunol* 2006; **177**(12)**:** 8708-13.

260. LaRosa DF, Stumhofer JS, Gelman AE, Rahman AH, Taylor DK, Hunter CA *et al.* T cell expression of MyD88 is required for resistance to Toxoplasma gondii. *Proc Natl Acad Sci U S A* 2008; **105**(10)**:** 3855-60.

261. Rahman AH, Cui W, Larosa DF, Taylor DK, Zhang J, Goldstein DR *et al.* MyD88 plays a critical T cell-intrinsic role in supporting CD8 T cell expansion during acute lymphocytic choriomeningitis virus infection. *J Immunol* 2008; **181**(6)**:** 3804-10.

262. Song Y, Zhuang Y, Zhai S, Huang D, Zhang Y, Kang W *et al.* Increased expression of TLR7 in CD8(+) T cells leads to TLR7-mediated activation and accessory cell-dependent IFN-gamma production in HIV type 1 infection. *AIDS Res Hum Retroviruses* 2009; **25**(12)**:** 1287-95.

263. Matikainen S, Paananen A, Miettinen M, Kurimoto M, Timonen T, Julkunen I *et al.* IFN-alpha and IL-18 synergistically enhance IFN-gamma production in human NK cells: differential regulation of Stat4 activation and IFN-gamma gene expression by IFN-alpha and IL-12. *Eur J Immunol* 2001; **31**(7)**:** 2236-45.

264. Zhou J, Law HK, Cheung CY, Ng IH, Peiris JS, Lau YL. Differential expression of chemokines and their receptors in adult and neonatal macrophages infected with human or avian influenza viruses. *J Infect Dis* 2006; **194**(1)**:** 61-70.

265. Tighe RM, Liang J, Liu N, Jung Y, Jiang D, Gunn MD *et al.* Recruited exudative macrophages selectively produce CXCL10 after noninfectious lung injury. *Am J Respir Cell Mol Biol* 2011; **45**(4)**:** 781-8.

266. Richer E, Prendergast C, Zhang DE, Qureshi ST, Vidal SM, Malo D. N-ethyl-N-nitrosourea-induced mutation in ubiquitin-specific peptidase 18 causes hyperactivation of IFN-alphass signaling and suppresses STAT4-induced IFN-gamma production, resulting in increased susceptibility to Salmonella typhimurium. *J Immunol* 2010; **185**(6)**:** 3593-601.

267. Cook MC, Vinuesa CG, Goodnow CC. ENU-mutagenesis: insight into immune function and pathology. *Curr Opin Immunol* 2006; **18**(5)**:** 627-33.

268. Sievers F, Wilm A, Dineen D, Gibson TJ, Karplus K, Li W *et al.* Fast, scalable generation of high-quality protein multiple sequence alignments using Clustal Omega. *Molecular systems biology* 2011; **7:** 539.

269. Kelley LA, Sternberg MJ. Protein structure prediction on the Web: a case study using the Phyre server. *Nature protocols* 2009; **4**(3)**:** 363-71.

270. The PyMol Molecular Graphics System. version 1.7**:** Schrödinger, LLC.

271. Chow LH, Beisel KW, McManus BM. Enteroviral infection of mice with severe combined immunodeficiency. Evidence for direct viral pathogenesis of myocardial injury. *Lab Invest* 1992; **66**(1)**:** 24-31.

272. Godeny EK, Gauntt CJ. In situ immune autoradiographic identification of cells in heart tissues of mice with coxsackievirus B3-induced myocarditis. *Am J Pathol* 1987; **129**(2)**:** 267-76.

273. Cook DN, Beck MA, Coffman TM, Kirby SL, Sheridan JF, Pragnell IB *et al.* Requirement of MIP-1 alpha for an inflammatory response to viral infection. *Science* 1995; **269**(5230)**:** 1583-5.

274. Kishimoto C, Kawamata H, Sakai S, Shinohara H, Ochiai H. Role of MIP-2 in coxsackievirus B3 myocarditis. *J Mol Cell Cardiol* 2000; **32**(4)**:** 631-8.

275. Aly M, Wiltshire S, Chahrour G, Osti JC, Vidal SM. Complex genetic control of host susceptibility to coxsackievirus B3-induced myocarditis. *Genes Immun* 2007; **8**(3)**:** 193-204.

276. Coronado MJ, Brandt JE, Kim E, Bucek A, Bedja D, Abston ED *et al.* Testosterone and interleukin-1beta increase cardiac remodeling during coxsackievirus B3 myocarditis via serpin A 3n. *Am J Physiol Heart Circ Physiol* 2012; **302**(8)**:** H1726-36.

277. Blazejczyk M, Miron M, Nadon R. FlexArray: A statistical data analysis software for gene expression microarrays. Genome Quebec, Montreal, Canada. 2007.

278. Huang da W, Sherman BT, Lempicki RA. Systematic and integrative analysis of large gene lists using DAVID bioinformatics resources. *Nature protocols* 2009; **4**(1)**:** 44-57.

279. Huang da W, Sherman BT, Lempicki RA. Bioinformatics enrichment tools: paths toward the comprehensive functional analysis of large gene lists. *Nucleic Acids Res* 2009; **37**(1)**:** 1-13.

280. Leipner C, Borchers M, Merkle I, Stelzner A. Coxsackievirus B3-induced myocarditis in MHC class II-deficient mice. *Journal of human virology* 1999; **2**(2)**:** 102-14.

281. Heim A, Stille-Seigener M, Pring-Akerblom P, Grumbach I, Brehm C, Kreuzer H *et al.* Recombinant Interferons beta and gamma have a higher antiviral activity than interferon-alpha in coxsackievirus B3-infected carrier state cultures of human myocardial fibroblasts. *J Interferon Cytokine Res* 1996; **16**(4)**:** 283-7.

282. Ding L, Hanawa H, Ota Y, Hasegawa G, Hao K, Asami F *et al.* Lipocalin-2/neutrophil gelatinase-B associated lipocalin is strongly induced in hearts of rats with autoimmune myocarditis and in human myocarditis. *Circulation journal : official journal of the Japanese Circulation Society* 2010; **74**(3)**:** 523-30.

283. Ni J, Ma X, Zhou M, Pan X, Tang J, Hao Y *et al.* Serum lipocalin-2 levels positively correlate with coronary artery disease and metabolic syndrome. *Cardiovascular diabetology* 2013; **12**(1)**:** 176.

284. Goetz DH, Holmes MA, Borregaard N, Bluhm ME, Raymond KN, Strong RK. The neutrophil lipocalin NGAL is a bacteriostatic agent that interferes with siderophore-mediated iron acquisition. *Molecular cell* 2002; **10**(5)**:** 1033-43.

285. Chan YR, Liu JS, Pociask DA, Zheng M, Mietzner TA, Berger T *et al.* Lipocalin 2 is required for pulmonary host defense against Klebsiella infection. *J Immunol* 2009; **182**(8)**:** 4947-56.

286. Berger T, Togawa A, Duncan GS, Elia AJ, You-Ten A, Wakeham A *et al.* Lipocalin 2-deficient mice exhibit increased sensitivity to Escherichia coli infection but not to ischemia-reperfusion injury. *Proc Natl Acad Sci U S A* 2006; **103**(6)**:** 1834-9.

287. Nocon AL, Ip JP, Terry R, Lim SL, Getts DR, Muller M *et al.* The bacteriostatic protein lipocalin 2 is induced in the central nervous system of mice with west nile virus encephalitis. *J Virol* 2014; **88**(1)**:** 679-89.

288. Singer E, Marko L, Paragas N, Barasch J, Dragun D, Muller DN *et al.* Neutrophil gelatinase-associated lipocalin: pathophysiology and clinical applications. *Acta Physiol (Oxf)* 2013; **207**(4)**:** 663-72.

289. Cruz DN, Gaiao S, Maisel A, Ronco C, Devarajan P. Neutrophil gelatinase-associated lipocalin as a biomarker of cardiovascular disease: a systematic review. *Clinical chemistry and laboratory medicine : CCLM / FESCC* 2012; **50**(9)**:** 1533-45.

290. Forsyth S, Horvath A, Coughlin P. A review and comparison of the murine alpha1-antitrypsin and alpha1-antichymotrypsin multigene clusters with the human clade A serpins. *Genomics* 2003; **81**(3)**:** 336-45.

291. Horvath AJ, Irving JA, Rossjohn J, Law RH, Bottomley SP, Quinsey NS *et al.* The murine orthologue of human antichymotrypsin: a structural paradigm for clade A3 serpins. *J Biol Chem* 2005; **280**(52)**:** 43168-78.

292. Sipione S, Simmen KC, Lord SJ, Motyka B, Ewen C, Shostak I *et al.* Identification of a novel human granzyme B inhibitor secreted by cultured sertoli cells. *J Immunol* 2006; **177**(8)**:** 5051-8.

293. Wagsater D, Johansson D, Fontaine V, Vorkapic E, Backlund A, Razuvaev A *et al.* Serine protease inhibitor A3 in atherosclerosis and aneurysm disease. *International journal of molecular medicine* 2012; **30**(2)**:** 288-94.

294. Asakura M, Kitakaze M. Global gene expression profiling in the failing myocardium. *Circulation journal : official journal of the Japanese Circulation Society* 2009; **73**(9)**:** 1568-76.

295. Westphal E, Rohrbach S, Buerke M, Behr H, Darmer D, Silber RE *et al.* Altered interleukin-1 receptor antagonist and interleukin-18 mRNA expression in myocardial tissues of patients with dilatated cardiomyopathy. *Mol Med* 2008; **14**(1-2)**:** 55-63.

296. Eppig JT, Blake JA, Bult CJ, Kadin JA, Richardson JE. The Mouse Genome Database (MGD): comprehensive resource for genetics and genomics of the laboratory mouse. *Nucleic Acids Res* 2012; **40**(Database issue)**:** D881-6.

297. Saeed AI, Bhagabati NK, Braisted JC, Liang W, Sharov V, Howe EA *et al.* TM4 microarray software suite. *Methods in enzymology* 2006; **411:** 134-93.

298. Saeed AI, Sharov V, White J, Li J, Liang W, Bhagabati N *et al.* TM4: a free, open-source system for microarray data management and analysis. *Biotechniques* 2003; **34**(2)**:** 374-8.

299. Ashburner M, Ball CA, Blake JA, Botstein D, Butler H, Cherry JM *et al.* Gene ontology: tool for the unification of biology. The Gene Ontology Consortium. *Nat Genet* 2000; **25**(1)**:** 25-9.

300. Carbon S, Ireland A, Mungall CJ, Shu S, Marshall B, Lewis S. AmiGO: online access to ontology and annotation data. *Bioinformatics* 2009; **25**(2)**:** 288-9.

301. Schmittgen TD, Livak KJ. Analyzing real-time PCR data by the comparative C(T) method. *Nature protocols* 2008; **3**(6)**:** 1101-8.

302. Bongfen SE, Rodrigue-Gervais IG, Berghout J, Torre S, Cingolani P, Wiltshire SA *et al.* An N-ethyl-N-nitrosourea (ENU)-induced dominant negative mutation in the JAK3 kinase protects against cerebral malaria. *PLoS One* 2012; **7**(2)**:** e31012.

303. Coghill EL, Hugill A, Parkinson N, Davison C, Glenister P, Clements S *et al.* A gene-driven approach to the identification of ENU mutants in the mouse. *Nat Genet* 2002; **30**(3)**:** 255-6.

304. Gondo Y. Trends in large-scale mouse mutagenesis: from genetics to functional genomics. *Nat Rev Genet* 2008; **9**(10)**:** 803-10.

305. Michaud EJ, Culiat CT, Klebig ML, Barker PE, Cain KT, Carpenter DJ *et al.* Efficient gene-driven germ-line point mutagenesis of C57BL/6J mice. *BMC genomics* 2005; **6:** 164.

306. Sakuraba Y, Sezutsu H, Takahasi KR, Tsuchihashi K, Ichikawa R, Fujimoto N *et al.* Molecular characterization of ENU mouse mutagenesis and archives. *Biochemical and biophysical research communications* 2005; **336**(2)**:** 609-16.

307. Augustin M, Sedlmeier R, Peters T, Huffstadt U, Kochmann E, Simon D *et al.* Efficient and fast targeted production of murine models based on ENU mutagenesis. *Mamm Genome* 2005; **16**(6)**:** 405-13.

308. Beutler B, Du X, Xia Y. Precis on forward genetics in mice. *Nat Immunol* 2007; **8**(7)**:** 659-64.

309. Sandanger O, Ranheim T, Vinge LE, Bliksoen M, Alfsnes K, Finsen AV *et al.* The NLRP3 inflammasome is up-regulated in cardiac fibroblasts and mediates myocardial ischaemia-reperfusion injury. *Cardiovascular research* 2013; **99**(1)**:** 164-74.

310. Austin CP, Battey JF, Bradley A, Bucan M, Capecchi M, Collins FS *et al.* The knockout mouse project. *Nat Genet* 2004; **36**(9)**:** 921-4.

311. Collins FS, Rossant J, Wurst W. A mouse for all reasons. *Cell* 2007; **128**(1)**:** 9-13.

312. Beckers J, Wurst W, de Angelis MH. Towards better mouse models: enhanced genotypes, systemic phenotyping and envirotype modelling. *Nat Rev Genet* 2009; **10**(6)**:** 371-80.

313. Brown SD, Moore MW. Towards an encyclopaedia of mammalian gene function: the International Mouse Phenotyping Consortium. *Disease models & mechanisms* 2012; **5**(3)**:** 289-92.

314. Brown SD, Moore MW. The International Mouse Phenotyping Consortium: past and future perspectives on mouse phenotyping. *Mamm Genome* 2012; **23**(9-10)**:** 632-40.

315. Brown SD, Wurst W, Kuhn R, Hancock JM. The functional annotation of mammalian genomes: the challenge of phenotyping. *Annual review of genetics* 2009; **43:** 305-33.